FACULTY OF ENGINEERING AND ARCHITECTURE

Influence of supply temperature and booster technology on the energetic performance of a district heating network

Alixe Degelin
Student number: 01811037

Supervisors: Prof. dr. ir. Michel De Paepe, Dr. ir. Wim Beyne
Counsellors: Ir. Robin Tassenoy, Dr. ir. Toon Demeester, Ir. Elias Vieren

Master's dissertation submitted in order to obtain the academic degree of
Master of Science in Electromechanical Engineering

Academic year 2022-2023

GHENT UNIVERSITY

Ghent, June 2023
Alixe Degelin

Preface

This Master dissertation is the result of my first independent academic research activity. From the start, as an prospective electromechanical engineer, I was interested in the subject and willing to contribute to the research on energy efficient systems.

My Master dissertation trajectory was very rewarding and has strongly stimulated my academic curiosity. Therefore I like to express my sincere appreciation to my supervision team who played a decisive role in the progress and completion of this project. First, I would like to thank my supervisor, Prof. Dr. Ir. Michel De Paepe, for welcoming me into the research group and offering the idea for such an interesting research topic. I appreciate his support and the constructive feedback I received while writing this Master dissertation. I would also like thank Dr. Ir. Wim Beyne for his role as co-supervisor. Additionally, I highly value the assistance and guidance of my counsellors, Ir. Robin Tassenoy, Dr. Ir. Toon Demeester, and Ir. Elias Vieren. Their availability for stimulating discussions along with their critical but constructive feedback greatly improved the quality of this work.

I also extend my gratitude to Eline Himpe and Tim Wyffels, who were the contact persons of the collaboration between Ghent University and the City of Ghent. I had the opportunity to attend meetings on the district heating network in Muide-Meulestede, which generated valuable insights into the origins and developments of the project.

In November, I was given the opportunity to travel with Marieke Merckx (Ghent University) and Tom Van Nieuwenhove (City of Ghent) to the EUniverCities meeting in Innsbruck to present the university – city collaborative project. I would like to thank them for their kind invitation to bring me to this conference and offering the opportunity to introduce my research to a audience of policy makers. It was an interesting and very pleasant experience.

Lastly, I would like thank my family and close friends for their support and encouragement during the past five years.

Influence of supply temperature and booster technology on the energetic performance of a district heating network

Alixe Degelin

Supervisor: Prof. dr. ir. Michel De Paepe, Dr. ir. Wim Beyne
Counsellors: Ir. Robin Tassenoy, Dr. ir. Toon Demeester, Ir. Elias Vieren, Dr. ir. arch. Eline Himpe

Master's dissertation submitted in order to obtain the academic degree of
Master of Science in Electromechanical Engineering

Departement of Electromechanical, Systems and Metal Engineering
Chair:
Faculty of Engineering and Architecture
Ghent University
Academic year 2022–2023

Summary This master dissertation investigates the influence of the network supply temperature and the use of booster technology on the energetic performance of a district heating network with central heat pump. Chapter 1 provides an introduction on district heating networks and central heat pumps, and gives a brief description of the network considered in this work. In Chapter 2, the current state of the research on district heating networks, geothermal energy, heat pumps, electric heaters and piping is discussed and the scope of the research is introduced. Chapter 3 starts with explaining the investigated scenarios and discusses the methodology and assumptions. Chapter 4 is devoted to the description of the models in Dymola, which are used to simulate the investigated scenarios. In Chapter 5, the results are presented and discussed. In Chapter 6 a sensitivity analysis is performed and the influence on the results is discussed. In Chapter 7, a general conclusion is formulated.

Keywords: District heating, central heat pump, energy efficiency, energy system analysis, Modelica, booster heat pump

MASTER THESIS 2022-2023
Research group Sustainable Thermo-Fluid Energy Systems
Department of Electromechanical, Systems and Metal Engineering – Ghent University, UGent

INFLUENCE OF SUPPLY TEMPERATURE AND BOOSTER TECHNOLOGY ON THE ENERGETIC PERFORMANCE OF A DISTRICT HEATING NETWORK

Alixe Degelin, Robin Tassenoy, Toon Demeester, Elias Vieren, Wim Beyne, Michel De Paepe
Department of Electromechanical, Systems and Metal Engineering
Ghent University
Sint-Pietersnieuwstraat 41, B9000 Gent, Belgium
E-mail: alixe.degelin@ugent.be

ABSTRACT

This study investigates the influence of the supply temperature on the primary energy use and energy efficiency of a district heating network supplied by a central heat pump, taking into account the need for booster heat pumps or booster electric heaters. The simulations consider network supply temperatures ranging from 10 °C to 75 °C and distinguish between refurbished and non-refurbished buildings. The simulation of the network is performed using the IDEAS and Buildings libraries in Dymola (Modelica). This study shows that lowering the supply temperature to 45°/55°C for non-refurbished buildings and to 45°C for refurbished buildings in combination with a booster heat pump results in the lowest total primary energy use. In the case of refurbished buildings, the trade-off between a network at 55°C without booster and a network at 10°C with individual heat pumps is highly sensitive to the performance of the central heat pump. Implementing measures to decrease the temperature needed for space heating offers significant benefits, as it can improve the overall energy efficiency from 291% to 449%.

NOMENCLATURE

D	$[m]$	Diameter pipe
DH		District heating
DHW		Domestic hot water
E	$[MWh]$	Electric energy
f	$[-]$	Darcy friction factor
HP		Heat pump
l	$[m]$	Length pipe
LTDH		Low temperature district heating
$\dot{m}$	$[kg/s]$	Mass flow rate
p	$[Pa]$	pressure
Q	$[MWh]$	Thermal energy
COP		Coefficient of performance
SH		Space heating
T	$[K]$ or $[°C]$	Temperature
ULTDH		Ultra low temperature district heating
Special characters		
η	$[-]$	Efficiency
ρ	$[kg/m^3]$	Density

INTRODUCTION

The use of fossil fuels for heating in buildings accounted for 35% of energy-related greenhouse gas emissions in Europe in 2020 [1], highlighting the need for significant improvements in energy efficiency and use. To achieve a fully decarbonized energy system by 2050, Heat Roadmap Europe targets an increase in district heating (DH) up to 50% of the total heating and cooling demand in Europe [2]. District heating networks consist of a number of buildings or consumers, which are heated by a network of pipes. The main advantage compared to conventional, individual heating technologies is the possibility to decarbonize the heating system by integrating renewable energy sources, geothermal energy and waste heat [3].

DH can be categorized into multiple generations based on the operating temperature range. The first three generations utilized steel pipes to provide steam or pressurized water above 70 °C [3, 4]. Although high network supply temperatures are suitable for high temperature radiators and domestic hot water (DHW) preparation, they suffer from low energy efficiency and substantial heat losses [3]. Currently, there is a trend towards reducing the network supply temperature to minimize heat losses, enable the use of pre-insulated (twin) pipes, and integrate renewable energy sources. This approach is referred to as the fourth generation of district heating networks, with a distinction made between low temperature district heating (LTDH) with supply temperatures of 50-70 °C and ultra-low temperature district heating (ULTDH) operating at tem-

peratures below 50 °C [5]. However, the use of low temperature district heating networks presents some challenges. To prevent the proliferation of legionella in DHW, the DH supply temperature must be raised above 55 °C with the aid of a supplementary booster unit when water is stored locally [5]. Another limitation of DH at low temperatures is its limited application potential in old buildings, where high supply temperatures are required for space heating (SH). Given that 75% of buildings in the EU are not energy efficient and only 1% of the building stock is renovated every year [6], hybrid solutions and appropriate temperature regimes are necessary.

Several studies have examined the effects of decreasing the DH supply temperature on energy efficiency and the importance of booster units such as heat pumps (HPs) and electric heaters.

Köfinger et al. [7] described economically and ecologically optimized concepts for LTDH in four case studies in Austria. The authors conclude that a couple of technical solutions are feasible, including temperature boosting using electric heaters or booster HPs, but LTDH implies higher investment cost on the demand side and the economic performance of LTDH mainly depends on availability and prices of the heat source. The researchers also state that optimum design and opertional strategies highly depend on the local conditions and can not be solved in a generalized way. Ommen et al. [8] investigated the effect of changing the DH temperature in terms of total heat cost for the consumers, carbon emissions and primary fuel consumption. Based on the results, the authors recommended "the use of 65-70 °C as the optimal forward temperature for DH networks, since lower temperatures require high investment, among others DH booster HP units in each dwelling". Yang and Svendsen [9] investigated the actual performance of a case of ULTDH in Denmark containing a central heat pump and local boosters and compared the performance to medium and low temperature DH supplied by a CHP plant and central heat pump respectively. It seems to be viable to meet the heat demand with supply temperature of 47°C most of the year. Both ULTDH (47°C and LTDH (55/25°C) show lower heat losses compared to medium temperature DH (70°C/40°C).

Depending on the network supply temperature and the state of the building, a booster unit is required for DHW preparation and/or SH. Zvingilaite et al. [10] analysed the feasibility of a micro heat pump for DHW in LTDH (40°C) and compared the thermodynamic and economic performance of HPs with electric heating. From cost perspective, HP use is not the most beneficial concept under stated technology and energy prices, but the electricity consumption is reduced by more than six times. The cost feasibility is thus highly dependent on the on the electricity prices, compared to the prices of the district heat. Østergaard and Andersen [11] investigated the optimal use of HPs in DH systems with heating based on electricity. The researchers compared two alternatives of DH with a central HP, with and without a booster HP. Results show that the primary energy demand is lower using booster HPs compared to individual boilers, individual HPs or DH without boosting. Yang et al. [12] studied the performance of five different configurations of boosting units in single-family houses supplied with ULTDH. Electric heaters combined with heat exchangers showed better energetic and economical performances compared to heat pumps, which have a higher set-point temperature due to the storage of DHW.

Previous studies have shown that the optimal DH supply temperatures and technologies are heavily influenced by local conditions, making it difficult to draw general conclusions. In a DH network powered by a central heat pump, the supply temperature affects not only the end user's energy use and heat losses but also the performance of the central heat source. Some studies have explored the use of DH networks with a central heat pump as the heat source, but only in combination with buildings where the temperature requirement for DHW is the primary factor limiting the reduction of the supply temperature.
However, this particular study takes into account a DH network in an urban neighbourhood comprising non-refurbished and refurbished buildings, which is a common scenario. In non-refurbished buildings, the supply temperature for radiators imposes a lower limit on the network's supply temperature. As a result, the temperature at which a booster unit becomes necessary is elevated. Therefore, this study aims to investigate the influence of the supply temperature and booster unit on the performance of the central heat pump and the overall network for both refurbished and non-refurbished buildings. A network in Ghent, which is part of a pilot project, is used as a case study.

METHODOLOGY

Case description

This study investigates the influence of the supply temperature in a DH network in Ghent, which is supplied by a central heat pump. The network consists of 35 houses and provides heat for both SH and DHW. The network is located alongside a football field, under which geothermal energy is extracted. Besides the energy use of the end-user, also the energy use the central heat pump and the circulation pumps are evaluated with varying supply temperature. Supply temperatures, ranging from 10 °C to 75 °C, are compared in terms of primary energy use and energy efficiency. The simulations are performed using the IDEAS and Buildings libraries in Dymola (Modelica).

The investigated scenarios are displayed in Table 1. Four scenarios with non-refurbished buildings and four with refurbished buildings are included. In non-

Table 1: Investigated scenarios.

	State of the building	Network temperature	Booster technology		Booster technology usage	
			Heat pump	*Electric heater*	*Domestic hot water*	*Space heating*
1	Non-refurbished	75 °C				
2	Non-refurbished	55 °C	X			X
3	Non-refurbished	55 °C		X		X
4	Non-refurbished	45 °C	X		X	X
5	Refurbished	55 °C				
6	Refurbished	45 °C	X		X	
7	Refurbished	45 °C		X	X	
8	Refurbished	10 °C	X		X	X

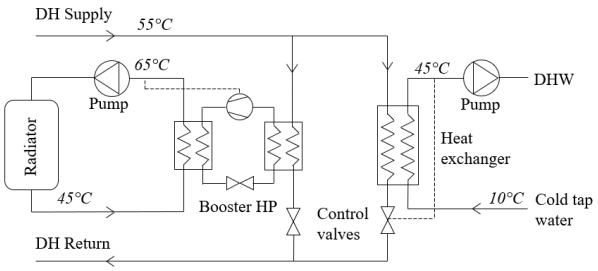

Figure 1: Schematic overview of scenario 2.

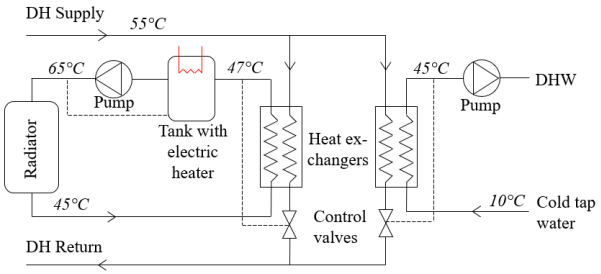

Figure 2: Schematic overview of scenario 3.

refurbished buildings a radiator supply temperature of 65 °C is assumed, while in refurbished buildings with underfloor heating 35 °C is sufficient [13]. DHW temperature of 45 °C meets the requirements for DHW use in the kitchen and bathroom [14].
Scenario 1 and 5 do not require a booster unit and exchange heat from the district heating network using a heat exchanger. All other scenarios require a booster HP or booster electric heater for SH, DHW or both. In scenarios with a booster HP, the evaporator side is connected to the DH network and the condenser side to the substation as shown in the schematic of scenario 2 (Figure 1). In scenarios with an electric heater, the water in the substation is preheated by the DH network via a heat exchanger, and further heated with a resistive electric heater as shown in the schematic of scenario 3 (Figure 2).

District heating network

The central heat pump is a water source heat pump and connected to the geothermal boreholes which provide a constant water flow rate at 10 °C [15]. The network forms a ring topology of 315 m with 35 connection points. The pressure of the piping network is set to 6 bar, according to the operating pressure of pre-insulated Flexstar UNO pipes for district heating [16]. The pressure drop in the piping network is determined using the Darcy – Weisbach equation:

$$\Delta p = \frac{8 l f \dot{m}^2}{D^5 \rho \pi^2} \tag{1}$$

Where Δp is the pressure loss in the pipe [Pa], l is the length of the pipe [m], f is the Darcy friction factor, $\dot{m}$ is the mass flow rate through the pipe [kg/s], D is the diameter of the pipe [m] and ρ is the density of the passing fluid [kg/m^3]. The pressure over a substation is assumed to be 0.5 bar [17]. Pipe dimensions are chosen such that the pressure drop in the pipes with maximum mass flow rate is limited to 300 Pa/m [18]. Heat losses are calculated using the heat transfer coefficient provided by the manufacturer [16]. The soil temperature is set to 10 °C at a pipe depth of 0.8 m. The heat exchanger effectiveness is assumed to be 80% [19].

The coefficient of performance of the central heat pump is estimated by the formula presented in the study of Jesper et al. [20] and shown in Equation 2.

$$COP = a \left(\Delta T_{lift} + 2b\right)^c \tag{2}$$

Where COP is the coefficient of performance [-], ΔT_{lift} is the temperature difference [K] between evaporator inlet and condenser outlet temperature and a, b and c are fit parameters. The fit parameters are $a = 1.4480 \cdot 10^{12}$, $b = 88.730$, $c = -4.9460$. The lift temperature can be calculated as the difference between the desired network temperature and the temperature of the ground water.

Buildings and occupants

Five different categories of occupants are selected to introduce variations in DHW consumption and heat-

Table 2: Annual SH demand before and after refurbishment and DHW consumption per occupant category.

Profile	SH Demand before refurbishment	SH Demand after refurbishment	DHW consumption
FTE, FTE, School, School	18.000 kWh	13.000 kWh	143 l/day
FTE, PTE, School	16.000 kWh	11.000 kWh	116 l/day
Retired, retired	17.000 kWh	12.000 kWh	89 l/day
FTE, FTE, School, Student	15.000 kWh	10.000 kWh	114 l/day
FTE, FTE	12.000 kWh	8.000 kWh	80 l/day

ing behaviour, and are included equally. The categories are shown in Table 2, where FTE = full time employed, PTE = part time employed, School = children living full time at home, Student = children living only during the weekends at home, Retired = always at home.

Space heating demand profiles are generated according to the approach described in the BDEW guideline [21], using weather data of Ghent of 2019 [22]. Small variations are introduced in the demand profile to avoid 100% simultaneity, based on the occupant's behaviour. An estimation of the annual heat demand of the buildings is made based on the mean gas consumption of a Belgian household (17.000 kWh/year) [23] and a gas invoice of one of the selected buildings. Table 2 provides an overview of the annual heat demand before and after refurbishment, as used in the simulations.

The required temperature for DHW in the kitchen and bathroom is 45 °C [24]. In the simulations, the setpoint temperature for DHW is 45 °C when heat is directly exchanged and 55 °C when the water is stored [25]. DHW profiles are generated with DHWcalc from Universität Kassel [26]. The mean draw-off is estimated using the Event-based Residential Occupant Behaviour (EROB) model [27].

The performance map of the booster heat pump is provided by Daikin. The performance of the electric heater is assumed to be 100%, as in Zvingilaite et al. [10].

Modelling

The simulations are performed using the Modelica programming language in Dymola. Besides the models available in the Modelica Standard Library, IDEAS library and Building library, a new pipe model is used to reduce simulation time. For the purpose of simulating a district heating network mass flow rate, pressure drop and temperature are the most important parameters. Therefore, a simple pipe model is created, taking heat losses to the ambient and pressure losses into account. For each of the eight investigated scenarios, a corresponding house model is built. Those house models are connected in a larger model which represents the district heating network, including supply and return pipes, circulation pumps and a heat source.

RESULTS

In Figure 3, the total primary energy use is presented for scenarios 1 to 4, which all concern non-refurbished buildings. The annual total energy use is calculated by summing the electric energy use of the circulation pumps, all booster units and the central heat pump. Scenario 2 (55°C, heat pump for SH) shows with 207.2 MWh/year the lowest total energy use of all investigated scenarios, followed by scenario 4 (45°C, heat pump for SH and DHW) with 213.1 MWh/year. The superior performance of the central heat pump and booster heat pumps in these scenarios, as shown in Table 3, accounts for this outcome. By reducing the DH network temperature, the COP of the central heat pump improves and heat losses in the network decrease, resulting in lower energy use compared to scenario 1 (75°C, no booster), which has a total energy use of 279.7 MWh/year. However, scenario 1 only exhibits a 35% higher total energy use than scenario 2. When investment cost for the end-user is a constraint, scenario 1 could be a viable option. On the other hand, in scenario 3 (55°C, electric heater for SH) with 535.4 MWh/year, the energy use is 2.6 times higher than in scenario 2. The largest share of the heat production in scenario 3 is performed by the electric heater, which has a much lower performance than the central heat pump or a booster heat pump. This causes the high energy use of the booster electric heater compared to the central heat pump and circulation pumps. The circulation pumps in all scenarios contribute to less than 1% of the total energy use.

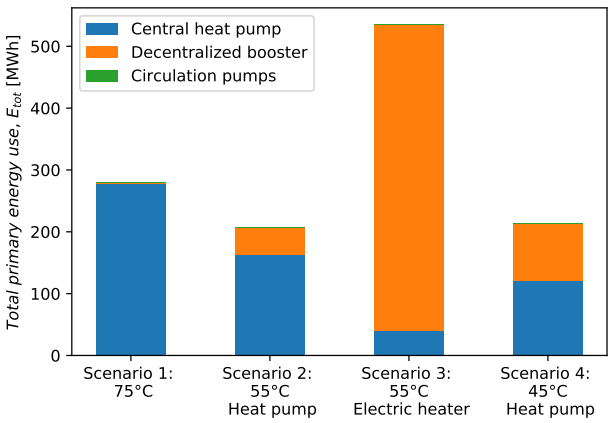

Figure 3: Comparison of the total primary energy use for scenarios 1 to 4 with non-refurbished buildings.

Table 3: Coefficient of performance of the booster units and central heat pump.

Scenario	**1**	**2**	**3**	**4**	**5**	**6**	**7**	**8**
Booster unit	-	12.7	1	6.6	-	7.7	1	3.2
Central HP	2.3	3.6	3.6	4.5	3.6	4.5	4.5	-

Figure 4 compares the total energy use of scenarios 5 to 8, which all concern refurbished buildings. Among these scenarios, scenario 6 (45°C, heat pump for DHW) shows the lowest total energy use with 96.7 MWh/year, followed by scenario 7 (45°C, electric heater for DHW) with 123.3 MWh/year. In scenario 7, the network preheats the cold tap water, reducing the share of heat generated by the electric heater. This reduces the effect of the lower performance of the electric heater compared to the booster heat pump. The total energy use in scenario 7 is only 28% higher than in scenario 6. If the end-user's investment cost is a limiting factor, an electric heater for DHW preparation is certainly worth considering. Scenario 5 (55°C, no booster) with a supply temperature of 55°C results in reduced performance of the central heat pump and increased heat losses, leading to a higher total energy use (with 130.8 MWh/year) compared to scenarios 6 and 7 with a supply temperature of 45°C. Scenario 8 (10°C, heat pump for SH and DHW) results in the highest total energy use with 138.3 MWh/year. It is remarkable that the reduction in heat losses by lowering the network temperature to 10°C is counteracted by the booster heat pump's lower performance compared to the central heat pump in the other scenarios.

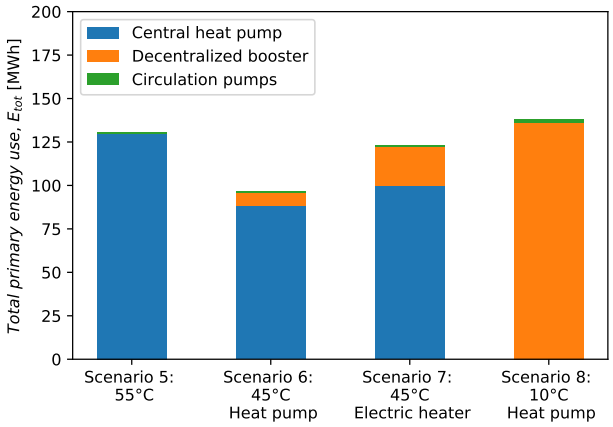

Figure 4: Comparison of the total primary energy use for scenarios 5 to 8 with refurbished buildings.

The total energy use is compared to the total useful energy, which in this case refers to the thermal energy delivered for SH and DHW. This comparison is expressed as the energy efficiency of the DH network. The energy efficiency is defined by Equation 3.

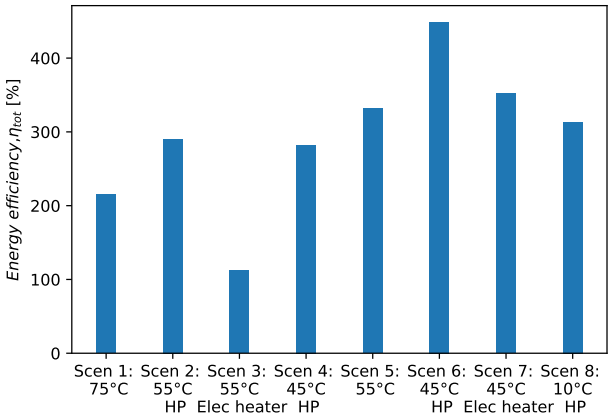

Figure 5: Comparison of the total energy efficiency of the DH network for scenarios 1 to 8.

$$\eta_{tot} = \frac{Q_{SH} + Q_{DHW}}{E_{pump} + E_{booster} + E_{CH}} = \frac{Q_{SH} + Q_{DHW}}{E_{tot}} \tag{3}$$

Where η_{tot} is the energy efficiency of the network [-], Q_{SH} and Q_{DHW} are the thermal energy delivered for SH and DHW [MWh], E_{pump}, $E_{booster}$ and E_{CH} are the electric energy used by the circulation pumps, the booster units and the central heat pump [MWh], and E_{tot} is the total used electric energy [MWh]. Figure 5 illustrates the overall system energy efficiency for both non-refurbished buildings (scenarios 1 to 4) and refurbished buildings (scenarios 5 to 8). The figure clearly demonstrates that a DH network serving refurbished buildings results in higher energy efficiency across all investigated scenarios. The most efficient scenario among the refurbished buildings (scenario 6) achieves an efficiency of 449%, whereas the most efficient scenario among the non-refurbished buildings (scenario 2) achieves an efficiency of 291%. This indicates that measures to reduces the temperature requirements for SH are beneficial to increase the overall energy efficiency of the network.

SENSITIVITY ANALYSIS

Table 4 presents the results of a sensitivity analysis on the total primary energy use by varying the COP of the central heat pump by +/-20% of its original value. Observing the table, it is evident that the results of scenarios 1 and 5 are most impacted by variation of the COP of the central heat pump. This can be attributed to the absence of booster units in these scenarios, making the central heat pump's performance relatively more influential. For non-refurbished buildings, the overall conclusion remains unchanged. However, in the case of refurbished buildings, the ranking of scenarios 5, 7, and 8 is affected by variations in the COP of the central heat pump, as can be seen in Figure 6. When the COP of the central heat pump decreases, scenario 8 remains unaffected as it does not

Table 4: Influence of variations of the COP of the central heat pump on the total primary energy use.

Scenario	1	2	3	4	5	6	7	8
COP +20%	-16.6%	-13.1%	-1.3%	-11.0%	-16.6%	-15.3%	-13.5%	-
COP -20%	+24.9%	+19.7%	+1.9%	16.5%	+24.8%	+22.9%	+20.3 %	-

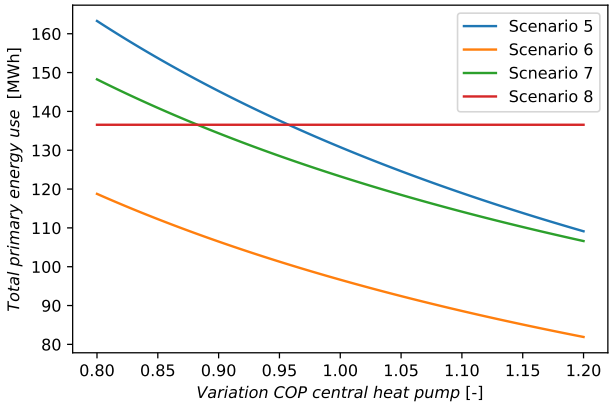

Figure 6: Influence on total primary energy use with a variation of +/-20% of the COP of the central heat pump.

involve the use of a central heat pump, and it outperforms scenarios 5 and 7. Nevertheless, scenario 6 remains the preferred scenario in terms of total energy use.

CONCLUSION

The aim of this study was to investigate the total energy use and energy efficiency of a district heating network with a central heat pump under different network supply temperatures. The study is based on a planned pilot project in Ghent, involving 35 residential buildings. Eight scenarios were investigated, considering both non-refurbished and refurbished buildings, along with booster heat pumps and booster electric heaters. The findings for non-refurbished buildings demonstrate that lowering the supply temperature to 55°C and 45°C, along with the addition of a booster heat pump, reduces heat losses and improves the performance of the central heat pump, resulting in the lowest total energy use and highest energy efficiency. However, when booster units are not used and the network supply temperature is set at 75°C, the total energy use is only 35% higher compared to the optimal scenario. The scenario at 75 °C is worth considering when the investment cost of booster heat pumps is high. The use of electric heaters to increase the temperature for space heating is found to be unfavourable, as it leads to 2.6 times higher total energy use compared to using a booster heat pump and almost twice as high as the scenario without booster units.

For refurbished buildings, a supply temperature of 45°C with decentralized booster heat pumps demonstrates the lowest energy use and highest energy efficiency. The use of booster electric heaters results in only a 28% increase in total energy use and may be an economically viable alternative. The results for the scenario with a supply temperature of 55°C (without booster units) and the scenario with a supply temperature of 10°C (with decentralized heat pumps) are similar, as the heat losses at 55°C are counterbalanced by the slightly higher performance of the central heat pump compared to the decentralized heat pumps.
A sensitivity analysis shows that the coefficient of performance of the central heat pump is a crucial parameter in the analysis of the scenarios with refurbished buildings as it changes the ranking of the scenarios. However, the optimal scenario remains unchanged.

REFERENCES

[1] E. E. Agency, "Greenhouse gas emissions from energy use in buildings in Europe," Oct. 2022. https://www.eea.europa.eu/ims/greenhouse-gas-emissions-from-energy.

[2] A. University, "Press-Release_roadmap-towards-a-decarbonised-EU-HC-sector.pdf," Dec. 2019. https://heatroadmap.eu/wp-content/uploads/2019/12/Press-Release$_{R}oadmap - towards - a - decarbonised - EU - HC - sector.pdf$.

[3] H. Lund, S. Werner, R. Wiltshire, S. Svendsen, J. E. Thorsen, F. Hvelplund, and B. V. Mathiesen, "4th Generation District Heating (4GDH): Integrating smart thermal grids into future sustainable energy systems," *Energy*, vol. 68, pp. 1–11, Apr. 2014.

[4] A. R. Mazhar, S. Liu, and A. Shukla, "A state of art review on the district heating systems," *Renewable and Sustainable Energy Reviews*, vol. 96, pp. 420–439, Nov. 2018.

[5] M. Pellegrini and A. Bianchini, "The Innovative Concept of Cold District Heating Networks: A Literature Review," *Energies*, vol. 11, p. 236, Jan. 2018. Number: 1 Publisher: Multidisciplinary Digital Publishing Institute.

[6] D. Romanov and B. Leiss, "Geothermal energy at different depths for district heating and cooling of existing and future building stock," *Renewable and Sustainable Energy Reviews*, vol. 167, p. 112727, Oct. 2022.

[7] M. Köfinger, D. Basciotti, R. R. Schmidt, E. Meissner, C. Doczekal, and A. Giovannini, "Low temperature district heating in Austria: Energetic, ecologic and economic comparison of four case studies," *Energy*, vol. 110, pp. 95–104, Sept. 2016.

[8] T. Ommen, W. B. Markussen, and B. Elmegaard, "Lowering district heating temperatures – Impact to system performance in current and future Danish energy scenarios," *Energy*, vol. 94, pp. 273–291, Jan. 2016.

[9] X. Yang and S. Svendsen, "Ultra-low temperature district heating system with central heat pump and local boosters for low-heat-density area: Analyses on a real case in Denmark," *Energy*, vol. 159, pp. 243–251, Sept. 2018. Place: Oxford Publisher: Pergamon-Elsevier Science Ltd WOS:000442973300022.

[10] E. Zvingilaite, T. Ommen, B. Elmegaard, and M. L. Franck, "LOW TEMPERATURE DISTRICT HEATING CONSUMER UNIT WITH MICRO HEAT PUMP FOR DOMESTIC HOT WATER PREPARATION," p. 9, 2012.

[11] P. A. Østergaard and A. N. Andersen, "Booster heat pumps and central heat pumps in district heating," *Applied Energy*, vol. 184, pp. 1374–1388, Dec. 2016.

[12] X. Yang, H. Li, and S. Svendsen, "Evaluations of different domestic hot water preparing methods with ultra-low-temperature district heating," *Energy*, vol. 109, pp. 248–259, Aug. 2016. Place: Oxford Publisher: Pergamon-Elsevier Science Ltd WOS:000382591000021.

[13] B. Elmegaard, T. S. Ommen, M. Markussen, and J. Iversen, "Integration of space heating and hot water supply in low temperature district heating," *Energy and Buildings*, vol. 124, pp. 255–264, July 2016.

[14] T. Ommen and B. Elmegaard, "Exergetic evaluation of heat pump booster configurations in a low temperature district heating network," p. 15, 2012.

[15] Vlaanderen, "Warmtepomp." https://www. vlaanderen.be/zoek?q=temperatuur %20grondwater.

[16] B. Pipes, "FLEXSTAR pipe system – The flexible and reliable star | BRUGG Pipes." https://www.bruggpipes.com/en/flexstar/.

[17] H. Tol and S. Svendsen, "Improving the dimensioning of piping networks and network layouts in low-energy district heating systems connected to low-energy buildings: A case study in Roskilde, Denmark," *Energy*, vol. 38, pp. 276–290, Feb. 2012.

[18] I. Best, J. Orozaliev, and K. Vajen, "Impact of Different Design Guidelines on the Total Distribution Costs of 4th Generation District Heating Networks," *Energy Procedia*, vol. 149, pp. 151–160, Sept. 2018.

[19] Y. Luo, Y. Shi, and N. Cai, "Chapter 2 - Distributed hybrid system and prospect of the future Energy Internet," in *Hybrid Systems and Multi-energy Networks for the Future Energy Internet* (Y. Luo, Y. Shi, and N. Cai, eds.), pp. 9–39, Academic Press, Jan. 2021.

[20] M. Jesper, F. Schlosser, F. Pag, T. G. Walmsley, B. Schmitt, and K. Vajen, "Large-scale heat pumps: Uptake and performance modelling of market-available devices," *Renewable and Sustainable Energy Reviews*, vol. 137, p. 110646, Mar. 2021.

[21] BDEW, "BDEW Guideline." https://www.bdew.de/.

[22] Meteoblue, "Weather Archive Ghent." https://www.meteoblue.com/en/weather/archive/era5/ghent_belgium_2797656.

[23] VREG, "Energieverbruik," Dec. 2018. https://www.vreg.be/nl/energieverbruik.

[24] X. Yang and S. Svendsen, "Achieving low return temperature for domestic hot water preparation by ultra-low-temperature district heating," *Energy Procedia*, vol. 116, pp. 426–437, June 2017.

[25] A. zorg en gezondheid, "Legionella | Zorg en Gezondheid." https://www.zorg-en-gezondheid.be/per-domein/preventie/legionella.

[26] U. Jordan and K. Vajen, "DHWcalc: PROGRAM TO GENERATE DOMESTIC HOT WATER PROFILES WITH STATISTICAL MEANS FOR USER DEFINED CONDITIONS," 2005.

[27] S. Verbruggen, M. Delghust, J. Laverge, and A. Janssens, "Stochastic Occupant Behavior Model Based on Activity And Occupancy Patterns," (Rome, Italy), pp. 2310–2317.

Contents

List of Figures

List of Tables

Nomenclature

Abbreviations

1GDH First generation district heating

2GDH Second generation district heating

3GDH Third generation district heating

4GDH Fourth generation district heating

5GDHC Fifth generation district heating and cooling

BDEW Bundesverband der Energie- und Wasserwirtshaft

BHE Borehole heat exchanger

CHP Combined heat and power

COP Coefficient of performance

DH District heating

DHW Domestic hot water

EROB Event-based residential occupant behaviour

FTE Full-time employed

GHG Greenhouse gas

GWP Global warming potential

HEX Heat exchanger

HP Heat pump

LTDH Low temperature district heating

NZEB Nearly zero energy building

PTE Part-time employed

PV Photovoltaic

RES Renewable energy sources

SH Space heating

ULTDH Ultra low temperature district heating

Greek Symbols

ϵ	Roughness
η	Efficiency
ρ	Density
ε	Heat exchanger effectiveness

Letters

$\dot{m}$	Mass flow rate
$\dot{Q}$	Thermal power
c_p	Specific heat capacity
D	Diameter
E	Electric energy
f	Darcy friction factor
fr	Fraction
k	Gain
l	length
P	Power
p	Pressure
Q	Thermal energy
Re	Reynolds number
T	Temperature
Td	Derivative time constant
Ti	Integral time constant
U	Heat transfer coefficient
V	Volume

Subscripts

C	Cold
CH	Central heat pump
diff	Differential
fric	Friction
H	Hot
i	Inner

max	Maximum
min	Minimum
nom	Nominal
o	Outer
sub	Substation
tot	Total

Chapter 1

Introduction

1.1 Setting the scene

In Europe, the use of fossil fuels for heating in buildings accounted for 35% of energy-related greenhouse gas emissions in 2020 [1], highlighting the need for significant improvements in energy efficiency and use. To achieve a fully decarbonized energy system by 2050, Heat Roadmap Europe targets an increase in district heating (DH) up to 50% of the total heating and cooling demand in Europe compared to 12% in 2019 [2]. District heating networks consist of a number of buildings or consumers, which are heated by a network of pipes. Possible heat sources for DH networks include combined heat and power (CHP) plants, waste heat from industrial processes or combustion of waste, geothermal heat, heat pumps and conventional boilers [3]. The required heat can be delivered from centralized plants or distributed heat production units, which allows any available heat source to be used. The main advantage compared to conventional, individual heating technologies is the possibility to decarbonize the heating system by integrating renewable energy sources [4].

While district heating is not a new technology and has been employed in Eastern Europe for over a century, intensive research over the past four decades has focused on harnessing the potential of district heating as a sustainable heating solution [3]. Eastern European states have more developed DH infrastructure, but Scandinavian countries have demonstrated higher efficiency in heat production and better use of low-carbon heat sources [3]. Denmark, where two third of the residential dwellings is connected to a district heating network, serves as the leading country in terms of heat planning strategies, energy efficiency and wide variety of technical solutions and heat sources [5]. In Finland, district heating covered 45% of the space heating demand in 2020 [6], while in Sweden, it accounted for 55% of the heat supply to buildings in 2014 [7]. These countries predominantly rely on biomass and heat recovery for their heat supply [6, 7, 8]. On the other hand, Flanders has only 58 district heating networks with a total length of 92 km, with a 34.1% share of renewable energy in heat production in 2019 [9]. The district heating market in Flanders is still developing, providing an opportunity to increase the use of renewable energy sources in the heating sector, thereby reducing CO_2-emissions and improving energy efficiency.

In addition to biomass and waste heat, the use of large-scale heat pumps as central heat source is expected to play a crucial role in future district heating networks [3]. One advantage of heat pumps is their ability to integrate low-temperature heat from geothermal boreholes, treated sewage water, and industrial excess heat into the district heating network [10]. By utilizing low-temperature heat, a part of the heating demand for residential dwellings can be met by using heat which is otherwise lost. Sweden has already installed large-scale heat pumps since 1980 to absorb excess electricity from nuclear power plants and provide heat for DH [7]. Nowadays,

large-scale heat pumps can benefit from excess electricity generated by wind or solar farms [11]. This integration of heat pumps with renewable electricity sources enables the combination of the electricity and thermal systems into a smart energy system [4].

1.2 Case description

The district of Muide-Meulestede in the city of Ghent has been selected as a pilot project for achieving full decarbonization and electrification of the heating system by 2030 [12]. To reach this target, multiple small-scale projects are being enrolled. One of these projects is the design and implementation of a DH network that utilizes a central heat pump as heat source, as can be seen in Figure 1.1. The plan includes the installation of 30 geothermal boreholes, each 150 meters deep, located beneath and around an existing football field. These boreholes serve as heat source for the central heat pump. The DH network will supply heat to a total of 35 private residential dwelling, meeting their space heating (SH) and domestic hot water (DHW) requirements. The buildings in the area primarily date back to the 1950s and have undergone varying degrees of refurbishment. In later stages of the project, the potential of integrating solar photovoltaics on the surrounding buildings for supplying electricity to the central heat pump, as well as the use of thermal storage, may be investigated.

The performance of the heat pump depends on the temperature difference between the heat source (geothermal boreholes) and the heat sink (the DH network). A larger temperature difference leads to lower heat pump performance. Consequently, the supply temperature of the DH network becomes a crucial design parameter with an important impact on overall energy use and energy efficiency. To enhance the performance of the central heat pump, the supply temperature can be reduced. However, this may necessitate the use of decentralized booster units to increase the temperature locally. The following chapters of this study quantitatively analyse and discuss the influence of the supply temperature on the DH network in Ghent.

In this research, a comparison of eight scenarios is conducted by modelling the network in Dymola (Modelica). The influence of the supply temperature on the energy use and energy efficiency is examined for the district heating network in Ghent, where a central heat pump is used as heat source. The network is introduced briefly in Section 1.2. Chapter 2 provides an overview of existing research related to similar district heating networks, the use of geothermal energy for large-scale heat pumps, heat pumps in district heating systems, the integration of electric heaters in district heating, and considerations regarding piping. In Chapter 3, the methodology employed in this research is described, including the investigated scenarios and the parameters used. Chapter 4, is devoted to the description of the models, used for the simulation of the investigated scenarios. In Chapter 5, the results of the simulations are presented, compared and discussed. A sensitivity analysis is conducted in Chapter 6. Finally, the research concludes with Chapter 7, summarizing the findings of the study.

Figure 1.1: Overview of the district heating network in Ghent: the residential dwellings connected to the network (red), the area for geothermal heat extraction (green), the potential for the installation of solar photovoltaics (yellow).

Chapter 2

Literature

2.1 District heating

District heating (DH) consists of a number of buildings or consumers, which are heated by a network of pipes. The piping network contains supply and return pipes which deliver heat for SH, DHW or process heat. Different heat sources can be used in one network including fossil fuels, renewable energy sources (RES), thermal energy storage, HPs and a CHP plant [13]. DH networks are developed to improve the energy efficiency and reduce environmental impact compared to localized boilers by using a central heat production and by distributing to final users [14]. The main advantage compared to conventional, individual heating technologies is the option to decarbonize the heating system by integrating renewable energy sources [3].

2.1.1 Evolution of district heating networks

DH can be classified in multiple generations, according to the operating temperature range. Table 2.1 summarizes the features, improvements and drawbacks of the described generations. The first generation district heating (1GDH) was introduced in the late 19^{th} century and used steam as a heat carrier. The introduction of a DH network offered an opportunity to replace individual boilers, but also introduced the risk of steam explosions. These technologies are now considered outdated, since the high temperature steam networks show a low energy efficiency and substantial losses [4]. The second generation district heating (2GDH), emerging from 1930, used pressurized water (>100°C) for fuel savings. This technology was dominant until 1970, because of the reliable operation and high flexibility [4]. Introduced in the 1970s, the third generation district heating (3GDH) emerged using pressurized water below 100°C for better energy efficiency and security of supply, often in combination with CHP. The insulation cost of the piping system lowered due to lower operating temperatures compared to 2GDH. Most networks throughout the world still use 3GDH [14]. Figure 2.1 illustrates the tendencies towards lower temperatures and increasing use of renewable energy resources.

2.1.2 Low temperature district heating networks

Fourth generation district heating networks

Fourth generation district heating (4GDH) is currently being developed and used in small scale projects [3]. Operating temperatures are lowered to 30-70°C, decreasing the heat losses in the network. Lowering the supply temperature may, on the other hand, increase the mass flow rates, causing increased flow losses. However, Mazhar et al. [3] state that "Contrary to many previous studies that argue that a lower primary temperature results in higher flow rates and pumping expenses, the overall effect is positive, both in terms of power requirements of the auxiliary

Table 2.1: Comparison four generations of district heating.

	1GDH	2GDH	3GDH	4GDH	Ref.
Period of best application	1880-1930	1930-1980	1980-2020	2020-2050	[4]
Heat carrier	Steam	Pressurized hot water	Pressurized hot water	Low-temperature water	[4]
Operating temperatures	>150°C	>100°C	<100°C	30-70°C	[3, 4]
Pipes	Insulated steel pipes	Insulated steel pipes	Pre-insulated steel pipes	Pre-insulated (twin) pipes	[4, 3]
Type of building	Apartments and service sector buildings in urban areas	Apartments and service sector buildings 200-300kWh/m^2	Apartments, service sector buildings and family houses 100-200kWh/m^2	New buildings <25kWh/m^2, existing buildings 50-150 kWh/m^2	[4]
Radiators	High-temperature radiators (>90°C)	High-temperature radiators (90°C)	Medium-temperature radiators and floor heating	Floor heating, low-temperature radiators	[4]
Domestic hot water	DHW tank directly heated with steam	DHW tank heated to 60°C	DHW tank heated to 60°C	Booster unit necessary	[4]
Improvements	Replacement of individual boilers, reduction of risk boiler explosion	Reliable operation, high flexibility, fuel savings	Lower distribution temperatures, security of supply, prefabrication of pipes	Best overall energy efficiency, lower heat losses, lower investment cost, integration of renewable energy sources, possible integration in smart energy systems, use of HP, reduced pipeline thermal stress	[4, 3, 13, 14]
Drawbacks	Low energy efficiency, high heat losses, risk of steam explosions	Low energy efficiency	Difficult integration of renewable sources	Risk of legionella proliferation, hardly applicable for old building stock	[4, 3, 13, 14]

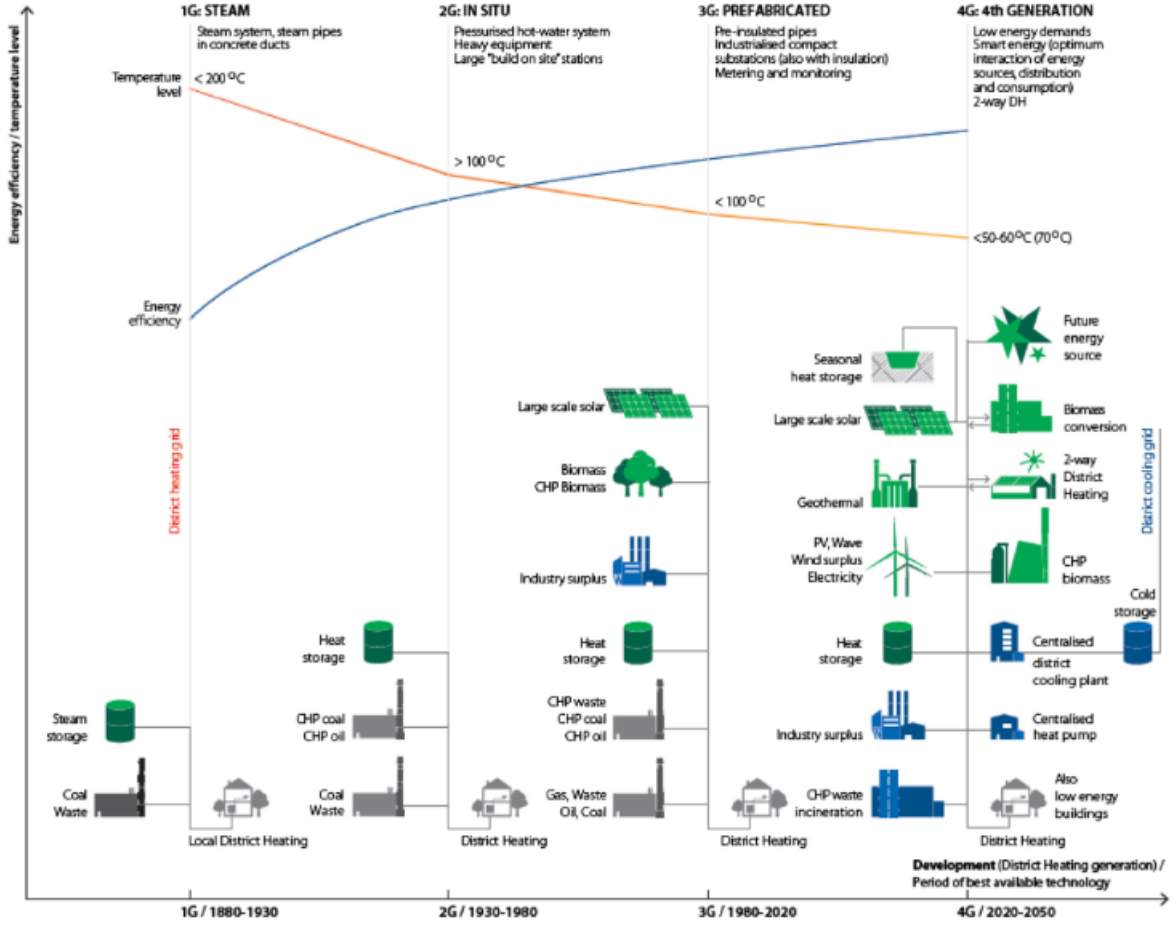

Figure 2.1: Evolution of district heating networks in four generations [4].

equipment and the heat losses". In literature a distinction is made between low temperature district heating (LTDH) with supply temperatures of 50-70°C and ultra-low temperature district heating (ULTDH), operating at <50°C [14]. Lower operating temperatures decrease the investment cost of piping insulation and reduces the pipeline thermal stress [13]. Twin pipes can be introduced, in which the supply and return pipes are embedded in the same insulation material. Low temperatures also offer the opportunity to introduce low grade RES – such as solar or geothermal power – and the use of HPs. The integration of 4GDH in smart energy systems – where gas, electricity and thermal power are combined and controlled – is currently being investigated [4].

Challenges

The use of 4GDH also implies some challenges. An important drawback of 4GDH is the risk of proliferation of legionella in DHW [14]. A supplementary booster unit must be provided to elevate the temperature above 55°C [15]. Another restriction of DH at low temperatures is its limited application in old building stock, where SH requires high supply temperatures. Space heating with 4GDH is mainly done using floor heating or low-temperature radiators in new or newly renovated building with a heat demand of <150kWH/m² [4]. Since most urban areas still have an old building stock, hybrid solutions or suitable temperature regimes are needed.

Future district heating networks

A couple of papers have been published on fifth generation district heating and cooling (5GDHC), but the concept is not defined clearly and differs from paper to paper [16]. Most often mentioned characteristics of 5GDHC are the use of near ground temperature, the combination of heating and cooling, the integration of local waste heat sources and the placement of heat pumps at the end-users [16].

Independent of the used name or concept, there is a clear trend noticeable in the past research into DH systems [3, 4]:

- Decreasing supply and return temperature, reducing heat losses and increasing energy efficiency.
- Increasing use and integration of local RES, low-grade waste heat and decentralised sources in order to decarbonise the heating system.
- Exploring the possible integration in smart energy systems.

2.1.3 Heat demand and temperature regimes

The main limitation of the use of LTDH is the high heat demand in old buildings. Currently 75% of the buildings in the EU are not energy efficient and every year only 1% of the building stock is being renovated [17]. Also the rate of construction of new buildings is estimated to be around 1-3% per year [18]. This means that 85-95% of the EU buildings is expected to be standing by 2050 [19]. In order to increase the energy performance of the European building stock, the Energy Performance of Buildings Directive required that all new building were nearly-zero energy by the end of 2020 and will be zero-emission by the end of 2030 [20]. Future urban areas will therefore unavoidably consist of a mix of old, renovated and new buildings, having different energy performances and heat demands.

Reduction of heat demand

The increase of energy efficiency and the reduction of heat demand focuses mainly on SH. In buildings using floor heating, the supply temperature can be lowered to 35°C [21]. Measures can be taken to lower the heat demand for SH, while the use of DHW stays relatively constant and is primarily dependant on the number of residents [22]. In nearly zero-energy buildings (NZEB), DHW can reach 40-50% of the total energy use [23], and will therefore play an important role in determining the most energy-efficient supply temperature. A NZEB is defined by the European Commission as 'a building that has a very high energy performance, while the nearly zero or very low amount of energy required should be covered to a very significant extent by energy from renewable sources, including energy from renewable sources produced on-site or nearby' [20]. In Flanders, a minimum temperature of 55°C is required to avoid the proliferation of legionella, according to Agentschap zorg en gezondheid [24]. For storage systems of hot water, the temperature of the water needs to be heated above 55°C once a week [15].

Temperature regimes and boosting

Important reasons for lowering the supply temperature are the reduction of heat losses, integration of cost efficient RES, reduced piping insulation and cheaper materials for pipes and other components [25]. Research has been done to investigate the impact of lowering the DH supply temperature on energy efficiency and the role of boosting units such as HPs and electric heaters.

In Table 2.2 an overview is given of previous studies on lowering the supply temperature in DH networks. Köfinger et al. [25] described economically and ecologically optimized concepts for LTDH in four case studies in Austria. The authors conclude that a couple of technical solutions are feasible, including temperature boosting using electric heaters or booster HPs, but LTDH implies higher investment cost on the demand side and the economic performance of LTDH mainly depends on availability and prices of the heat source. The researchers also state that optimum design and opertional strategies highly depend on the local conditions and can not be solved in a generalized way. Ommen et al. [26] investigated the effect of changing the DH temperature in terms of total heat cost for the consumers, carbon emissions and primary fuel consumption. Based on the results, the authors recommended "the use of 65-70 °C as the optimal forward temperature for DH networks, since lower temperatures require high investment, among others DH booster HP units in each dwelling". Elmegaard et al. [27] compared different concepts for SH and DHW in conventional DH and LTDH with both electric heating and HPs. The authors' calculations show that the decrease in heat loss in LTDH does not compensate the electricity demand to cover the electricity consumption of the booster units. Yang and Svendsen [28] investigated the actual performance of a case of ULTDH in Denmark containing a central heat pump and local boosters and compared the performance to medium and low temperature DH supplied by a CHP plant and central heat pump respectively. It seems to be viable to meet the heat demand with supply temperature of 47°C most of the year. Both ULTDH (47°C) and LTDH (55/25°C) show lower heat losses compared to medium temperature DH (70°C/40°C).

Table 2.2: Previous studies on lowering the supply temperature in DH networks.

Reference	T_{supply}	**Central heat source**	**Booster unit**
Köfinger et al. [25]	49°C - 58°C	Return pipe high temperature DH / HP	Electric heater / HP
Ommen et al. [26]	40°C - 110°C	CHP / HP	Booster HP
Elmegaard et al. [27]	45°C - 80°C	CHP	Electric heater/ HP
Yang and Svnedsen [28]	47°C	HP	Electric heater / HP
	55°C	HP	-
	70°C	CHP	-

When lowering the supply temperatures below 55°C, additional boosting units needs to be applied for the preparation of DHW. Several studies have investigated the energetic and economic performance of different lay-outs of booster heat pumps and electric heaters. Zvingilaite et al. [29] analysed the feasibility of a micro heat pump for DHW in LTDH (40°C) and compared the thermodynamic and economic performance of HPs with electric heating. From cost perspective, HP use is not the most beneficial concept under stated technology and energy prices, but the electricity consumption is reduced by more than six times. The cost feasibility is thus highly dependent on the electricity prices, compared to the prices of the district heat. Østergaard and Andersen [30] investigated the optimal use of HPs in DH systems with heating

based on electricity. The researchers compared two alternatives of DH with a central HP, with and without a booster HP. Results show that the primary energy demand is lower using booster HPs compared to individual boilers, individual HPs or DH without boosting. Yang et al. [31] studied the performance of five different configurations of boosting units for DHW in single-family houses supplied with ULTDH. Electric heaters combined with heat exchangers showed better energetic and economical performances compared to heat pumps, which have a higher set-point temperature due to the storage of DHW.

Previous studies show that lowering the supply temperature reduces heat losses, but necessitates a booster unit when temperature requirements for DHW and SH cannot be met. Booster heat pumps offer a good performance, while electric heaters may be more interesting regarding the investment cost. However, the discussed studies assume the DHW temperature requirement is the main limiting factor in lowering the supply temperature. This assumption does not hold true for non-refurbished buildings with radiator heating. Consequently, the conclusions drawn from these studies cannot be directly applied to urban areas with a diverse mix of old, refurbished, and new buildings in their building stock.

2.2 Geothermal energy

By the end of 2021, global renewable generation capacity increased to 3 064 GW, of which the share of solar and wind energy has grown the most [32]. Solar and wind energy mainly produce electricity, which can be used for generating heat by HPs, but suffer from its intermittent character. Geothermal energy on the other hand, is a non-intermittent and largely available source that can be used for both heating and cooling [17]. Geothermal HP systems can contribute to decarbonizing the heating sector, since efficiencies are higher than with traditional combustion based heaters [33] and renewable electricity can be used.

2.2.1 Classification

No universal definition or classification exists since different criteria can be used, such as fluid temperatures, depth of drilling, open or closed systems, horizontal or vertical installation [17, 34]. In this literature review, the classification of Romanov et al. [17] is used, based on fluid temperatures and suitability for different DH generations. Table 2.3 provides an overview of the different geothermal systems.

Table 2.3: Overview of shallow, medium and deep geothermal systems, adapted from [17].

Geothermal system	**Fluid temperature**	**Generation DH**	**Drilling depth**	**SH**	**DHW**
Shallow	<25°C	ULTDH	1.5-150m	HP	HP
Medium	25-90°C	LTDH	150-3000m	HP/HEX/direct	HP/HEX/direct
Deep	>90°C	2GDH/3GDH	>3000m	HEX/direct	HEX/direct

Shallow geothermal systems

Shallow geothermal systems have a drilling depth range of 1.5 m-150 m and deliver low temperature heat [17]. These systems utilize either open or closed loops to extract heat. In an open loop system, local groundwater or surface water is extracted and passed through a heat exchanger to exchange heat. The water is then returned to its source. The advantage of an open systems is the constant supply temperature of the source. However, open loops systems also show some important disadvantages and are often not allowed. Open loop systems have more inherent environmental risks and equipment is more prone to corrosion and fouling [35]. Closed loop systems are commonly used and make use of a heat transfer fluid circulating in a piping system. Heat transfer occurs through the pipe walls [35]. Closed loops can be divided into horizontal and vertical configurations, depending on the installation of the borehole heat exchangers (BHE) [17]. In horizontal systems, BHE are placed parallel with the earth's surface at a depth of 1.5-2 m deep [17]. The installation cost is relatively low, but the proximity of the earth's surface causes a daily and annual variation of the source temperature [36]. In vertical systems, typical drilling depths are between 100 and 150 m for large-scale applications, mostly dependent on local licensing rules [34]. The most common type of borehole lay-out are U-tubes and coaxial tubes [17]. The heat extraction is higher compared to horizontal systems, but drilling cost of the boreholes as well [34]. Consequently, vertical loop systems are more economical for larger applications [35]. Shallow geothermal systems extract low temperature heat and as a consequence require HPs to deliver sufficient heat for SH and DHW. Nevertheless, technologies for shallow geothermal systems are more advanced than medium and deep ones, and more research is done describing optimal design and new materials to increase efficiency [17]. Overall, shallow geothermal systems are characterized by following advantages and disadvantages:

- Advantages: Flexible lay-out, lowest drilling and installation cost, advanced research and increasing performances.
- Disadvantages: Lowest heat output.

Medium-deep geothermal systems

The current situation of medium-deep geothermal systems is described in the work of Romanov et al. [17]. Medium-deep geothermal systems can increase the heat output with drilling depths up to 3 km, which can be advantageous for urban environments with limited space. The heat can be used both directly as indirectly using HPs or heat exchangers (HEX) for SH and DHW. Besides production of heat, medium-deep BHE may also be an attractive solution for thermal energy storage. The main downside of medium-deep systems is the high drilling cost. That is why depleted oil and gas wells could be transformed into BHE, but this is accompanied by hydro-geological, environmental and legal requirements. Currently, there are only a few such systems in the world. The main advantages and disadvantages of medium-deep geothermal systems are listed below:

- Advantages: Higher heat output, possibility for thermal energy storage.
- Disadvantages: Higher drilling costs, environmental and legal constraints.

Deep geothermal systems

Romanov et al. [17] summarizes that deep geothermal energy is mainly interesting because the availability of thermal energy is several orders of magnitude higher compared to the global primary energy use. Electricity can be produced via direct steam, flash or binary cycles or heat

can be produced directly. The use of deep geothermal systems depends on geological conditions, such as boundaries of tectonic plates. The majority of places on earth do not have this favourable conditions, which limits the exploitation of deep geothermal heat. The implementation of deep geothermal heat extraction increases the risk of seismicity, which can lead to hostility and poor social acceptance. Limited available technologies for drilling and high upfront costs form big barriers for the up-scaling of deep geothermal energy. Below, the advantages and disadvantages of deep-geothermal systems are summarized:

- Advantages: High availability of geothermal heat, both electricity and heat production.
- Disadvantages: Seismicity risk, difficult social acceptance, very high drilling costs.

Shallow geothermal energy systems are currently the most developed and suitable option for utilizing DH networks in urban areas. While larger heat output systems are being explored, shallow geothermal systems are the most mature. The low temperature heat can not be used directly and requires additional heat pump technology to raise the temperature to a more practical level.

2.2.2 Variations in ground temperature

Daily and annual fluctuations

Geothermal energy is considered abundant and relatively constant and thus forms and interesting thermal resource. Nevertheless, meteorological conditions such as solar radiation, snow cover, rain, shade and air temperature influence the ground surface temperature [35, 37] and affects the performance of the heat system. The daily variances in meteorological conditions affect the ground temperature to a depth of 0.3-0.8 m [37], while seasonal effects are noticeable up to 10 m of depth [37, 38]. Figure 2.2 shows the annual ground temperature variations at different depths in Ottawa, Canada. The ground temperature range converges as the depth increases. Below the point at which meteorological conditions causes fluctuations, the ground temperature increases with depth at a rate of 30 °C/km, also called the geothermal gradient [37]. In Flanders, the ground temperature at a depth of 5-7 m is in the range of 10-12 °C and stable to use for geothermal heat pumps [39].

Figure 2.2: Annual ground temperature fluctuations at different depths [35, 37].

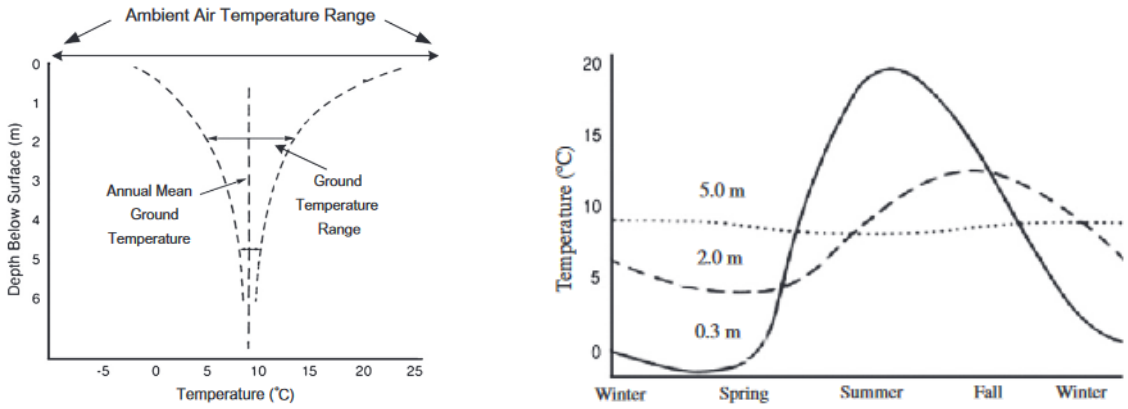

Temperature degradation

Besides the meteorological influences, also ground heat pump systems can alter the ground temperature. According to Li et al. [40] unbalance of heat load can cause the ground temperature to increase or decrease. When the cooling load of buildings is higher in summer than the

heating load in winter, the ground temperature will increase after a long time and the ability of rejecting heat will become worse and vise versa. The researchers showed that in a year when the cooling load was 3.59 higher than the heating load, the ground temperature increased by 1-5 °C compared to the previous year. Moreover, when only extracting heat, after 5 years the ground temperature will be reduced by 6 °C, and when only emitting heat, after 13 years the ground temperature will be over 35 °C. Luo et al. [38] observed the ground temperature decreasing if the thermal imbalance of the heat demand is high and a larger amount of heat is extracted. Duus & Schmitz [41] investigated the effect of changes in operation in order to obtain a efficient and sustainable use of geothermal energy. The researchers state that measurements within the geothermal field show that different effective measures, such as balancing the cooling and heating demand, exist to counteract the energy imbalance and thus a sustainable and energy efficient use of the geothermal energy can be achieved.
The extraction or emission of heat using heat pumps thus causes the increase or decrease of ground temperatures and decreases the system performance. In order to avoid the geothermal field to become unable to use, measures need to be taken to ensure balance between the energy extraction and emission.

2.3 Heat pumps

2.3.1 Role of heat pumps in district heating

Globally, about 10% of the heat demand in buildings is covered by heat pumps [42]. By replacing individual gas boilers by heat pumps, the majority of the current SH and DHW could be met with lower emissions [42]. In combination with DH, HPs offer the opportunity to use excess electricity of RES and waste heat or low-temperature natural heat [13]. From an economic and environmental point of view, LTDH networks using HP technologies are fully competitive. This is not the case for high temperature DH networks, where mainly fossil fuel generation technologies are economically more interesting [13]. Nevertheless, the trend in European DH systems shows a focus on improving efficiency in heat generation and transmission, using of RES and reducing impact on the environment and human health [43].

Technical characteristics and configurations

The heat pump is an efficient technology that achieves high energy efficiency based on thermodynamic cycles. A HP can deliver several units of thermal energy for each unit driving energy [13]. This ratio is called the coefficient of performance (COP), which is often greater than one for heat pumps. In the EU, a large diversity of applications and RES characterise the use of HPs in DH [43]. HPs can be divided is two categories: electrically driven HPs and thermally driven HPs [44]. Electrically driven heat pumps use electricity to drive the compression cycle, based on fossil or renewable resources such as wind turbines or PV panels. Thermally driven heat pumps, on the other hand, use heat or a gas engine to drive the compression cycle. Waste heat from industry or CHP plants can be used. Both types of HPs also have a low grade heat source, which can be ambient air, natural water sources like lakes and rivers, geothermal heat, waste heat etc.

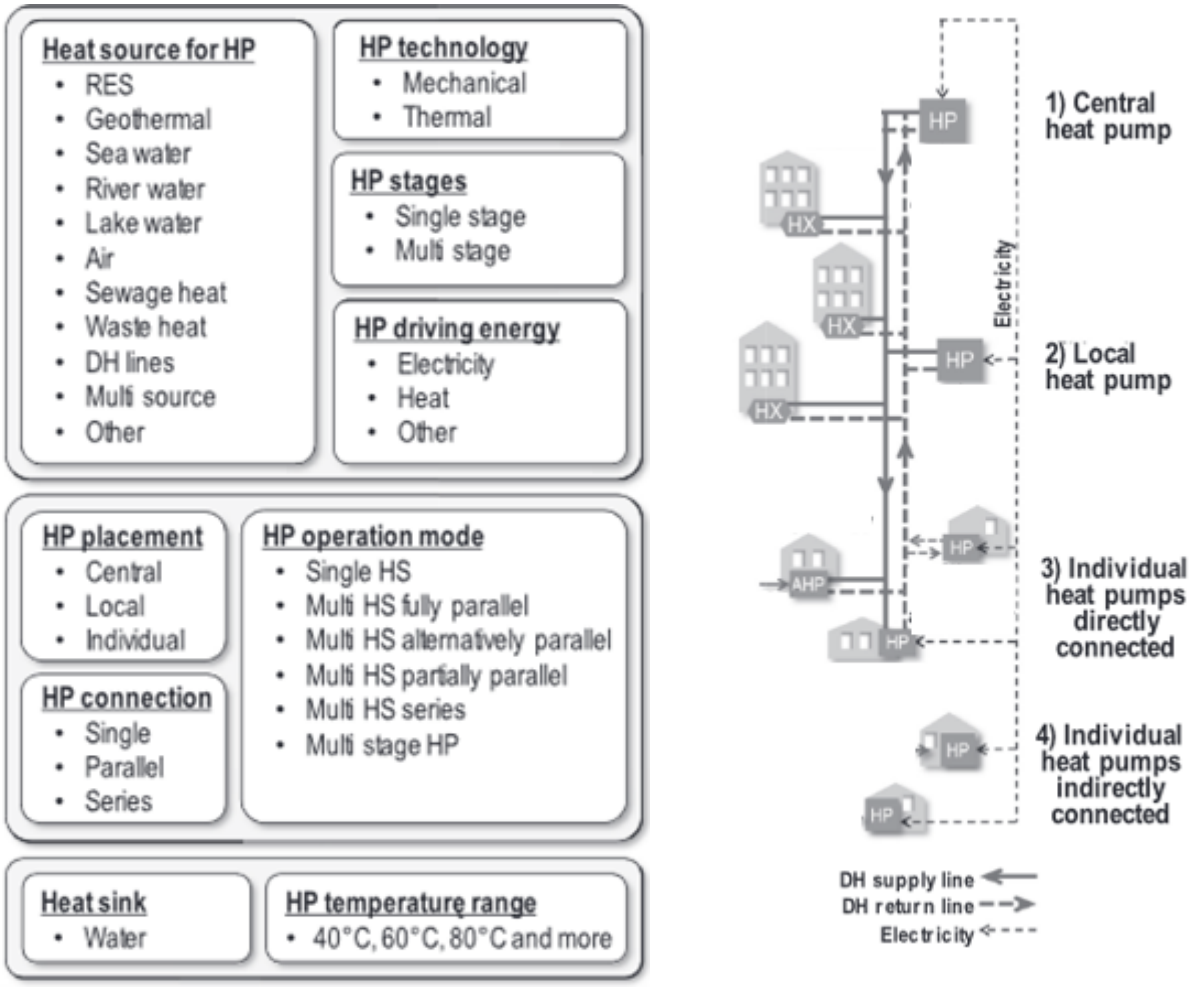

Figure 2.3: Characteristics and configurations of heat pumps in district heating, adapted from [13].

The placement and configuration of the HP strongly depends on the location and ability of the heat source [13]. Figure 2.3 shows four different configurations of HPs in DH networks:

1. A central heat pump requires a high thermal capacity to cover the full heating demand of the DH network. The heat pump forms the power station and can be configured in single or multi-stage, in series or parallel.

2. A local heat pump is placed in the network and depends on local resources. Local heat pumps can have a high or medium heat capacity and can introduce flexibility in the system.

3. Directly connected individual heat pumps are used to integrate RES and make use of the supply or return lines as heat source. Individual heat pumps offer the potential to locally boost the temperature, enabling a reduction of supply temperatures in the DH network.

4. Indirectly connected individual heat pumps are used in buildings which are not connected to the DH network and use local RES.

Improvements

In order to improve HP performance and use in the building sector, the International Energy Agency (IEA) points out in which research domains innovation is needed. The key improvements to be made are [42]:

- System-oriented solutions to optimise the building/district energy use with active control, storage and integration of solar photovoltaics (PVs).
- Compacted integrated solutions of both heat pump and storage.
- Efficiency improvements of buildings.
- Efficient and safe refrigerants with low or zero global warming potential (GWP).
- Improved acoustics and aesthetics.
- Improved drilling techniques to reduce surface footprint of geothermal solutions.

2.3.2 Large-scale central heat pumps

From the 1980s, large-scale heat pumps entered the market to provide heat for DH. David et al. [45] presented a database and status of the technology for applications in Europe. The focus is mainly on electricity driven heat pumps, because the large-scale HPs used excess of electricity of nuclear power and later renewable resources [45]. Large HPs are integrated in the DH system to consume affordable surplus energy and balance the variable electricity production [46]. The HPs in the survey of David et al. [45] achieve COP values between 2.65 and 6.5, with lower COP values for higher output temperatures. In the survey the maximum output temperature ranges from 42 °C to 90 °C. Although the high temperature requirements for DH were considered a barrier for the expansion of the technology [45], installed large-scale heat pumps proved to be able to deliver the required heat for both existing and newly developed DH systems. The trend of decreasing DH supply temperatures is even favourable for the implementation of HPs. Volkova et al. [47] point out that thermal storage is crucial for the reduction of greenhouse gas (GHG) emissions, because it allows HPs to operate when excess electricity of RES is available. The economic feasibility of using large-scale HPs is highly sensitive to electricity and fuel prices [46, 48, 49]. If electricity prises increase compared to fuel price levels, the potential for HPs will decrease and vice versa [48]. The competitiveness of HPs is also highly dependent on taxes and subsidies [49]. Biomass has been heavily subsidised in order to phase out fossil fuels and therefore compete directly against HPs [47]. When electricity prices are high, the heat cost lowers and increase the economic advantage of biomass CHP. Therefore, it is favourable to have both biomass CHP plants as HPs for heat supply [49].

2.3.3 Booster heat pumps

Booster heat pumps are used to increase the temperature of the system locally to provide DHW in LTDH or ULTDH. Booster heat pumps can be placed on the primary or secondary side of the tap water heat exchanger as showed in Figure 2.4a and Figure 2.4b respectively. According to Ommen & Elmegaard [50] a heat pump on the primary side of the tap water heat exchanger is superior in terms of COP and exergy efficiency at almost all temperature configurations of LTDH.
The specific lay-out of the DH booster HP is shown in Figure 2.4c. The inlet of the condenser is connected to the supply line of the DH network. The heated water is stored in a storage tank. Fresh water is heated through a heat exchanger and fed to the sanitary circuit. The heat pump evaporator can be supplied by the DH supply line or the return line of the storage tank/heat exchanger. Zvingilataite et al. [29] state that the option with the DH supply water feeding the

evaporator results in more stable operating conditions, since the temperature of the return line from the heat exchanger can vary, depending on the cold tap water temperature.

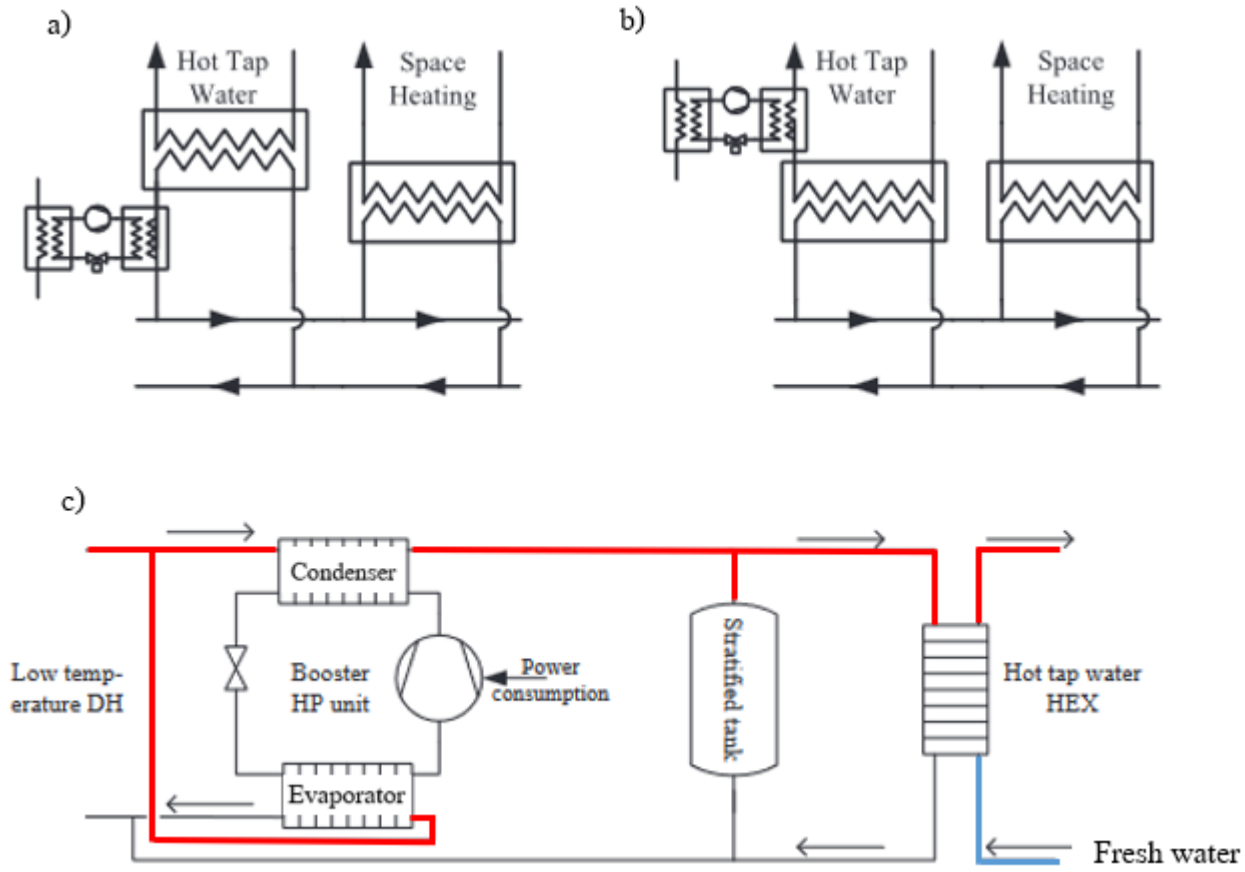

Figure 2.4: Booster heat pump lay out: a) HP on primary side of the heat exchanger b) HP on secondary side of the heat exchanger c) specific lay out booster HP (adapted from [26]).

2.4 Electric heater

In LTDH or ULTDH networks, electric heaters are often mentioned to provide elevated temperatures for DHW. The main reason for choosing electric heaters over booster HPs is the lower investment cost and simpler design, although electricity consumption is expected to be higher [29]. Therefore a trade-off exists between cost for the end-user and energy efficiency. Elmegaard et al. [27] compared different concepts for SH and DHW with conventional district heating with CHP. Results show that electricity consumption is highest when using a electric heater. Lund et al. [51] compared LTDH without any form of boosting with two scenarios of ULTDH with an electric heater and a booster HP. The authors found that capacity investments keep on decreasing with decreasing DH temperature as long as no booster element is needed. They state that even if the investments costs of LTDH and ULTDH would be the same, a larger investment in terms of building refurbishment is necessary to be able to implement ULTDH.
Although boosting is found to be not economically interesting at the moment, there is a trend towards lowering DH temperatures and electric heaters have been investigated for the purpose of DHW preparation. Zvingilaite et al. [29] proposed three different configurations using electric heating and a hot water storage tank. The set up using a storage tank which is preheated by the DH water and further heated by an immersed electric heater (Figure 2.5a) showed lowest

yearly costs compared to the other electric heater configurations and a scenario with booster HP. But the authors also note that the electricity consumption is 6 times higher than with a HP, increasing the importance of electricity prices. Yang et al. [31] on the other hand concluded that an in-line heater as supplementary heating device (Figure 2.5b) shows better energetic and economic performances compared to other configurations including a HP. The researchers state that the use of thermal energy storage requires more heat due to heat losses, which results in lower energy efficiency.

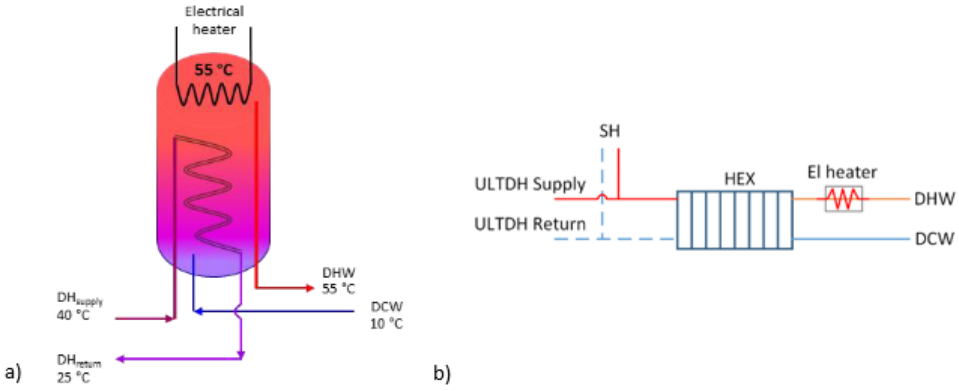

Figure 2.5: Best performing electric heater lay-out according to a) Zvingilaite et al. [29]: DH water flows through a coil and DHW is further heated up by an electrical heater installed in the tank and b) Yang et al. [31, 52]: DHW is heated by an instantaneous in-line HEX without storage.

The choice between electric heaters and booster HPs is mainly dependent on the choice between investment cost for the end user and energy efficiency. Electric heaters are simpler and require less investment costs, but often consume more electricity to provide DHW.

2.5 Piping

DH consists of a large amount of pipes distributing heat to multiple users. Optimization of design and pipe lay-out can not be overlooked, since distribution losses are usually in the range of 10-30 % [14] of the total delivered energy by the central heat source and circulation pumps. Distribution losses consist of heat losses, pressure losses and leakages. According to Mazhar et al. [3] heat losses are a major source of loss compared to flow losses. Heat losses usually are in the range of 5-20 % of the delivered energy, flow losses are in the range of 100-250 Pa/m [3]. Heat losses mainly depend on length of the transmission line, insulation and material of the piping, and external conditions such as ground temperature and meteorologic factors.
The reduction of DH supply temperature aims to lower the distribution heat losses in the network, but also benefits the use of other piping material or configuration. 3GDH made use of pre-insulated steel pipes directly buried into the ground [16]. In 4GDH, lower DH supply temperatures offer the possibility of using cheaper materials for pipes such as plastic, using twin pipes and decreasing insulation thickness and costs [3, 14]. In papers discussing 5GDHC, pipes are often not insulated at all since supply temperatures are close to ground temperature [16].
In order to decrease investment cost of piping and heat losses the type, insulation and dimensions of the pipe should be chosen with care. One of the most substantial parameters of a DH design is the selection of pipe diameters to minimize the investment cost and heat losses [53]. Pipe diameters are determined by maximal peak pressure drop or mass flow rate [53]. To minimize heat losses, insulation thickness can be increased, but results in higher investment costs [53].

According to Mazhar et al. [3] twin-pipes should be applied wherever possible since they show best performance to price ratio.

2.5.1 Pre-insulated, twin and triple pipes

Current DH networks mainly use pre-insulated pipes, but more improved concepts such as twin-pipes and triple-pipes are entering the market or being investigated in literature. In a network using pre-insulated pipes, one pipe is used for the supply of water and one for the return, as can be seen in Figure 2.6a. Different types of insulation are used such as PUR, PUR plus and PEX [54]. In twin pipes both supply and return pipes are embedded in the core of a larger casing filled with insulation to reduce heat losses [55], as in Figure 2.6b. Nowak-Oclon & Oclon [54] presented an economic analysis of a modern heating network using pre-insulated pipes and twin-pipes. The authors concluded that twin-pipes have a higher investment cost, but obtained the lowest heat loss, and thus were more cost-effective compared to the studied pre-insulated pipes. The results also show that the use of PEX insulation is economically more beneficial than PUR insulation. Khosravi & Arabkoohsar [56] investigated the compatibility of twin-pipes with ULTDH and LTDH and concluded that twin-pipes fit both systems, but that there is space for improvement of the insulation material.
The concept of triple pipes is introduced in literature, but is not commercially available [55]. The idea is to integrate a smaller secondary supply line to provide DHW at higher temperatures or for during demand peaks, as in Figure 2.6c. The return pipe has the largest cross-section, which is the sum of the two supply pipes [57]. Arabkoohsar et al. [57] compared the use of triple pipes to twin pipes based on existing DH temperatures for SH and DHW. The authors showed that triple pipes with DHW and SH supply lines could perform better in terms of thermal performance.

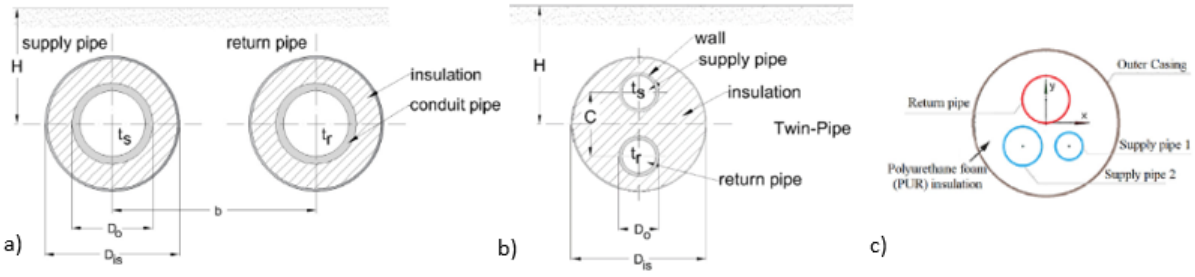

Figure 2.6: Piping cross-section: a) Pre-insulated pipes b) Twin pipes c) Triple pipes (adapted from [54, 55]).

For the current LTDH networks, pre-insulated pipes or twin pipes will probably be most interesting in terms of cost and thermal performance. When DH supply temperatures are lowered to ground temperature and DHW booster units are used, thermal performance looses importance and investment cost of piping will probably be a more important parameter. From that perspective, it can be questioned whether triple pipes have a role in that scenario.

2.6 Literature gap

Numerous studies have focused on DH systems examining the impact of reducing the supply temperature and have proposed suitable booster units to locally raise the temperature if necessary. Some studies have explored the use of DH networks with a central heat pump as the heat source, but only in combination with buildings where the temperature requirement for DHW is the primary factor limiting the reduction of the supply temperature.

However, this particular study takes into account a DH network in an urban neighbourhood comprising of non-refurbished and refurbished buildings, which is a common scenario in cities. In non-refurbished buildings, the supply temperature for radiators imposes a lower limit on the network supply temperature. As a result, the temperature at which a booster unit becomes necessary is elevated. Therefore, this study aims to investigate the influence of the supply temperature and booster unit on the performance of the central heat pump and the overall network for both refurbished and non-refurbished buildings.

Chapter 3

Methodology

For the DH network in Muide-Meulestede (Ghent) a suitable solution is required to provide SH and DHW by means of a central heat pump. The aim of this research is to provide a comparative study for this DH network on different temperature regimes in terms of primary energy use and energy efficiency. The choice of supply temperature in the DH network is influenced by the temperature requirements for SH and DHW, which are determined by the state of the building and their suitability for different technologies. To this end, eight scenarios are chosen and modelled for comparison, as shown in Table 3.1. In this chapter, the importance of the parameters used in the scenarios is discussed in Section 3.1, and the eight scenarios are explained in Section 3.2. The topology and size of the DH network is discussed in Section 3.3. In Section 3.4, the buildings and the booster technologies are described.

3.1 Parameters

3.1.1 Supply temperature

Depending on the central heat source and the temperature requirements of the buildings, the possible network supply temperature differs [51, 58]. In the case of Muide-Meulestede (Ghent), a central heat pump is used to provide heat for the network. Higher supply temperatures will decrease the performance of the central heat pump and increase the heat losses in the distribution network [30, 59]. On the other hand, the heat requirements of the buildings for SH and DHW will impose a lower limit on the supply temperature at which a booster technology is needed [30]. Therefore, different supply temperatures can be found in literature and case studies, ranging from 10 °C to 90 °C [25, 27, 30, 33, 53, 60, 61].

3.1.2 Space heating

The two considered SH technologies are radiators and underfloor heating. For radiators, the supply temperature is estimated to be 65 °C, with a temperature drop of 20 K [27, 62], whereas for underfloor heating, a supply temperature of 35 °C and a temperature drop of 10 K is assumed [27, 62]. Depending on the supply temperature of the network, a booster technology may be required to ensure sufficient heating capacity. Two alternative booster technologies are proposed in this study. Firstly, an electricity-driven water source heat pump is proposed as an alternative for an individual air source heat pump or ground water heat pump with individual boreholes. The booster heat pump is connected to the DH network at one side and to the SH circuit at the other. For remainder of this study, the DH network will be referred to as the primary side, while the circuits within the buildings will be referred to as the secondary side. The connection to the DH network eliminates the need for both an outdoor unit and an indoor unit, making it more favorable than installing an individual air source heat pump. Additionally, the connection to the DH network provides the possibility to utilize geothermal

energy as a heat source, eliminating the need for individual boreholes, especially in urban areas where space is limited. Secondly, an electric heater or electric boiler can be utilized as a booster technology during peak demand to increase the temperature of the radiator supply, and serves as an alternative for heating with natural gas or fuel oil. Although the heat pump is likely to outperform the electric heater in terms of electricity consumption, the investment cost for the former may be higher and is therefore included in the comparison.

3.1.3 Domestic hot water

The required temperature for DHW used in the kitchen and bathroom is 45 °C [50, 51, 52]. However, to prevent the growth of legionella bacteria, the stored DHW temperature should be occasionally elevated to 55 °C [31, 15, 24]. Depending on the DH network supply temperature, cold tap water at 10 °C is heated directly via a heat exchanger, or boosted by a heat pump or electric heater. This can be done either solely for DHW or in combination with hot water for SH.

3.1.4 State of the building

The state of a building and its level of insulation affect the heat demand and the most suitable heating technology to be employed. According to Zhang et al. [63], increasing insulation thickness in a building reduces heat losses, thereby lowering the heat demand when the occupants' behavior remains unchanged. On the other hand, it can be shown that by insulating a building, occupants tent to heat more rooms and prefer a higher level of comfort. Heat demand is thus not necessarily lower after refurbishment. This phenomenon is also called 'the rebound effect' [64]. The available heating technology is influenced by the building's heat demand and the state of the building [4]. In non-refurbished buildings, SH with radiators (65 °C) is more common, while underfloor heating (35 °C) and low-temperature radiators (50 °C) are more likely to be found in refurbished or new buildings.

3.2 Investigated scenarios

To analyze the energy efficiency and primary energy use of a DH network, which comprises a central heat pump and 35 houses, eight scenarios were proposed, simulated, and compared. These scenarios, presented in Table 3.1, are divided into four with non-refurbished buildings and four with refurbished buildings with varying network supply temperature. The non-refurbished buildings, depicted in scenarios 1 to 4, employ radiators with a supply temperature of 65 °C. On the other hand, the refurbished buildings in scenarios 5 to 8 use underfloor heating with a supply temperature of 35 °C. A booster unit is necessary for DHW, SH or both, based on the DH network temperature. The booster unit can be a heat pump or electric heater. The subsequent section explains the configuration of each scenario.

Scenario 1: non-refurbished, 75 °C, no booster

Scenario 1 employs a high network supply temperature of 75 °C and does not require booster technology. A schematic overview is given in Figure 3.1. In this scenario, a heat exchanger is used to heat water for SH and DHW purposes. Control valves, for both SH and DHW, regulate the amount of water extracted from the DH network to achieve the desired temperature.

Table 3.1: Investigated scenarios.

	State of the building	Network temperature	Booster technology		Booster technology use	
			Heat pump	*Electric heater*	*Domestic hot water*	*Space heating*
1	Non-refurbished	75 °C				
2	Non-refurbished	55 °C	X			X
3	Non-refurbished	55 °C		X		X
4	Non-refurbished	45 °C	X		X	X
5	Refurbished	55 °C				
6	Refurbished	45 °C	X		X	
7	Refurbished	45 °C		X	X	
8	Refurbished	10 °C	X		X	X

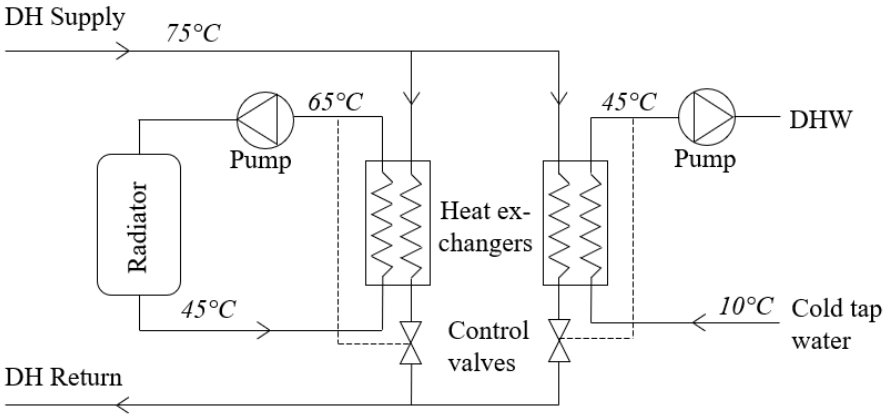

Figure 3.1: Schematic scenario 1: non-refurbished, 75 °C, no booster.

Scenario 2: non-refurbished, 55 °C, booster HP for SH

The network temperature in scenario 2 is lowered to 55 °C , which necessitates the use of a booster unit to fulfil the SH requirements. Figure 3.2 presents a schematic overview of scenario 2. A booster heat pump is used to elevate the temperature in the radiator circuit to 65 °C. The HP evaporator side is connected to the DH network. A control valve regulates the mass flow through the heat pump to achieve a DH return temperature of 25 °C. Similar to scenario 1, DHW preparation is carried out using a heat exchanger.

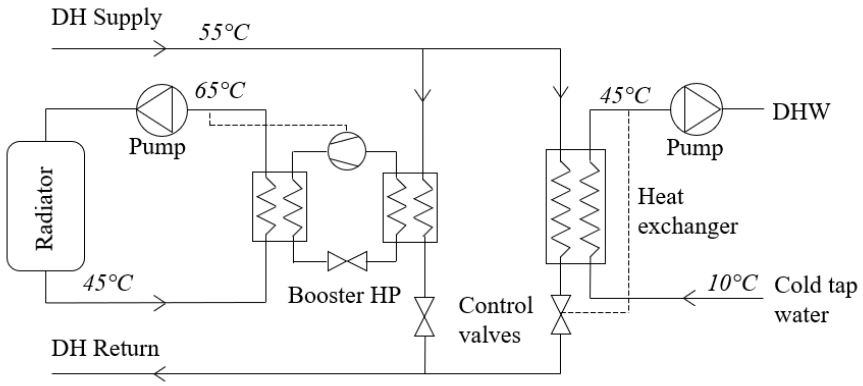

Figure 3.2: Schematic scenario 2: non-refurbished, 55 °C, booster HP for SH.

Scenario 3: non-refurbished, 55 °C, booster electric heater for SH

In scenario 3 the same network conditions as in scenario 2 are maintained, but an electric heater is employed to increase the radiator supply temperature. Figure 3.3 provides a schematic overview of scenario 3. The DH network connection is used to preheat the water in the radiator circuit to 47 °C via a heat exchanger. The resistive heater in the storage tank elevates the radiator supply temperature to 65 °C. DHW preparation is conducted through a heat exchanger, similar to scenarios 1 and 2.

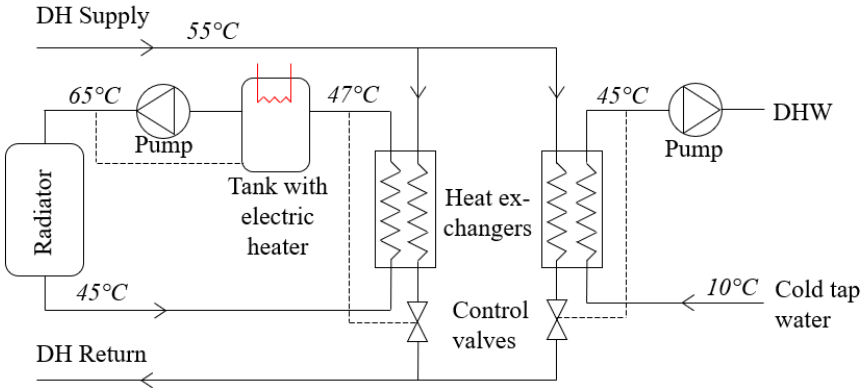

Figure 3.3: Schematic scenario 3: non-refurbished, 55 °C, booster electric heater for SH.

Scenario 4: non-refurbished, 45 °C, booster HP for SH and DHW

Scenario 4 involves a DH network temperature that is insufficient to elevate the cold tap water to 45 °C via a heat exchanger. Therefore, a heat pump is utilized to increase the temperature for both SH and DHW purposes. The schematic overview of scenario 4 is presented in Figure 3.4. The heat pump condenser temperature is set to 65 °C to fulfil the requirements of the radiator circuit. For DHW preparation, a storage tank with internal heat exchanger is employed. As the tap water is stored, the storage tank temperature must occasionally reach 55 °C to prevent legionella growth. A control valve regulates the mass flow from the heat pump to maintain the storage tank temperature between 45 °C and 55 °C.

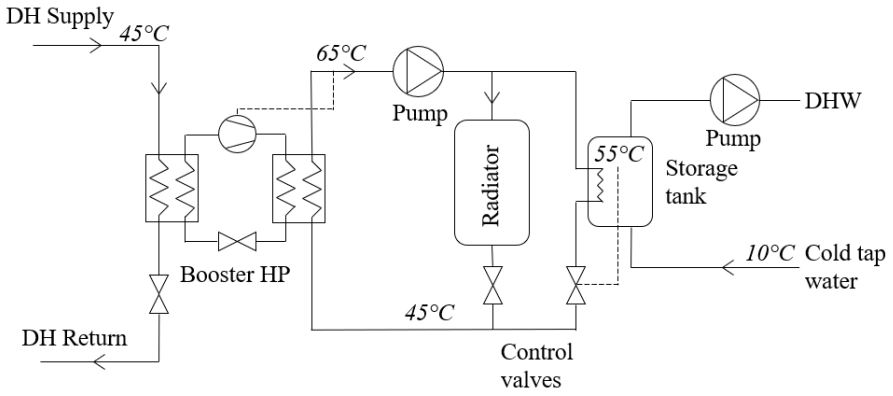

Figure 3.4: Schematic scenario 4: non-refurbished, 45 °C, booster HP for SH and DHW.

Scenario 5: refurbished, 55 °C, no booster

Since scenarios 5 to 8 involve refurbished buildings, the SH temperature requirements are reduced to 35 °C. As a result, with a DH network temperature of 55 °C, no booster unit is required. Figure 3.5 provides a schematic overview of scenario 5. Heat is exchanged from the network via heat exchangers, similar to scenario 1. Control valves regulate the DH mass flow the through the substation.

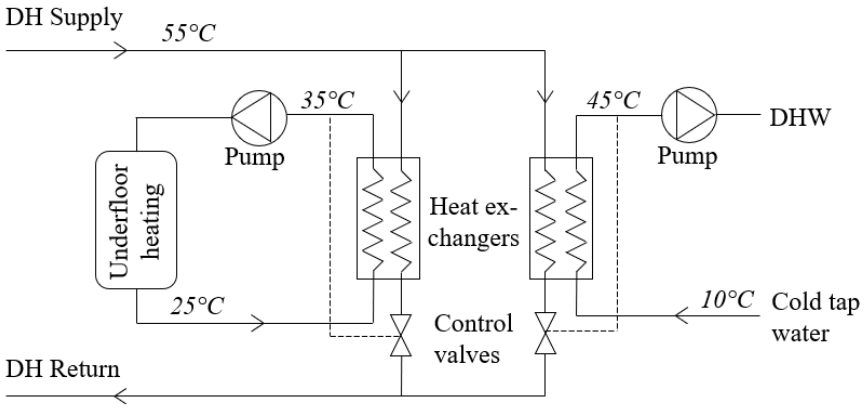

Figure 3.5: Schematic scenario 5: refurbished, 55 °C, no booster.

Scenario 6: refurbished, 45 °C, booster HP for DHW

Scenario 6 utilizes a booster heat pump for DHW preparation, since the DH network temperature is lowered to 45 °C. Figure 3.6 displays a schematic overview of scenario 6. The cold tap water is heated in the storage tank with an internal heat exchanger. A hystersis control loop is used to regulated the power of the heat pump, based on the temperature of the water in the storage tank. To elevate the temperature of the water in the underfloor heating circuit, heat is exchanged from the network with a heat exchanger, similar to scenario 5.

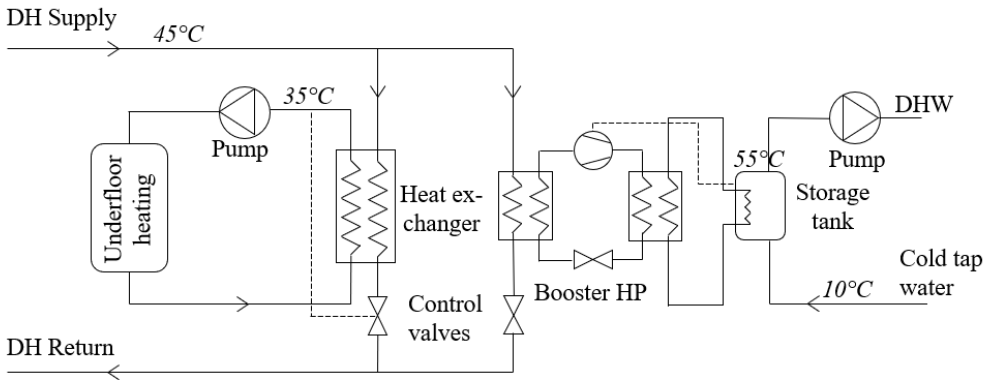

Figure 3.6: Schematic scenario 6: refurbished, 45 °C, booster HP for DHW.

Scenario 7: refurbished, 45 °C, booster electric heater for DHW

Scenario 7 is similar to scenario 6, except for the DHW preparation. Figure 3.7 shows a schematic overview of scenario 7. Instead of a heat pump, an electric heater is used to heat the cold tap water, which is preheated by the DH network. The water is stored in a tank and heated further by the electric heater. To prevent the growth of legionella, the temperature in the tank is raised to 55 °C. The underfloor heating circuit is heated by the DH network via a heat exchanger. Control valves regulate the mass flow through the primary side of the heat exchanger to ensure that the desired temperature is reached at the secondary side.

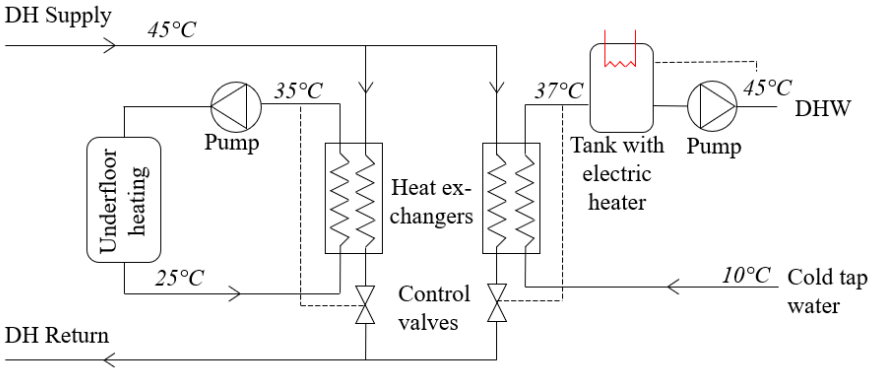

Figure 3.7: Schematic scenario 7: refurbished, 45 °C, booster electric heater for DHW.

Scenario 8: refurbished, 10 °C, booster HP for SH and DHW

In scenario 8, the DH network temperature is not increased by a central heat pump. Instead, the DH network temperature is the same as the borehole water temperature, which is 10 °C. As a result, a booster heat pump is needed in the substations to raise the temperature for SH and DHW. A schematic overview of scenario 8 is presented in Figure 3.8. To ensure the temperature of the DHW storage tank reaches 55 °C at certain moments, the heat pump condenser temperature is set to 55 °C. Mass flow rate from the heat pump is controlled by control valves.

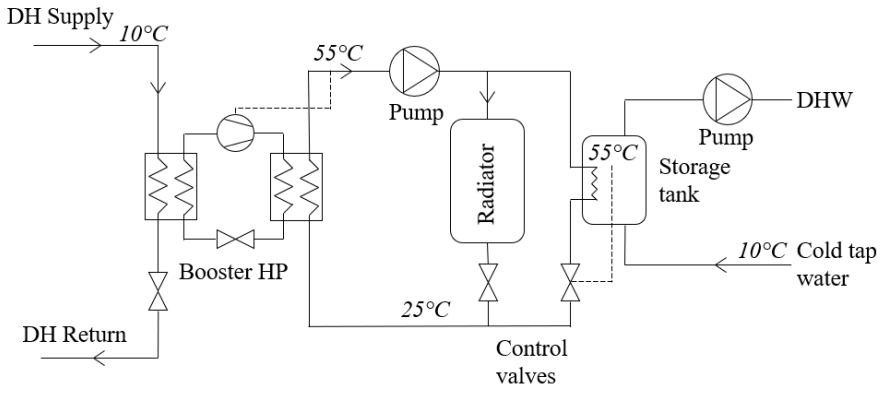

Figure 3.8: Schematic scenario 8: refurbished, 10 °C, booster HP for SH and DHW.

3.3 District heating network

In this section the topology and components of the DH network are discussed. The dimensions of the components are used in the models in Chapter 4. An overview of the assumptions made in this section can be found in Table 3.2.

Table 3.2: Assumptions for the sizing of the components in the distribution network.

Variable	**Symbol**	**Assumption**	**Ref.**
Operating pressure distribution network	p_{dist}	6 bar	[65]
Pressure drop over substation	Δp_{sub}	0.5 bar	[66, 67]
Pressure drop	$\Delta p/l$	300 Pa/m	[68]
Pipe roughness	ϵ	0.007 mm	[65]
Pinch point temperature HEX	ΔT_{HEX}	8 K	[29, 30, 50, 69]
Heat exchanger effectiveness	ε	0.8	[70]
Soil temperature	T_{soil}	10 °C	[65]
Pipe depth	-	0.8 m	[65]

3.3.1 Network topology

The topology of the network is shown in Figure 3.9 [71]. Geothermal energy is extracted centrally with boreholes of 150m depth under the parking lot of the football club. The water is transported to the neighbouring building, where a technical room is provided for the central heat pump. The network forms a circular loop along the backyards of the buildings. The total length of the ring is 290m and has 35 connection points. The supply pipe starts at the central heat pump and stops at the last customer. The return pipe starts at the first customer and

ends at the central heat pump. The supply pipe line consists of a segment from the heat pump towards the first consumer of 20 m and 34 segments between the consumers of 5 m each. The return pipe line consists of 34 segments between the customers of 5 m each and a segment towards the central heat pump of 100 m. In a ring topology the total pipe length is the same for every customer, resulting in equalised pressure differences between supply and return pipes. This makes it easier to control a system with a ring topology compared to a branched or linear topology [72].

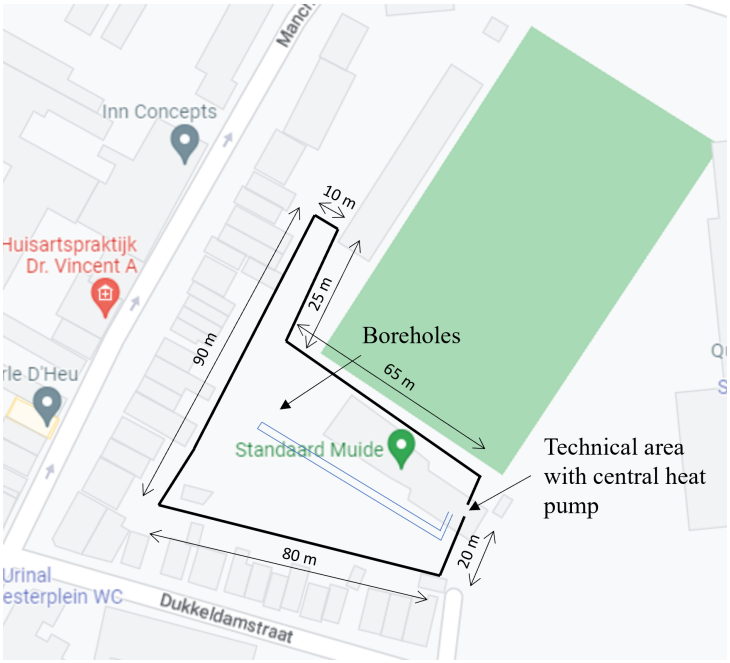

Figure 3.9: Overview of the network topology, adapter from [71].

3.3.2 Sizing of the network

This section discusses the sizing of components in the distribution network. It is important to note that the design of the network is not optimized as the scope of this work does not include design optimization. Therefore, decisions and calculations are made based on recommendations from existing research or available data provided by manufacturers. A summary of all assumptions made in the following calculations is provided in Table 3.2, and the chosen dimensions will be used in the models discussed in Chapter 4.

Pipe diameter

The distribution network starts at the central heat pump and transports the hot water towards all substations. It is assumed that the distribution network consists of pre-insulated Flexstar UNO® single pipes of BRUGG Pipes®[65]. Pipe dimensions, roughness and heat transfer coefficients are provided by the manufacturer. The data sheet can be found in Appendix A.1. The pressure of the piping network is set to 6 bar, according to the operating pressure of pre-insulated Flexstar UNO pipes [65]. The diameter of every pipe segment is calculated with the Darcy-Weisbach equation, as seen in Equation 3.1.

$$D = \sqrt[5]{\frac{8 f \dot{m}^2}{\frac{\Delta p}{l} \rho \pi^2}} \tag{3.1}$$

Where D is the pipe diameter [m], f is the Darcy friction factor [-], $\dot{m}$ is the maximum mass flow rate [kg/s], Δp/l is the pressure drop [Pa/m] and ρ is the density of the fluid [kg/m^3]. According

to Best et al. [68], total distribution cost is lowest when designing the network with a maximum pressure drop of 300 Pa/m. The Darcy friction factor is calculated with the Haaland equation [73]. The Haaland equation is expressed in Equation 3.2 and is an approximation of the implicit Colebrook-White equation [74] and allows to calculate the friction factor directly.

$$\frac{1}{\sqrt{f}} = 1.8log\left(\left(\frac{\epsilon/D}{3.7}\right)^{1.11} + \frac{6.9}{Re}\right) \tag{3.2}$$

Where f is the Darcy friction factor [-], ϵ is the roughness of the pipe [m], D is the diameter of the pipe [m] and Re is the Reynolds number [-]. The maximum mass flow rate is determined iteratively for every pipe segment. Pipe diameters are chosen according to the available pipe dimensions in the datasheet of the manufacturer. The resulting pipe dimensions can be found in Appendix B.

Heat losses

To calculate heat losses in the piping network, the heat transfer coefficient provided by the manufacturer is used [65], as displayed in Table 3.3. The inner tube of the selected pipes is made of PEX. The pipes are equipped with insulation comprising of a PUR foam, a PE foil, and an LLD-PE casing, as illustrated in Figure 3.10. The soil temperature is assumed to be 10 °C, and the pipes are buried at a depth of 0.8 m. Table 3.3 shows the available pipe dimensions and corresponding heat transfer coefficients. Heat losses in the distribution network are calculated according to Equation 3.3.

$$\dot{Q} = U \cdot l \cdot (T_{water} - T_{soil}) \tag{3.3}$$

Where $\dot{Q}$ is the heat lost to the environment [W], U is the heat transfer coefficient [W/mK], l is the pipe length [m], T_{water} is the temperature of the water in the pipe and T_{soil} is the soil temperature [K].

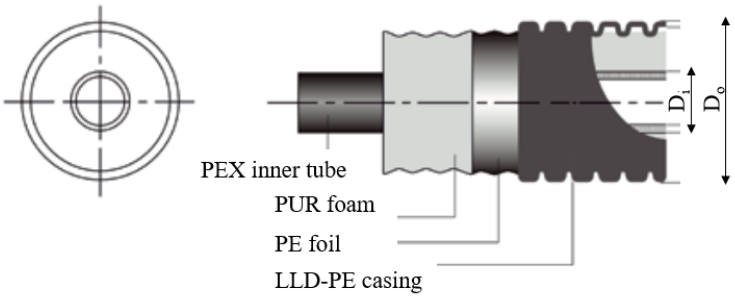

Figure 3.10: Pipe insulation layers (adapted from [65]).

Table 3.3: Pipe inner and outer diameter and heat transfer coefficient.

D_i **[mm]**	D_o **[mm]**	$U[W/mK]$
25	70	0.1470
32	70	0.1940
40	90	0.1880
50	90	0.2600
63	105	0.2890

Heat exchanger

A constant heat exchancher pinch point temperature of 8 K is assumed, as applied by Zvingilaite et al. [29], Ostergaard & Andersen [30], Ommen & Elmegaard [50] and Ochs et al. [69] to determine the required DH network temperature. In the scenarios described in Section 3.2, a temperature difference between the DH network and the required temperature in the DHW or SH circuit of 10 K is assumed (instead of 8 K) to account for potential temperature drops at the end of the DH supply line. The used heat exchanger model in Dymola is however characterized by the heat exchanger effectiveness, according to Equation 3.4 to 3.7.

$$\dot{Q}_{max} = C_{min} \left(T_{hot,in} - T_{cold,in}\right) \tag{3.4}$$

$$C_{min} = min \left(\dot{m}_{cold} c_{p,cold}, \dot{m}_{hot} c_{p,hot}\right) \tag{3.5}$$

$$\dot{Q}_{actual} = \dot{m}_{cold} c_{p,cold} \left(T_{cold,out} - T_{cold,in}\right) \tag{3.6}$$

$$\varepsilon = \frac{\dot{Q}_{actual}}{\dot{Q}_{max}} \tag{3.7}$$

where $\dot{Q}$ is the transfered heat [W], $\dot{m}$ is the mass flow rate [kg/s], c_p is the specific heat capacity [J/kg/K] and ε is the heat exchanger effectiveness [-]. Typical effectiveness of a plate heat exchanger is 70% to 90% in counter-flow mode according to [70]. In this work, an effectiveness of 80% is assumed for all heat exchangers which connect the DH network with the substation. The assumption of a constant pinch point temperature will thus not hold true in the simulations.

Circulation pump

A circulating pump is used to maintain a constant pressure of 6 bar. To select a suitable pump, the flow rate and differential pressure are required. The differential pressure is calculated according to Equation 3.8

$$\Delta p_{diff} = \Delta p_{fric} + \Delta p_{sub} \tag{3.8}$$

where Δp_{fric} is the actual friction loss [Pa] in the supply and return pipes according to Equation 3.1 and Δp_{sub} is the pressure drop over the substation [Pa], which is assumed to be 0.5 bar [66, 67]. The pressure loss over the substation includes the pressure loss over the heat exchanger, the control valves and bends. The maximum pressure drop over the pipes, with a design of 300 Pa/m and a total length of 290 m, is 0.87 bar. This results is a total differential pressure of 1.37 bar or or a head of 13.98 m. The maximum flow rate is determined iteratively by simulating the model and observe the maximum flow rate for every scenario. The maximum flow rate ranges from 1.4 kg/s (5.0 m^3/h) in scenario 3 to 7 kg/s (25.2 m^3/h) in scenario 8. Figure 3.11 displays the operating range of Wilo Stratos MAXO® pumps, of which the performance maps are implemented in the IDEAS library in Dymola.

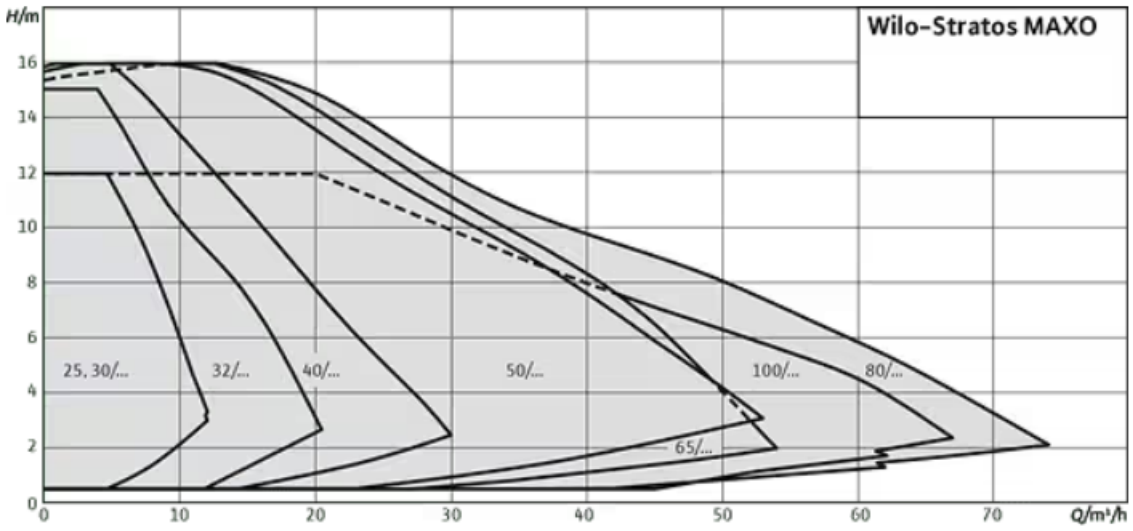

Figure 3.11: Operating range Wilo Stratos Maxo pumps [75].

The available performance maps in Dymola are limited to the pumps which deliver a head of 12 m. As a consequence, two pumps in series are needed to deliver the required pressure increase. Depending on the maximum mass flow rate, two pumps are chosen, as presented in Table 3.4. The data sheets can be found in Appendix A.2-A.6.

Table 3.4: Circulation pumps.

Scenario	Pump selection
1	Stratos MAXO 25/0,5-8 + Stratos MAXO 32/0,5-12
2	Stratos MAXO 25/0,5-8 + Stratos MAXO 30/0,5-12
3	Stratos MAXO 25/0,5-8 + Stratos MAXO 30/0,5-12
4	Stratos MAXO 32/0,5-8 + Stratos MAXO 40/0,5-12
5	Stratos MAXO 25/0,5-8 + Stratos MAXO 30/0,5-12
6	Stratos MAXO 25/0,5-8 + Stratos MAXO 30/0,5-12
7	Stratos MAXO 25/0,5-8 + Stratos MAXO 32/0,5-12
8	Stratos MAXO 40/0,5-8 + Stratos MAXO 50/0,5-12

Central heat pump

Since the penetration of large-scale heat pumps in the market in very low and performance data is often not made available by the manufacturer, Jesper et al. [76] developed a series of HP performance correlations that estimate the COP for a range of different temperature lifts based on real-world data. The recommended empirical expression in the study of Jesper et al. is used to estimate the COP of the central heat pump in this study. The expression is given in Equation 3.9.

$$COP = a\,(\Delta T_{lift} + 2b)^c\,(T_{h,out} + b)^d \tag{3.9}$$

Where COP is the coefficient of performance [-], ΔT_{lift} is the temperature difference [K] between evaporator inlet and condenser outlet temperature and a, b, c and d are fit parameters. The fit parameters are $a = 1.4480 \cdot 10^{12}$, $b = 88.730$, $c = -4.9460$, $d = 0.0000$. The ground water extracted via the geothermal boreholes is assumed to be 10 °C [39]. The lift temperature can be calculated as the difference between the desired network temperature and the temperature of the ground water. The resulting COP values are shown in Table 3.5.

Table 3.5: COP central heat pump.

Network temperature	**75 °C**	**55 °C**	**45 °C**
COP central heat pump	2.32	3.56	4.47

3.4 Buildings and occupants

In this section, the buildings and occupants are explained in more detail. The heat demand profiles for SH and DHW are discussed as well as the booster heat pump and booster electric heater.

3.4.1 Occupants

The number and type of occupants has an influence on both the DHW and SH demand. Five different categories are selected and distributed over the 35 buildings. The five different categories are listed in Table 3.6, where FTE = full time employed, PTE = part time employed, School = children living full time at home, Student = children living only during the weekends at home, Retired = always at home. All categories are included 7 times in the network.

Table 3.6: Occupant categories.

Category	**Occupants**
1	FTE, FTE, School, School
2	FTE, PTE, School
3	Retired, retired
4	FTE, FTE, School, Student
5	FTE, FTE

3.4.2 Space heating demand profile

Space heating demand profiles are generated according to the approach described in the Bundesverband der Energie- und Wasserwirtschaft (BDEW) guideline [77]. An hourly distribution of the SH demand of a single family house is generated, based on the annual heat demand of the building and weather data of Ghent of 2019 [78]. The heat demand is calculated according to Equation 3.10.

$$\dot{Q}(\theta) = KW \cdot h(\theta) \cdot F \cdot SF \tag{3.10}$$

Where $\dot{Q}$ is the heat demand in [W], θ is a daily mean temperature, KW is the daily consumption of a customer at 8 °C, h is a value depending on the daily mean temperature, F is a factor depending on the day of the week and SF is a factor depending on the hour. The daily mean temperature θ is a weighted moving average of the 3 previous days to account for thermal inertia, as can be seen in Equation 3.11.

$$\theta = \frac{T_t + 0.5 \cdot T_{t-1} + 0.25 \cdot T_{t-2} + 0.125 \cdot T_{t-3}}{1 + 0.5 + 0.25 + 0.125} \tag{3.11}$$

Figure 3.12 shows an example of a profile generated according to the BDEW guideline for a single family house of 10 MWh/year in Ghent. This profile can be scaled, depending on the annual heating demand.

Small variations are introduced in the demand profile to avoid 100% simultaneity, based on the occupant's estimated behaviour. Table 3.7 shows when the occupants are expected to be at home and to turn on the heating. These assumptions take into account work and school hours. Retired people are assumed to be always at home, and thus the generated demand profile, as in Figure 3.12, is directly applicable. For the other categories of occupants, scaling factors are introduced to differentiate between absence and presence. The heat demand is artificially increased by a factor 1.2 when the occupants are at home, and decreased with a factor 0.8 when the occupants are absent. Figure 3.13 shows the scaling factors for all occupant categories during one week. A comparison of the heat demand profile of all 5 occupant categories during one week is shown in Figure 3.14.

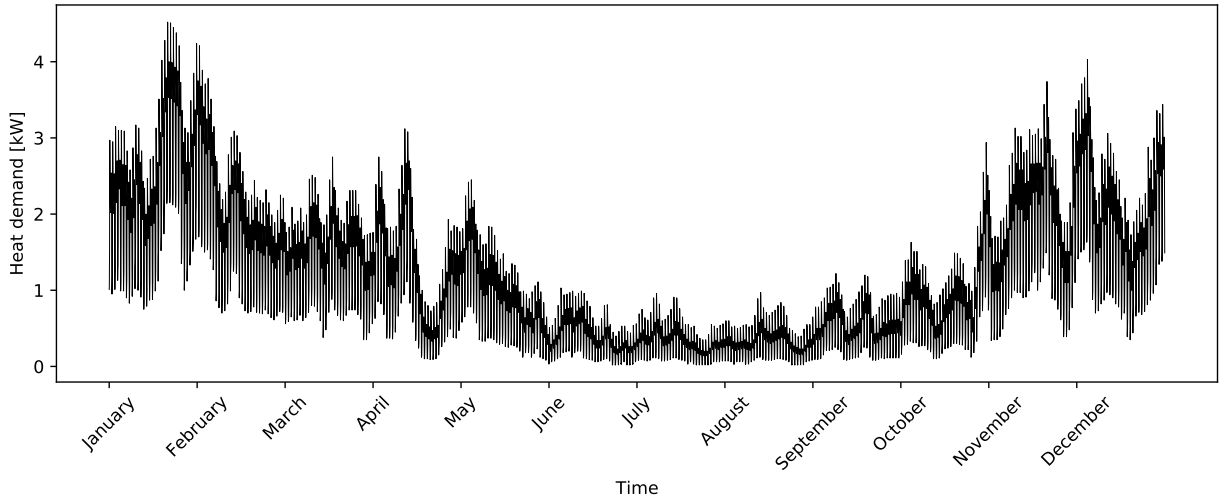

Figure 3.12: Heat demand profile according to the BDEW guideline of a single family house with a annual heat demand of 10 MWh/year.

Table 3.7: Timing of increased heating demand.

Profile	**Monday, Tuesday, Thursday, Friday**	**Wednesday**	**Saterday**	**Sunday**
FTE, FTE, School, School	7-9h, 16-22h	7-9h, 12-22h	7-22h	7-22h
FTE, PTE, School	6-9h, 16-22h	7-9h, 12-22h	7-22h	7-22h
Retired, retired	-	-	-	-
FTE, FTE, School, Student	7-9h, 18-22h	7-9h, 12-22h	7-22h	15-22h
FTE, FTE	7-9h, 19-23h	7-9h, 19-23h	7-22h	7-22h

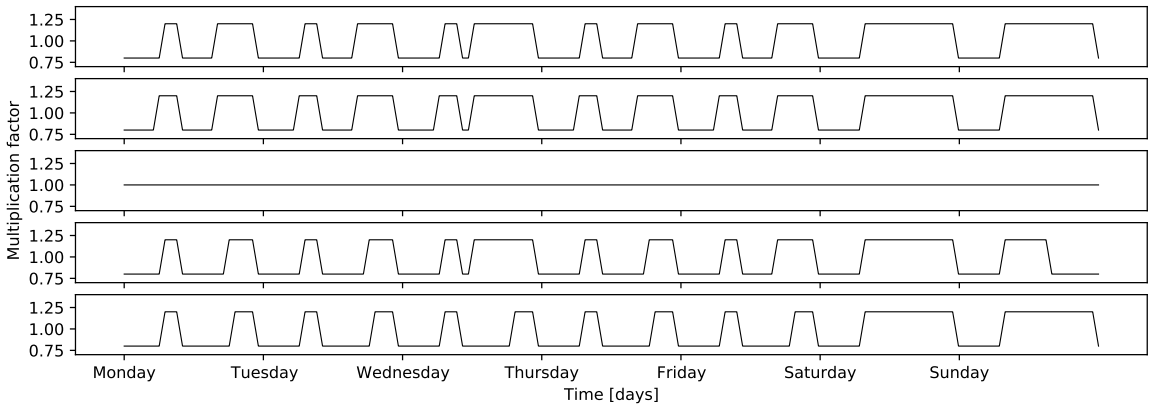

Figure 3.13: Scaling factor for occupant category 1 to 5 (top to bottom) during one week

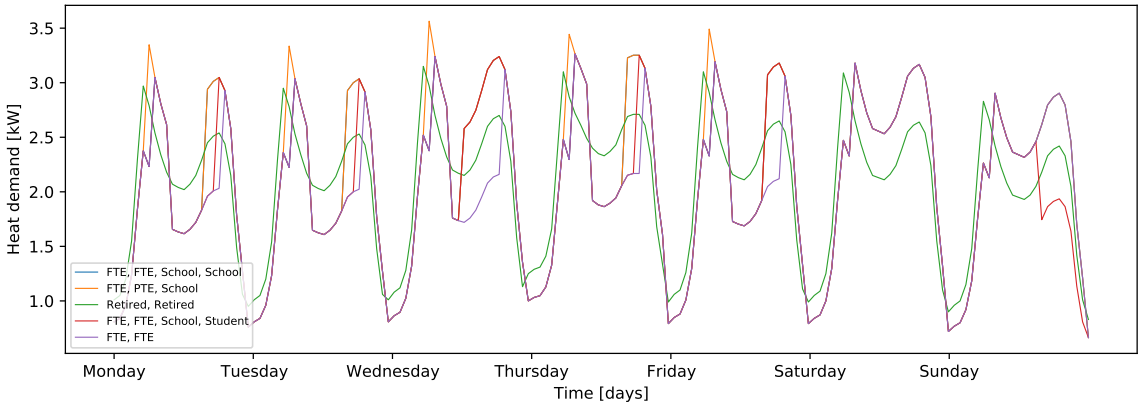

Figure 3.14: Heat demand profile after scaling of all 5 occupant categories during one week.

A distinction in annual heat demand is made, based on the type of occupant and the state of the building. According to the Belgian electricity and natural gas regulator VREG [79], a mean household consumed 17.000 kWh of natural gas, including 2.326 kWh for DHW and cooking in 2020 [80]. A gas invoice of one of the buildings of the Dukkeldamstraat was provided for the years 2021 and 2022, with values of 13.323,58 kWh/year and 12.826,74 kWh/year. Based on this available data and the type of occupant, an estimation of the annual heat demand is made. Table 3.8 shows the estimated annual heat demand per occupant category before and after refurbishment.

Table 3.8: SH demand before and after refurbishment per occupant category [kWh/year].

Profile	**SH Demand before refurbishment [kWh/year]**	**SH Demand after refurbishment [kWh/year]**
FTE, FTE, School, School	18.000	13.000
FTE, PTE, School	16.000	11.000
Retired, retired	17.000	12.000
FTE, FTE, School, Student	15.000	10.000
FTE, FTE	12.000	8.000

3.4.3 Domestic hot water demand profile

To simulate the consumption of DHW, demand profiles are generated with DHWcalc from Universität Kassel [81]. DHWcalc is a program that distributes DHW draw-offs throughout the year with statistical means, according to a probability function. The type of building (single or multi family house), the mean daily draw-off volume and holidays can be specified by the user. Figure 3.15 shows an example of a generated DHW profile for a single family building with a mean draw-off of 100l/day, with a timestep of 1 hour.

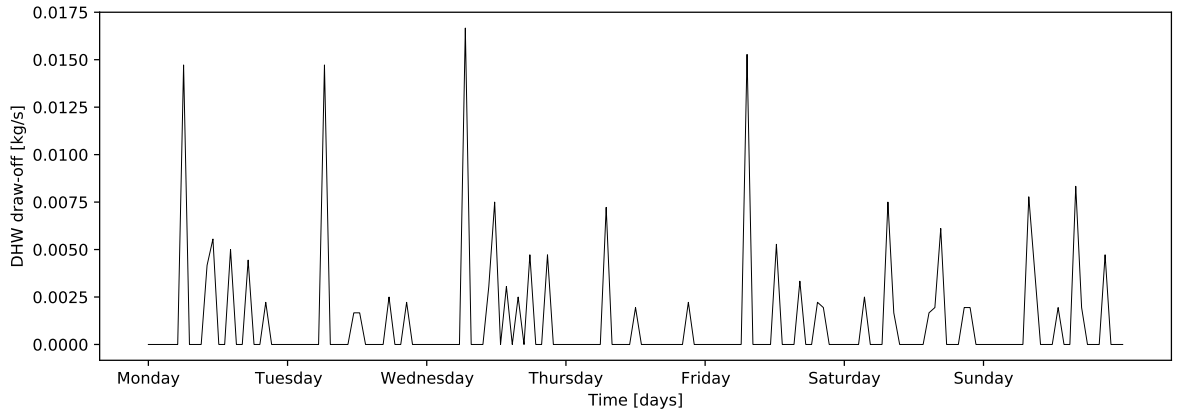

Figure 3.15: DHW draw-off profile of one week for a single family house with a mean draw-off of 100l/day.

The mean draw-off of DHW is estimated to be 30 l/pp/day at 60 °C by the Belgian Building Research Institute [82]. Depending on the number of occupants, the mean draw-off per person can vary, since hot water used for cooking or dish washing can be shared among occupants. The mean draw-off is estimated using the Event-based Residential Occupant Behaviour (EROB) [83], which is an expansion on the StROBe-model [84]. The EROB-model, which was developed in Python, generates DHW use per person at 60 °C based on the stochastic activity of the occupants. To calculate the draw-off of DHW at 45 °C, Equation 3.12 is used, knowing that hot water at 60 °C is mixed with cold tap water at 10 °C and assuming that the specific heat

capacity remains constant.

$$\dot{m}_{45°C} = \dot{m}_{60°C} \cdot \frac{60°C - 10°C}{45°C - 10°C} \tag{3.12}$$

Where $\dot{m}$ is the water mass flow rate [kg/s]. Table 3.9 provides the estimated DHW use per person per category of occupants.

Table 3.9: DHW use per person per day at 45 °C per occupant category.

N°	**Profile**	**Number of occupants**	**DHW use [l/pp/day]**	**DHW use [l/day]**
1	FTE, FTE, School, School	4	36	143
2	FTE, PTE, School	3	39	116
3	Retired, retired	2	41	89
4	FTE, FTE, School, Student	4	29	114
5	FTE, FTE	2	40	80

3.4.4 Booster heat pump

Daikin has provided performance data for a ground source heat pump used in collective housing. The data is confidential and therefore not displayed in this study. The performance map includes information about the COP and electrical power at full load for condenser outlet temperatures up to 60 °C and evaporator inlet temperatures up to 30 °C. However, since the heat pump's evaporator is connected to the DH network at temperatures higher than 30°C and a condenser outlet temperature of 65 °C is desired in the radiator circuit, the operating points are not included in the available performance map. To address this issue, the provided data is expanded by extrapolating the fraction of Carnot efficiency. The Carnot efficiency represents the maximum theoretical efficiency of an ideal thermodynamic cycle (as shown in Equation 3.13). The Carnot efficiency is calculated for the refrigerant cycle, for which the temperature differs from the water cycle by a pinch point temperature ΔT_{HEX}. In this study, the pinch point temperature in the heat exchanger of the heat pump is assumed to be 2.5 K [29, 50].

$$\eta_{Carnot} = \frac{T_H}{T_H - T_C} \tag{3.13}$$

Where η_{Carnot} is the Carnot efficiency [-], T_H is the temperature of the hot reservoir [K] and T_C is the temperature of the cold reservoir [K]. The fraction of Carnot is defined as in Equation 3.14.

$$fr = \frac{COP_{real}}{\eta_{Carnot}} \tag{3.14}$$

Wherer fr is the fraction of Carnot efficiency, COP_{real} is the actual COP of the heat pump and η_{Carnot} is the Carnot efficiency.

The available performance map provided by Daikin limits the condenser outlet temperature to 60 °C, but the desired temperature for the radiator circuit is 65 °C. To address this limitation, a graph (Figure 3.16a) is presented in which the fraction of Carnot efficiency is plotted against

the condenser temperature for different evaporator temperatures (represented by the solid line). To extend the available data beyond 60 °C, a second-order polynomial trendline is fitted to the existing data (represented by the dotted line).

Similarly, the evaporator temperature in the performance map is limited to 30 °C, but the desired temperature for the DH network is up to 55 °C. To extrapolate the available data, a graph (Figure 3.16b) is presented in which the fraction of Carnot efficiency is plotted against the evaporator temperature (represented by the solid line). In this case, a linear trend is perceived, and a linear trendline is used to extend the available data beyond 30 °C (represented by the dotted line).

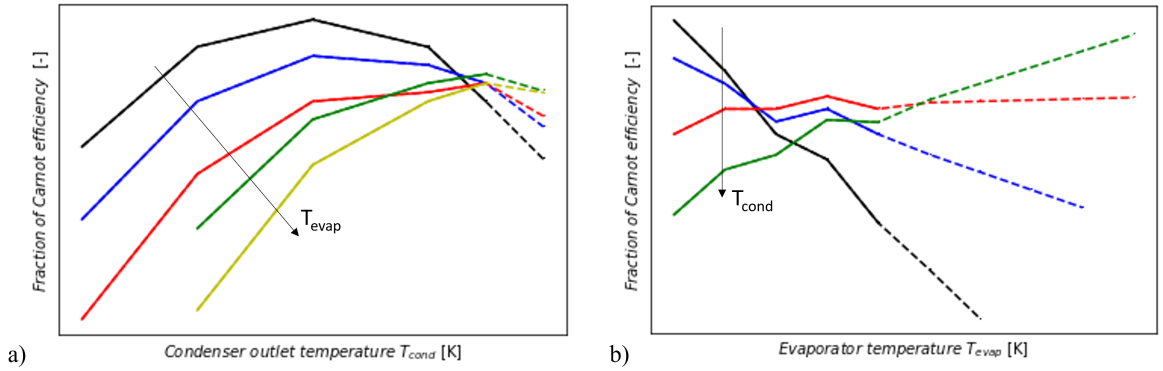

Figure 3.16: Expansion of the performance map: a) expansion of T_{cond} up to 65 °C (dotted line), b) expansion of T_{evap} up to 55 °C (dotted line).

3.4.5 Booster electric heater

As an alternative for a booster heat pump, an instantaneous electric heater is proposed. The electric heater is modelled as an immersive heater which adds heat directly into a storage tank. The size of the storage tank for DHW water is set to 150 l and the water is stored at 55 °C [31]. The performance of the electric heater is assumed to be 100%, as in Zvingilaite et al. [29].

Chapter 4

Dymola

For the modelling of the network, the software Dymola of Dassault Systèmes is used. Dymola makes use of the Modelica language, which is a language for component-oriented modelling of complex physical systems in multiple fields such as mechanics, electrics, hydraulics and thermodynamics [85]. Dymola, which is short for Dynamic Modeling Laboratory, provides an intuitive interface for model creation, testing, simulation and post-processing [86]. Libraries with components are available to use, both commercial and free. For the modelling and simulation in this work, the Modelica Standard Library (version 4.0.0) [87], IDEAS library (version 3.0.0) [88] and Buildings Library (version 9.0.0) [89] are used. For easier understanding of the figures presented in this section, Appendix C provides a description of the used components and their respective icons.

4.1 Description of the house models

For each scenario, a house model is built, resembling the heating and booster technologies for SH and DHW. In this section, the house models are shown and the control is discussed. In Section 4.2, the house models are connected into a district heating network with piping, a circulation pump and central heat source.

Scenario 1: non-refurbished, 75 °C, no booster

In scenario 1 water for SH and DHW is heated via a heat exchanger. An image of the Dymola model can be seen in Figure 4.1. Water from the district heating network enters the house model via port 'DH_Supply' and leaves via port 'DH_Return'. The left side of the model represents the SH circuit, and the right side the DHW circuit. A valve is added on both sides to control the mass flow rate from the district supply line through the heat exchangers. The valve actuation is controlled with a limited PID controller to reach the desired temperature at the secondary side of the heat exchanger. To determine the PID constants, a pulse signal is applied and the response is generated in a simulation. The signal and the response are used in an online tool to define suitable PID constants [90]. The mass flow rate at the secondary side is dictated by the SH and DHW demand. The 'SH_demand' and 'DHW_demand' ports are used to receive data from a data file outside the model. A mass flow controlled pump transports the amount of hot water that is requested by the occupants. The settings used in scenario 1 are given in Table 4.1.

Table 4.1: Simulation settings scenario 1.

Component	Simulation settings
PID valves	k = 0.014, Ti = 25 s, Td = 12 s
Valve SH	$\dot{m}_{nom}$ = 0.11 kg/s, Δp_{nom} = 0.5 bar
Valve DHW	$\dot{m}_{nom}$ = 0.08 kg/s, Δp_{nom} = 0.5 bar
Heat exchangers	$\varepsilon = 0.8$

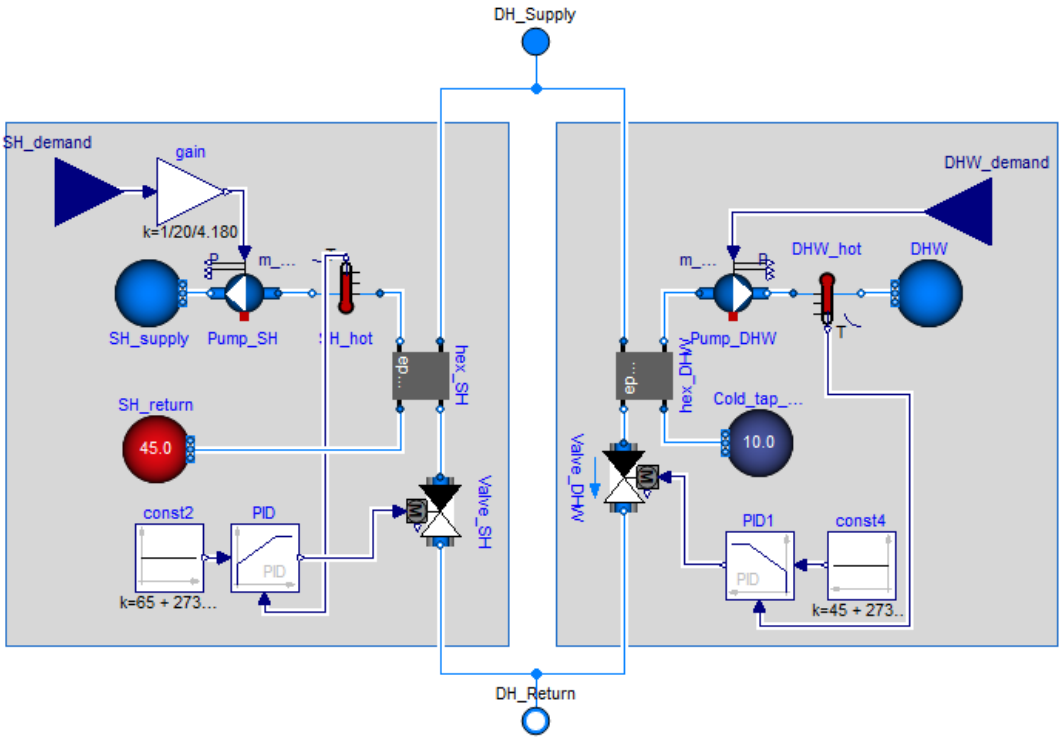

Figure 4.1: Dymola model of scenario 1: non-refurbished, 75 °C, no booster.

Scenario 2: non-refurbished, 55 °C, booster HP for SH

The DH supply temperature in scenario 2 is 55°C. DHW preparation is possible with a heat exchanger, but a booster unit is needed to elevate the temperature to 65°C for SH. Figure 4.2 presents an image of the Dymola model of scenario 2. A booster HP of 10 kW is installed in this case, based on the SH peak demand in the buildings. The heat pump is connected to the DH network at the evaporator side, and to the SH circuit at the condenser side. Modulation is used to control the heat pump, instead of on-off control. On-off control leads to time-consuming simulations due to the high number of events. Modulation on the other hand, smoothly controls the electrical power of the heat pump. The COP of the working point is then held constant, while the electric power is scaled. Variations of the COP in part load are not taken into account. A PID controller is used to assure the condenser outlet temperature is equal to 65°C. A valve between the heat pump and DH network controls the mass flow rate in the evaporator heat exchanger. The valve is controlled with the same PID controller of the heat pump. In this

way, the valve opening is synchronised with the working of the heat pump, and the return temperature can be set to 25°C by choosing the appropriate nominal mass flow rate. DHW heating is done using a heat exchanger and a control valve, assuring a DHW temperature of 45°C, similar to scenario 1. The constants used in the simulation are displayed in Table 4.2.

Table 4.2: Simulation settings scenario 2

Components	**Simulation settings**
Booster heat pump	P_{nom} = 10 kW
PID booster heat pump	k = 0.0125, Ti = 75 s, Td = 0 s
PID valve DHW	k= 0.014, Ti = 25 s, Td = 12 s
Valve SH	$\dot{m}_{nom}$ = 0.05 kg/s, Δp = 0.5 bar
Valve DHW	$\dot{m}_{nom}$ = 0.08 kg/s, Δp = 0.5 bar
Heat exchanger	ϵ = 0.8

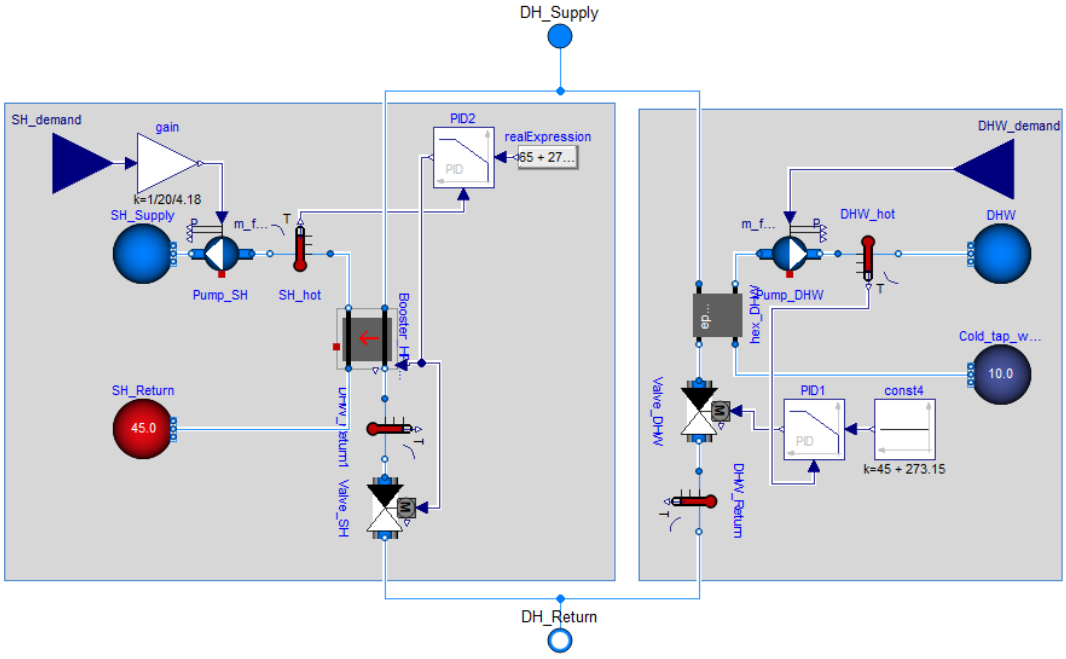

Figure 4.2: Dymola model of scenario 2: non-refurbished, 55 °C, booster HP for SH.

Scenario 3: non-refurbished, 55 °C, booster electric heater for SH

In scenario 3, the SH temperature is boosted with an electric resistive heater element. Figure 4.3 presents the Dymola model of scenario 3. The water for SH is first preheated to 47°C. The resistive heater is assumed to perform at 100 % efficiency. In the model, this is represented by a prescribed heat flux in a mixing volume. In practice, a resistive heater has a fixed power and should be turned on and off according to the temperature in the mixing volume. However, in the simulation model, a PID controller scales and controls the power of the heat flux. By

measuring the temperature in the mixing volume, the heat flux is regulated to achieve a setpoint temperature of 65°C, as on-off control could lead to numerous events in the simulation, increased simulation times, and larger data files. Similar to scenarios 1 and 2, the DHW is heated with a heat exchanger, and the mass flow is controlled using a valve to reach a setpoint temperature of 45°C. The settings used in scenario 3 are listed in Table 4.3.

Table 4.3: Simulation settings scenario 3.

Components	**Simulation settings**
PID valves	k= 0.014, Ti = 25 s, Td = 12 s
Valve SH	$\dot{m}_{nom}$ = 0.03 kg/s, Δp = 0.5 bar
Valve DHW	$\dot{m}_{nom}$ = 0.08 kg/s, Δp = 0.5 bar
Mixing volume	V = 200 l
Heat flux	Q_{max} = 10 kW
Heat exchangers	ϵ = 0.8

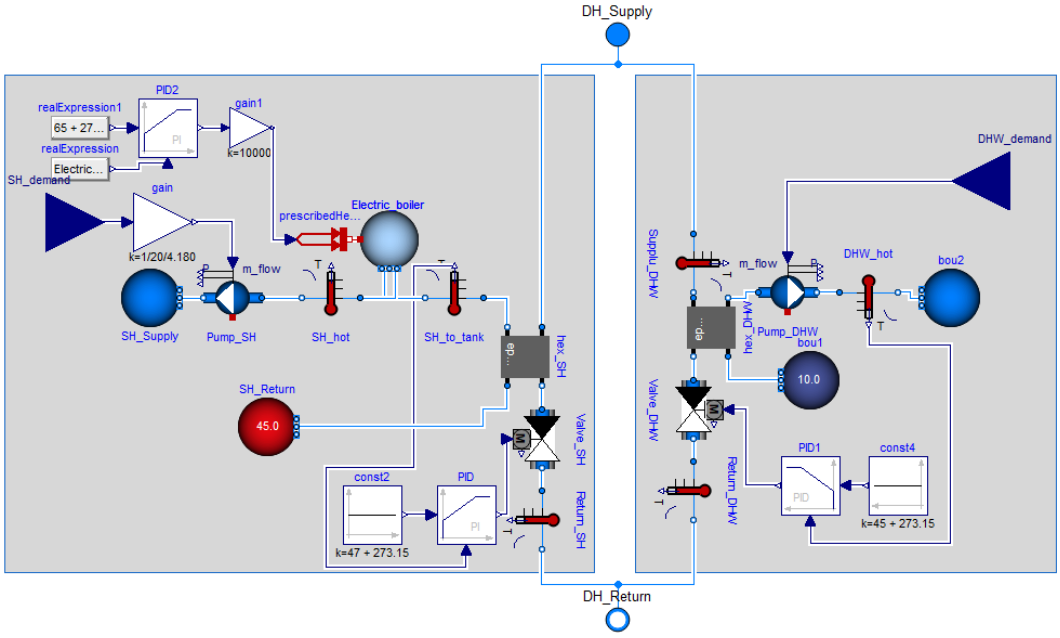

Figure 4.3: Dymola model of scenario 3: non-refurbished, 55 °C, booster electric heater for SH.

Scenario 4: non-refurbished, 45 °C, booster HP for SH and DHW

In scenario 4, a booster heat pump is needed to meet the SH and DHW temperature requirements, as the DH network temperature is set to 45°C. The Dymola model for this scenario is presented in Figure 4.4. The evaporator of the booster heat pump is connected to the DH network, and the condenser side is linked to a circuit that supplies the radiators and a storage tank for DHW. In practice, the water circulates directly through the radiators. In the model

however, the circuit of the booster heat pump and the radiator circuit are separated with a heat exchanger. To mimic the real situation the effectiveness of the heat exchanger is set to 1. The mass flow rate through the heat exchanger is regulated by a valve using a PID controller, as in scenarios 1 to 3. The hot water coming from the booster heat pump also circulates through a storage tank via an internal heat exchanger, raising the temperature in the tank. A hysteresis loop controls the mass flow rate through the internal heat exchanger, by opening a valve when the tank temperature drops to 45°C, and closing again when the temperature reaches 60°C. Similar to scenario 2, modulation is used to size the power output of the heat pump. The nominal power of the heat pump is set to 10 kW, based on the peak SH and DHW demand. A PID controller is employed to define the level of modulation and opening of the valve, controlling the mass flow rate through the evaporator side. The nominal mass flow rate through the valve is chosen such that the return temperature is 25°C. Table 4.4 provides an overview of the settings used in the simulation of scenario 4.

Table 4.4: Simulation settings scenario 4.

Components	**Simulation settings**
Booster heat pump	P_{nom} = 10 kW
PID valves and heat pump	k= 0.014, Ti = 25 s, Td = 12 s
Valve SH	$\dot{m}_{nom}$ = 0.1 kg/s, Δp = 0.5 bar
Valve DHW	$\dot{m}_{nom}$ = 0.1 kg/s, Δp = 0.5 bar
Valve heat pump	$\dot{m}_{nom}$ = 0.09 kg/s, Δp = 0.5 bar
Storage tank	V = 150 l
Hysteresis	T_{min} = 45 °C, T_{max} = 60 °C
Heat exchanger	ϵ = 1

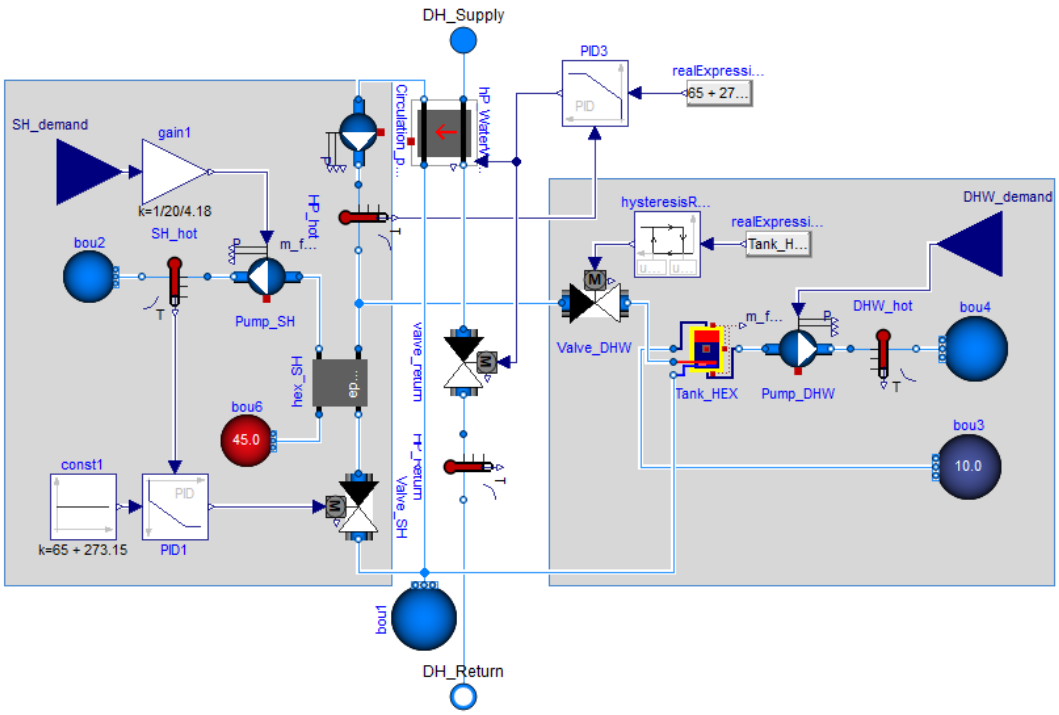

Figure 4.4: Dymola model of scenario 4: non-refurbished, 45 °C, booster HP for SH and DHW.

Scenario 5: refurbished, 55 °C, no booster

Scenario 5 differs from the previous four scenarios in that it considers refurbished buildings instead of non-refurbished ones. The key difference is the use of underfloor heating instead of radiators, which reduces the requirements for the DH network temperature. The lower limit for the DH network temperature is now determined by the DHW preparation requirements. In this scenario, the DH network temperature is set to 55°C, but the model is quite similar to scenario 1, as shown in Figure 4.5. Heat exchangers are used to increase the water temperature for SH and DHW, and valves regulate the mass flow from the DH network using a PID controller to achieve the desired temperature level. No booster heat pump or electric heater is necessary. The simulation settings for scenario 5 are presented in Table 4.5.

Table 4.5: Simulation settings scenario 5.

Component	**Simulation settings**
PID valves	k = 0.014, Ti = 25 s, Td = 12 s
Valve SH	$\dot{m}_{nom}$ = 0.21 kg/s, Δp_{nom} = 0.5 bar
Valve DHW	$\dot{m}_{nom}$ = 0.08 kg/s, Δp_{nom} = 0.5 bar
Heat exchangers	$\varepsilon = 0.8$

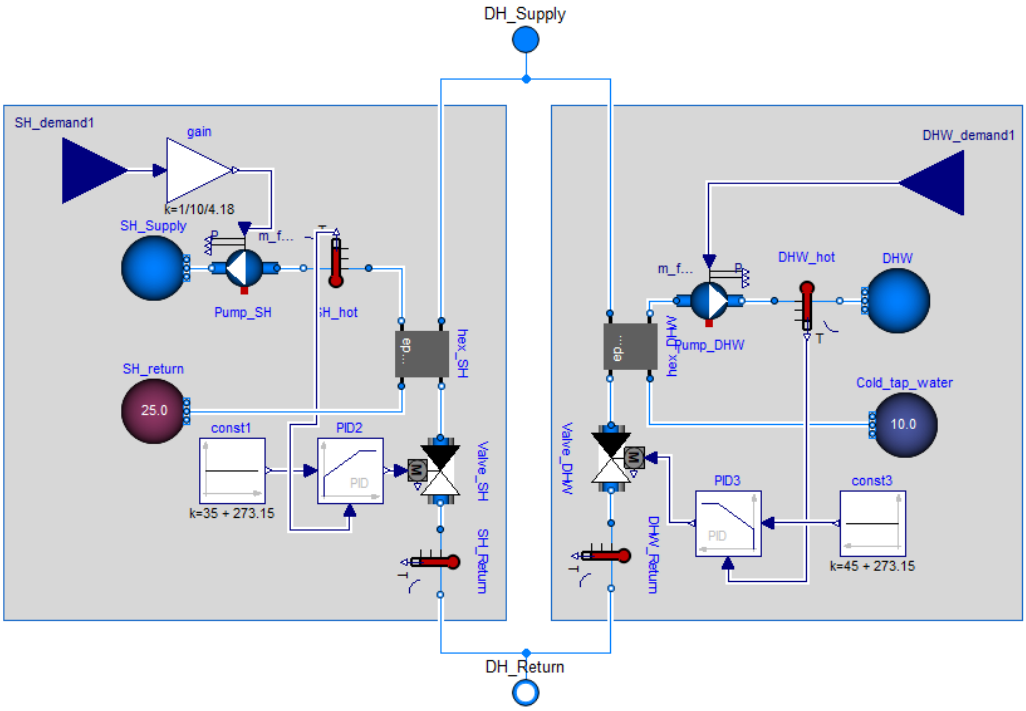

Figure 4.5: Dymola model of scenario 5: refurbished, 55 °C, no booster.

Scenario 6: refurbished, 45 °C, booster HP for DHW

In scenario 6, the DH network temperature has been reduced to 45°C, which means that a booster heat pump is necessary for DHW preparation. The Dymola model of scenario 6 can be seen in Figure 4.6. The right hand side of the figure shows the DHW preparation. The heat pump model is connected to the DH network at the evaporator side, and to a circuit with storage tank at the condenser side. The water in the circuit is heated and passes through the storage tank with an internal heat exchanger, elevating the temperature in the storage tank. A hysteresis control loop is used to control the heat pump power. When the temperature in the storage tank drops below 45°C the heat pump is turned on, until 55°C is reached. The opening of the valve at the evaporator side of the heat pump is controlled with the same hysteresis loop. On the left hand side, the water for SH is heated with a heat exchanger, as in scenario 5. A valve controls the mass flow through the heat exchanger to ensure that the water temperature reaches 35°C. Table 4.6 presents an overview of the simulation settings used in scenario 6.

Table 4.6: Simulation settings scenario 6.

Components	Simulation settings
Booster heat pump	$P_{nom} = 2$ kW
Valve SH	$\dot{m}_{nom} = 0.1$ kg/s, $\Delta p = 0.5$ bar
Hysteresis	$T_{min} = 45$ °C, $T_{max} = 55$ °C
Valve DHW	$\dot{m}_{nom} = 0.1$ kg/s, $\Delta p = 0.5$ bar
Storage tank	V = 150 l
Heat exchanger	$\epsilon = 0.8$

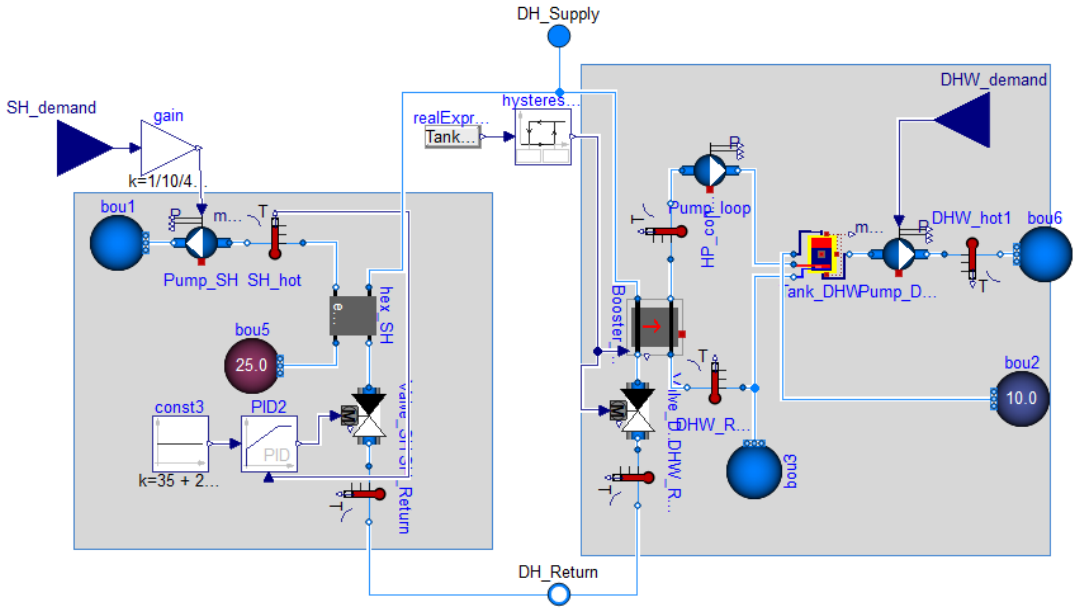

Figure 4.6: Dymola model of scenario 6: refurbished, 45 °C, booster HP for DHW.

Scenario 7: refurbished, 45 °C, booster electric heater for DHW

Scenario 7 maintains the DH network temperature of scenario 6, but instead of using a booster heat pump, an electric heater is employed to increase the DHW temperature. Figure 4.7 depicts the Dymola model for scenario 7. Cold tap water is initially preheated to 37°C using a heat exchanger and then stored in a mixing volume, which represents the storage tank. A PID controller regulates the valve opening to achieve the setpoint temperature of 37°C. The electric heater is assumed to be 100% efficient and is represented in the model by a prescribed heat flux of 2000 W. A hysteresis loop is utilized to control the temperature in the storage tank. When the temperature falls below 45°C, the electric heater is activated, and when it exceeds 60°C, the electric heater is turned off. The heating of water for SH is performed as in scenarios 5 and 6, and can be seen on the left-hand side of the figure. Table 4.7 provides an overview of the simulation settings applied in scenario 7.

Table 4.7: Simulation settings scenario 7.

Components	Simulation settings
Electric heater	$P_{nom} = 2$ kW
PID valves	k= 0.014, Ti = 25 s, Td = 12 s
Valve SH	$\dot{m}_{nom} = 0.11$ kg/s, $\Delta p = 0.5$ bar
Valve DHW	$\dot{m}_{nom} = 0.1$ kg/s, $\Delta p = 0.5$ bar
Storage tank	V = 150 l
Hysteresis	$T_{min} = 45$ °C, $T_{max} = 60$ °C
Heat exchangers	$\epsilon = 0.8$

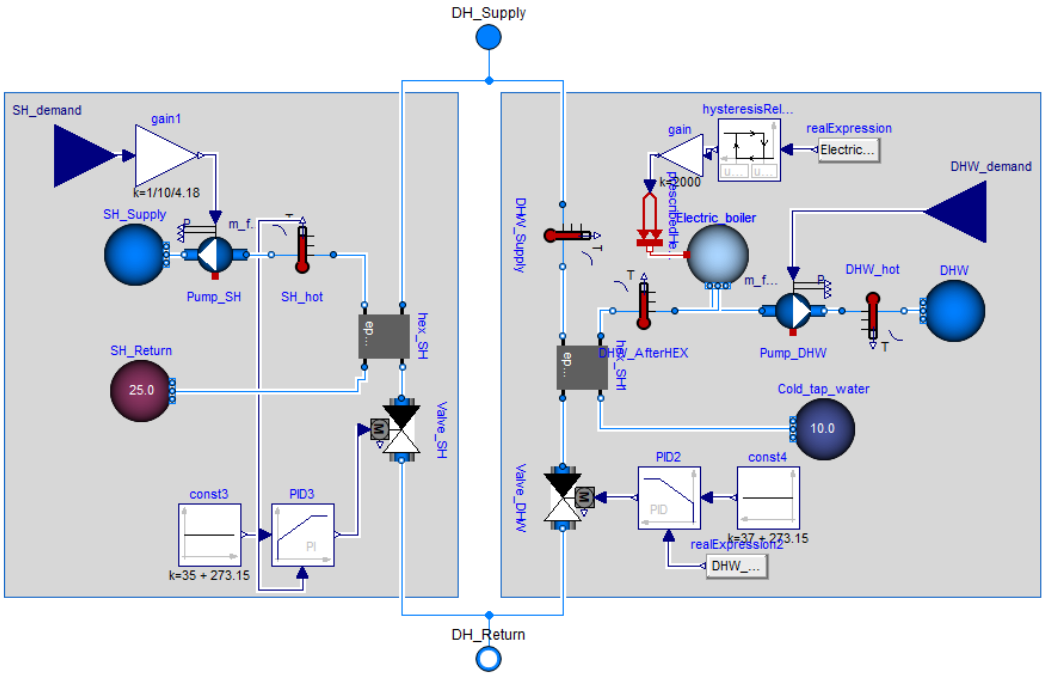

Figure 4.7: Schematic and Dymola model of scenario 7: refurbished, 45 °C, booster electric heater for DHW.

Scenario 8: refurbished, 10 °C, booster HP for SH and DHW

In scenario 8, the water of the DH network is not heated centrally, but distributed at the temperature of the water of the boreholes at 10°C. Individual water-water heat pumps are employed to provide SH and DHW in the buildings. Figure 4.8 illustrates the Dymola model for scenario 8, which is quite similar to the model for scenario 4, with the exception of the SH setpoint temperature being 35°C in this case. To meet the DHW requirements, the heat pump condenser outlet temperature is 55°C. Table 4.8 offers an overview of the simulation settings implemented in scenario 8.

Table 4.8: Simulation settings scenario 8.

Components	**Simulation settings**
Booster heat pump	P_{nom} = 15 kW
PID valves and heat pump	k= 0.014, Ti = 25 s, Td = 12 s
Valve SH	$\dot{m}_{nom}$ = 0.1 kg/s, Δp = 0.5 bar
Valve DHW	$\dot{m}_{nom}$ = 0.1 kg/s, Δp = 0.5 bar
Valve heat pump	$\dot{m}_{nom}$ = 0.5 kg/s, Δp = 0.5 bar
Storage tank	V = 150 l
Hysteresis	T_{min} = 45 °C, T_{max} = 55 °C
Heat exchanger	ϵ = 1

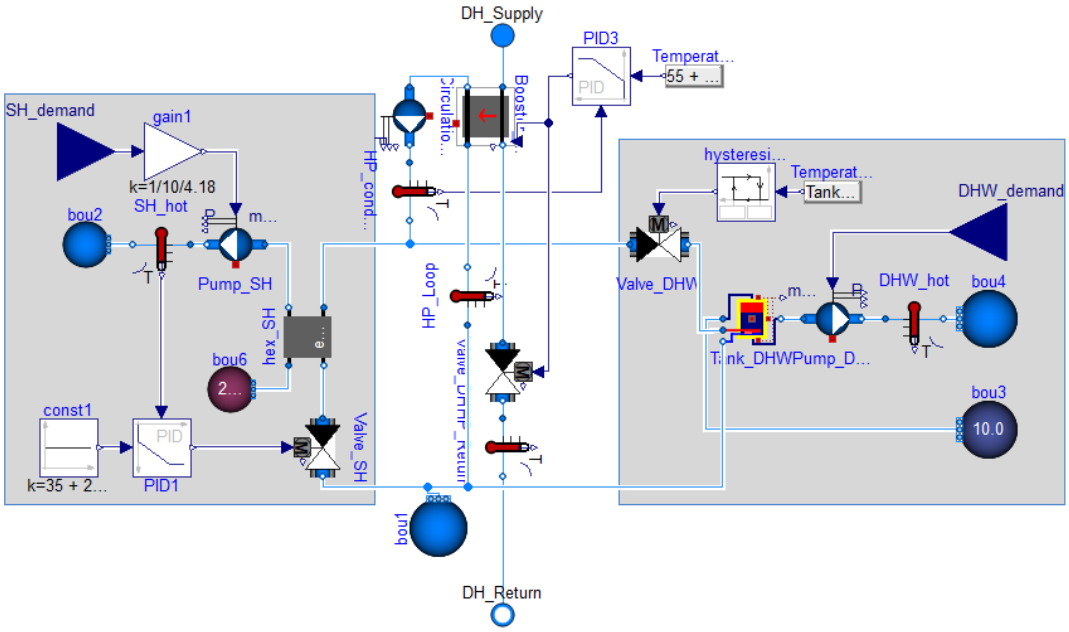

Figure 4.8: Dymola model of scenario 8: refurbished, 10 °C, booster HP for SH and DHW.

4.2 Description of the network model

The house models presented in Section 4.1 serve as the basis for constructing the DH network model, which is illustrated in Figure 4.9. The network consists of 35 houses which are interconnected by a supply pipe line and a return pipe line. Due to the repetitive character of the network lay-out, arrays are used for the ease of modifying the used house model and pipe dimensions for the different scenarios. The use of arrays allows to include a model multiple times without displaying it in the diagram view. Interconnections between the repeated models

can be described in the text view. The model shown in Figure 4.10 contains one of the house models and a pipe segment of the supply and the return pipe. This model is repeated with the use of arrays and is represented by the brown house in Figure 4.9. The central heat pump is not included in the Dymola model, but represented by an ideal source with given temperature and pressure. The performance and electricity consumption of the central heat pump are computed during post-processing using the mass flow rate through the network and the temperature at the end of the return pipe. Circulation pumps (see Table 3.4) are used to compensate for pressure losses in the network. One pump ensures a constant pressure increase of 0.5 bar to compensate for the constant pressure loss of 0.5 bar over the substation. The second pump is used to compensate the pressure loss in the pipes, which depends on the mass flow rate. The building in the middle of the network, the 18th house in this instance, is expected to have the greatest pressure loss. To maintain a pressure drop of 0.5 bar across the substation at all times, a PID controller regulates the delivered pressure increase of the second pump by changing the speed of the pump. Two tables containing data for SH and DHW demand are included in the model and connected to the corresponding house.

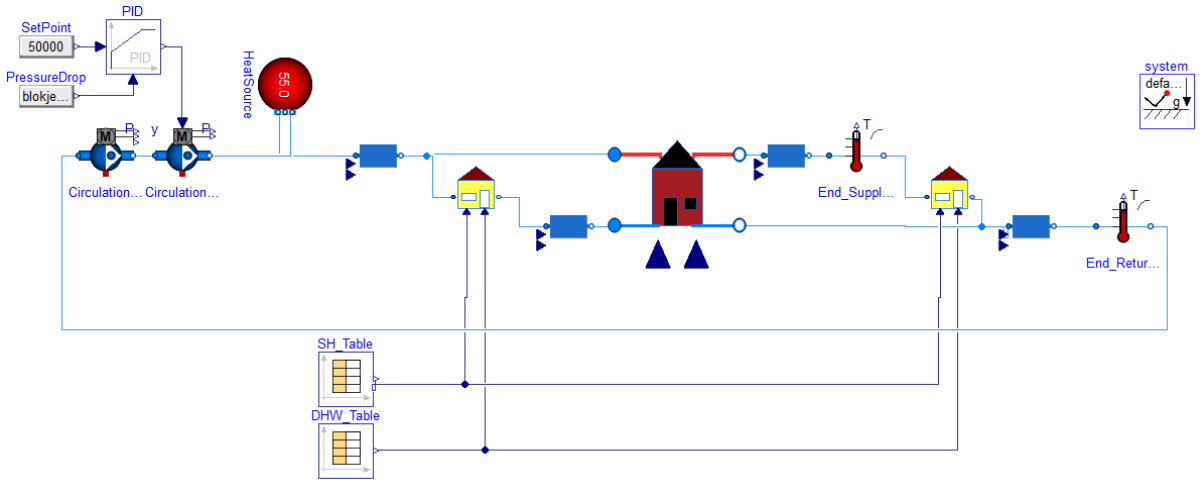

Figure 4.9: District heating network model.

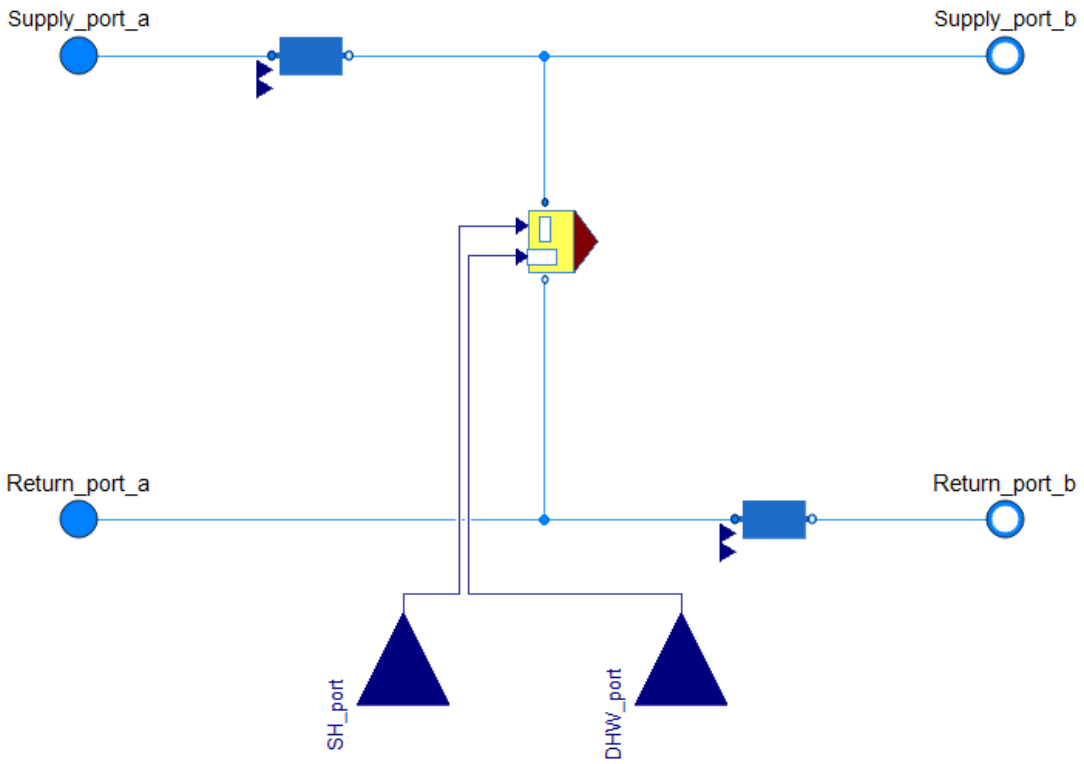

Figure 4.10: House model with supply and return pipe segment to be repeated with an array.

4.2.1 Pipe model

The Modelica Standard Library provides a dynamic pipe model. In this model, the pipe is divided in segments and for each segment the partial differential equations are solved, also called the finite volume method [91]. This model leads to long simulation times. For the purpose of simulating a district heating network, only mass flow rate, pressure drop and temperature are important parameters. Therefore, a less complex pipe model is created and used in the DH network model. The created pipe model can be seen in Figure 4.11.

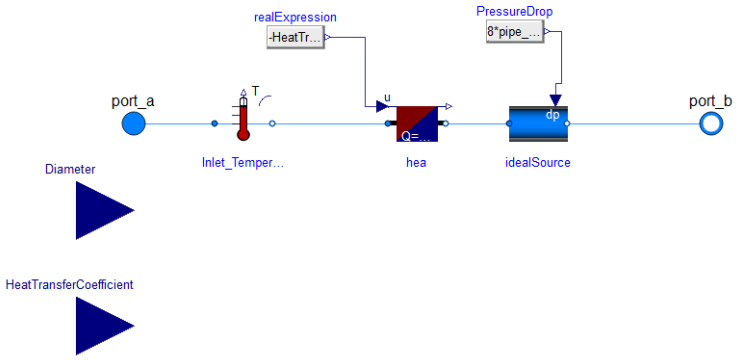

Figure 4.11: New pipe model.

The model imposes a heat loss and pressure drop on the passing flow. Heat is extracted with an ideal heater. Using the inlet temperature, the corresponding heat loss is calculated as in Equation 4.1:

$$\dot{Q} = U \cdot l \cdot (T_{inlet} - T_{soil}) \tag{4.1}$$

Where $\dot{Q}$ is the extracted heat [W], U is the heat transfer coefficient of the pipe [W/mK], l is the length of the pipe [m], T_{inlet} is the temperature at the pipe's inlet [K] and T_{soil} is the temperature of the soil [K].

An ideal pressure source introduces a pressure drop in the pipe. The pressure is calculated with the Darcy - Weisbach equation, given in Equation 4.2:

$$\Delta p = \frac{8lf\dot{m}^2}{D^5\rho\pi^2} \tag{4.2}$$

Where Δp is the pressure loss in the pipe [Pa], l is the length of the pipe [m], f is the Darcy friction factor, $\dot{m}$ is the mass flow rate through the pipe [kg/s], D is the diameter of the pipe [m] and ρ is the density of the passing fluid [kg/m^3].

Only the inlet temperature, mass flow rate and friction factor are variable during simulation. The density of the fluid depends on the medium used in the models. In this case, 'Simple liquid water medium' is used, which has a constant density of 995.586 kg/m^3 [92]. Length, diameter and heat coefficient of the pipe are parameters requested from the end user. The Darcy friction factor is calculated using the Haaland equation [73], as described in Equation 3.2.

Chapter 5

Results

This chapter presents the results of a comparison of the eight proposed scenarios for an renewable energy-based DH network in terms of primary energy use and energy efficiency. The analysis begins by observing thermal power of the central heat pump. Next, the heat losses in the network are compared to highlight the importance of the supply and return temperature. Finally, a comparison of the primary energy use and energy efficiency of the scenarios is made, which takes into account the energy use of the circulation pumps, the central heat pump, and decentralized booster units. It is important to note that scenario 6 is simulated in a slightly different manner compared to the other scenarios. The explanation and discussion can be found in Appendix D. In Table 5.1, the investigated scenarios are repeated for ease of following the interpretation of the results.

Table 5.1: Investigated scenarios.

	State of the building	**Network temperature**	**Booster technology**		**Booster technology usage**	
			Heat pump	*Electric heater*	*Domestic hot water*	*Space heating*
1	Non-refurbished	75 °C				
2	Non-refurbished	55 °C	X			X
3	Non-refurbished	55 °C		X		X
4	Non-refurbished	45 °C	X		X	X
5	Refurbished	55 °C				
6	Refurbished	45 °C	X		X	
7	Refurbished	45 °C		X	X	
8	Refurbished	10 °C	X		X	X

5.1 Central heat pump

The thermal and electric power of the central heat pump, as well as the total mass flow rate and temperature drop in the network are given in Table 5.2. The size of the central heat pump corresponds to the share of the thermal energy that it delivers to the end-users. That is why in scenarios 1 and 5, where the network operates without booster units, the thermal power is greatest for respectively non-refurbished and refurbished buildings. It can also be noticed that the decreased SH demand in refurbished buildings results in a reduced thermal power of the heat pump, which offers the possibility to opt for a smaller central heat pump or to include more buildings in the network. In scenarios with a booster unit, the size of the central heat pump can be reduced since the thermal energy demand is partially covered by the booster units. In such cases, the size of the central heat pump is mainly determined by the mass flow rate and temperature drop in the network. Scenario 3 (55°C, electric heater for SH) exemplifies this, where both the mass flow rate and temperature drop are low, resulting in lower thermal power requirements for the central heat pump. This can be explained by the limited temperature drop

in the heat exchanger for SH.

Table 5.2: Thermal and electric power of the central heat pump, and mass flow rate and temperature drop in the network.

Scenario	**Symbol**	**1**	**2**	**3**	**4**	**5**	**6**	**7**
Network supply temperature [°C]	T_{supply}	75	55	55	45	55	45	45
Refurbished	-	No	No	No	No	Yes	Yes	Yes
Thermal power central heat pump [kW]	$\dot{Q}_{CH}$	330	300	110	270	260	185	210
Electric power central heat pump [kW]	$P_{el,CH}$	142	84	31	60	72	41	47
Max total mass flow rate [kg/s]	$\dot{m}_{tot,max}$	2.87	2.25	1.40	2.88	2.29	2.7	2.66
Average temperature drop [°C]	$T_{supply} - T_{return}$	25.8	22.3	8.7	22.7	18.1	16.7	13.7

Figure 5.1 displays the distribution of the thermal power of the central heat pump over the course of one year for scenarios 1 and 5 (non-refurbished and refurbished, no booster). It can be observed that the central heat pump operates at part load for a significant portion of the time. Although differences in part load efficiency have not been considered, they may have an important impact on the total energy consumed by the central heat pump. Nevertheless, an analysis of the electric power curves reveals that the part load fraction is nearly identical across all scenarios, allowing for valid comparisons between them.

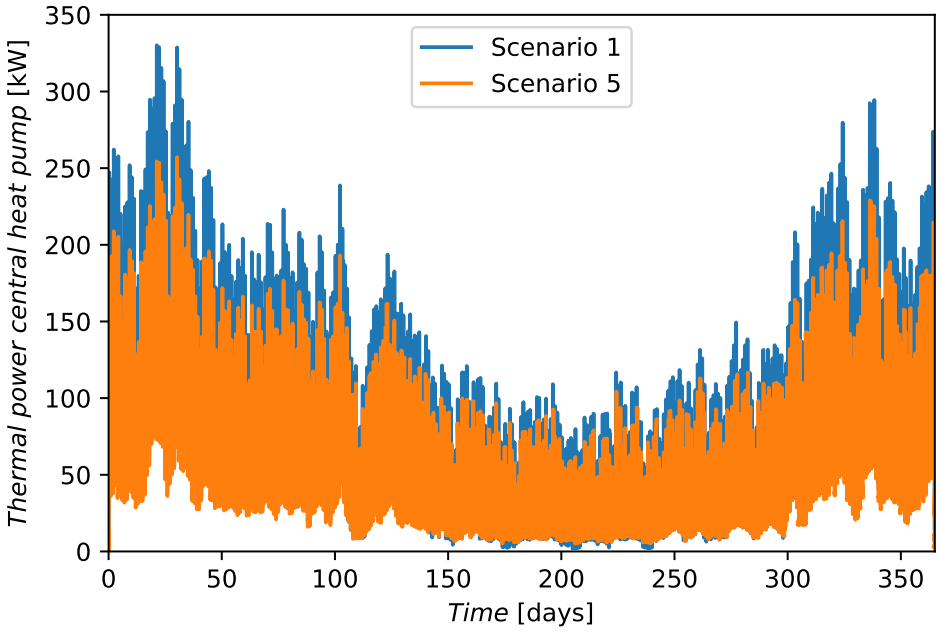

Figure 5.1: Thermal power central heat pump in scenarios 1 and 5 during one year.

5.2 Heat losses

Heat losses in the distribution network are caused by the temperature difference between the water in the network and the surrounding soil. Consequently, these losses are closely linked to the temperature of the water in the supply and return pipes. In Figure 5.2, the heat losses are presented in decreasing order of the network supply temperature. As expected, a clear trend of decreasing heat losses is observed as the network supply temperature decreases. However, scenarios 2, 3, and 5 share the same network supply temperature. The variation in heat losses among these scenarios can be attributed to the difference in the average return temperature, as a significant portion of the heat losses occurs in the return pipe. The same principle applies to scenarios 4, 6, and 7.

In scenarios that employ a heat pump as booster unit the return temperature is lower, compared to scenarios where heat is extracted from the network through a heat exchanger. This is a consequence of the limited temperature drop in a heat exchanger, which depends on the temperature of the medium on the secondary side, in this case water returning from the radiator circuit or cold tap water. Booster heat pumps can reach lower return temperatures in comparison to direct heat exchange or electric heaters, resulting in reduced heat losses.

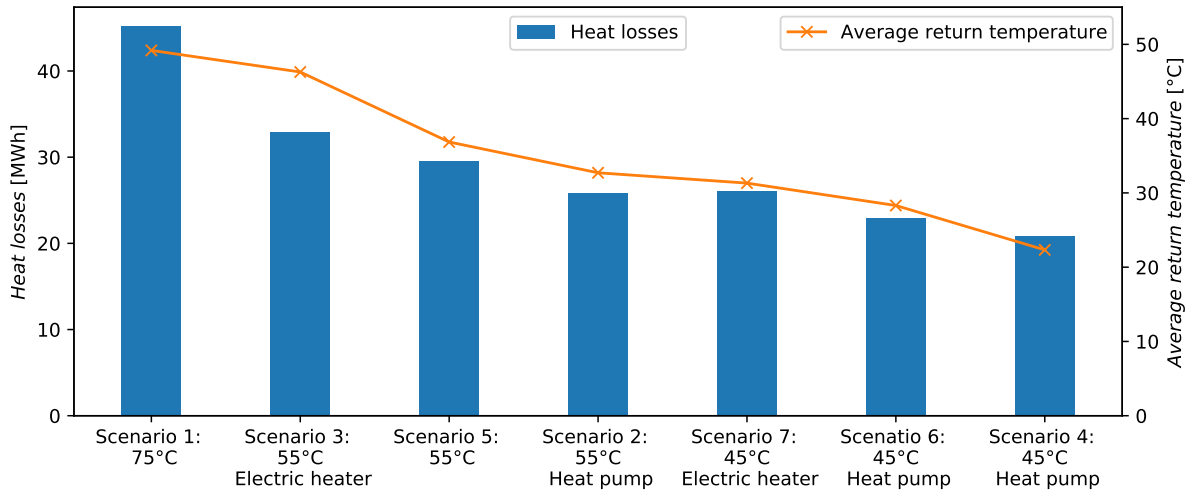

Figure 5.2: Comparison of the heat losses and the average return temperature.

Table 5.3 displays the total annual heat losses in the network. The relative heat loss can be expressed as a fraction of the thermal energy delivered by of the central heat pump, as described in Equation 5.1.

$$fr_{losses} = \frac{Q_{losses}}{Q_{CH}} \tag{5.1}$$

Where fr_{losses} is the relative heat loss [-], Q_{losses} is the annual heat loss in the network [MWh] and Q_{CH} is the annual thermal energy delivered by the heat pump [MWh]. By expressing the amount of heat losses as a fraction of the thermal energy delivered by of the central heat pump, it can be quantified how large the share of the heat losses is compared to the useful delivered heat. In most scenarios the relative heat loss accounts for 3.8-7 % of the total delivered heat. Comparing this to values mentioned in literature (5.0-27.8 % [3, 93, 94]), the heat losses are considered low in most scenarios and contribute to a high overall energy efficiency. This is probably a consequence of the limited size and compact lay-out of the DH network, since networks with larger distances between the consumers suffer from relatively higher heat losses.

Scenario 3 shows the highest relative heat loss of 22.9%. This can be explained by the limited delivered heat by the central heat pump and the relatively high return temperature.

Table 5.3: Absolute and relative heat losses in the piping network.

Scenario	**Symbol**	**1**	**2**	**3**	**4**	**5**	**6**	**7**
Heat losses [MWh]	Q_{losses}	45.1	25.8	32.9	20.8	29.6	22.9	26.0
Thermal energy central heat pump [kWh]	Q_{CH}	647	581	144	543	463	395	447
Relative heat loss [%]	fr_{losses}	7.0	4.4	22.9	3.8	6.4	5.8	5.8

The heat losses in the network also influence the temperature at the end of the supply pipe. In Chapter 3, it was assumed that the temperature drop is limited to 2 °C. Observing the average temperature at the end of the supply pipe in Table 5.4 shows that this is not always the case. This should be considered in the final design of the network.

Table 5.4: Temperature drop in supply pipe.

Scenario	**1**	**2**	**3**	**4**	**5**	**6**	**7**
Temperature drop supply pipe [°C]	3.0	1.8	1.8	3.4	1.9	2.6	1.7

5.3 Primary energy use and energy efficiency

The total energy use in the DH system is determined by circulation pumps, the central heat pump, and the decentralized booster units. The annual total energy use for these three components is calculated by summing the electric energy use of the circulation pumps, all booster units and the central heat pump. The total energy use is compared to the total useful energy, which in this case refers to the thermal energy delivered for SH and DHW. This comparison is expressed as the energy efficiency of the DH network. The energy efficiency is defined by Equation 5.2.

$$\eta_{tot} = \frac{Q_{SH} + Q_{DHW}}{E_{pump} + E_{booster} + E_{CH}} = \frac{Q_{SH} + Q_{DHW}}{E_{tot}} \tag{5.2}$$

Where η_{tot} is the energy efficiency of the network [-], Q_{SH} and Q_{DHW} are the thermal energy delivered for SH and DHW [MWh], E_{pump}, $E_{booster}$ and E_{CH} are the electric energy used by the circulation pumps, the booster units and the central heat pump [MWh], and E_{tot} is the total used electric energy [MWh]. The following sections discuss the results and explain the observed trends. Table 5.7 at the end of the chapter presents the performance, energy use and efficiency of all components in the investigated scenarios.

5.3.1 Scenarios 1 to 4: non-refurbished buildings

The comparison of the scenarios with non-refurbished buildings is discussed in this section. In Figure 5.3, the total primary energy use is presented and the distribution of the energy use

over the central heat pump, booster heat pumps and circulation pumps is visualized. Scenario 2 (55°C, heat pump for SH) shows with 207.2 MWh/year the lowest total energy use of all investigated scenarios, followed by scenario 4 (45°C, heat pump for SH and DHW) with 213.1 MWh/year. The superior performance of the central heat pump and booster heat pumps in these scenarios, as shown in Table 5.5, accounts for this outcome. By reducing the DH network temperature, the COP of the central heat pump improves and heat losses in the network decrease, resulting in lower energy use compared to scenario 1 (75°C, no booster), which has a total energy use of 279.7 MWh/year. However, scenario 1 only exhibits a 35% higher total energy use than scenario 2. When cost constraints are considered, scenario 1 could be a viable option. On the other hand, in scenario 3 (55°C, electric heater for SH) with 535.4 MWh/year, the energy use is 2.6 times higher than in scenario 2. The largest share of the heat production in scenario 3 is performed by the electric heater, which has a much lower performance than the central heat pump or a booster heat pump. This causes the high energy use of the booster electric heater compared to the central heat pump and circulation pumps. The circulation pumps in all scenarios contribute to less than 1% of the total energy use.

Based on this analysis, it can be concluded that a DH network at 45°C or 55°C with decentralized booster heat pumps for SH or both SH and DHW results in the lowest total energy use. However, if cost limitations are a concern, a DH network without decentralized boosters and a supply temperature of 75°C could be considered. It is not advisable to use electric heaters as booster units for SH, as it would transfer the largest share of the heat generation from the central heat pump to the decentralized electric heaters with lower performance.

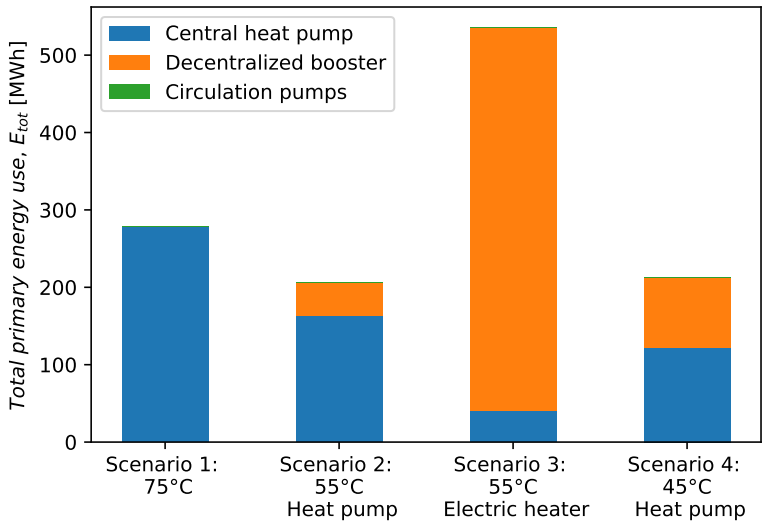

Figure 5.3: Comparison of the total primary energy use for scenarios 1 to 4 with non-refurbished buildings.

Table 5.5: Performance booster units and central heat pump in scenario 1 to 4.

Scenario	**1**	**2**	**3**	**4**
COP booster units	-	12.7	1	6.6
COP central heat pump	2.3	3.6	3.6	4.5

5.3.2 Scenarios 5 to 8: refurbished buildings

This section focuses on discussing scenarios related to refurbished buildings. Figure 5.4 compares the total energy use of scenarios 5 to 8, while Table 5.6 presents the performance of the central heat pump and booster units. Among these scenarios, scenario 6 (45°C, heat pump for DHW) shows the lowest total energy use with 96.7 MWh/year, followed by scenario 7 (45°C, electric heater for DHW) with 123.3 MWh/year. In scenario 7, the network preheats the cold tap water, reducing the share of heat generated by the electric heater. This reduces the effect of the lower performance of the electric heater compared to the booster heat pump. The total energy use in scenario 7 is only 28% higher than in scenario 6. If the end-user's investment cost is a limiting factor, an electric heater for DHW preparation is certainly worth considering. Scenario 5 (55°C, no booster) with a supply temperature of 55°C results in reduced performance of the central heat pump and increased heat losses, leading to a higher total energy use (with 130.8 MWh/year) compared to scenarios 6 and 7 with a supply temperature of 45°C. Scenario 8 (10°C, heat pump for SH and DHW) results in the highest total energy use with 138.3 MWh/year. It is remarkable that the reduction in heat losses by lowering the network temperature to 10°C is counteracted by the booster heat pump's lower performance compared to the central heat pump in the other scenarios.

For refurbished buildings, a DH network at 45 °C with decentralized heat pumps shows lowest energy use, but also electric heaters may be considered as the energy use is only 28% and investment cost may be the key factor in the decision making for this network. From the analysis above, it is also clear that the performance of the central heat pump is a crucial parameter, and that the reduction of heat losses by lowering the supply temperature does not necessarily result in the lowest energy use. Therefore, in Chapter 6 a sensitivity analysis is performed on the COP of the central heat pump and the heat transfer coefficient of the pipes to quantify the effect on total energy use and the drawn conclusions.

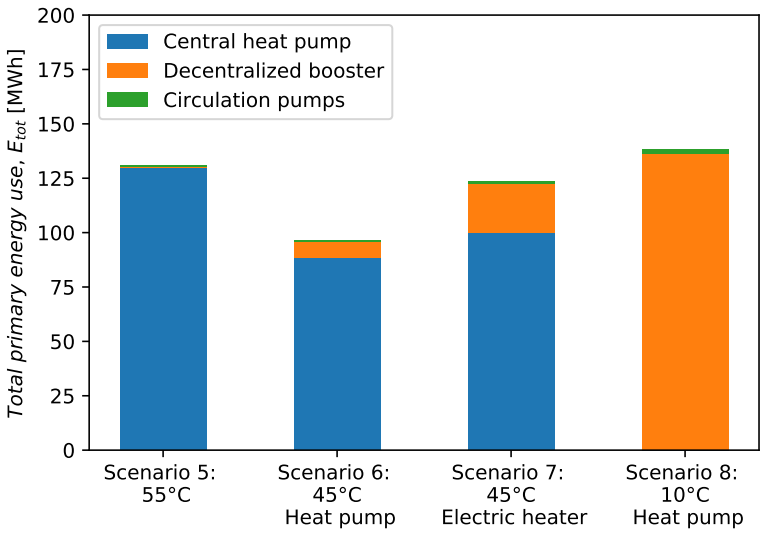

Figure 5.4: Comparison of the total primary energy use for scenarios 5 to 8 with refurbished buildings.

Table 5.6: Performance booster units and central heat pump in scenario 5 to 8.

Scenario	**5**	**6**	**7**	**8**
COP booster units	-	7.7	1	3.2
COP central heat pump	3.6	4.5	4.5	-

5.3.3 Energy efficiency

Figure 5.5 illustrates the overall system energy efficiency for both non-refurbished buildings (scenarios 1 to 4) and refurbished buildings (scenarios 5 to 8). When comparing the energy efficiency, the difference in SH demand is taken into account. The figure clearly demonstrates that a DH network serving refurbished buildings results in higher energy efficiency across all investigated scenarios. The most efficient scenario among the refurbished buildings (scenario 6) achieves an efficiency of 449%, whereas the most efficient scenario among the non-refurbished buildings (scenario 2) achieves an efficiency of 291%. This indicates that measures to reduces the temperature requirements for SH are beneficial to increase the overall energy efficiency of the network.

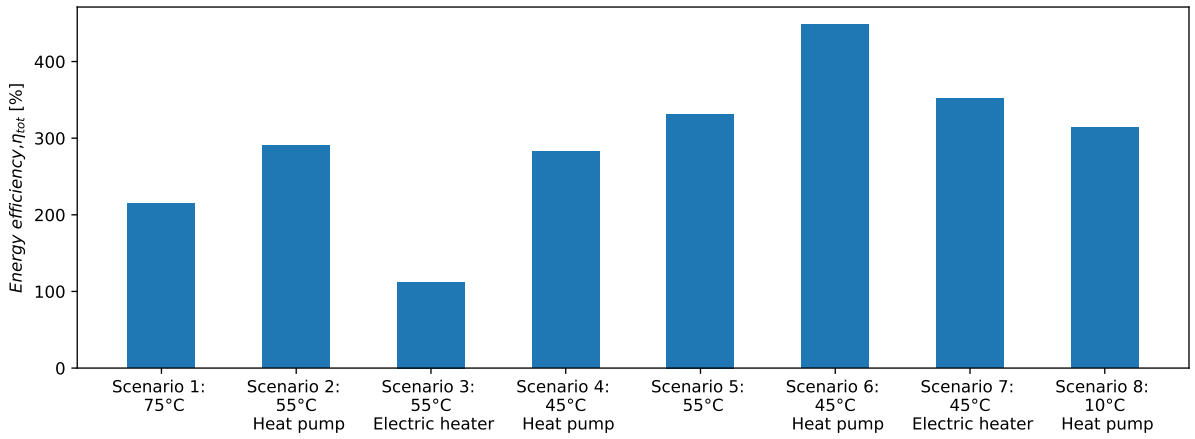

Figure 5.5: Comparison of the total energy efficiency of the DH network for scenarios 1 to 8.

Table 5.7: Performance, energy use and energy efficiency of scenario 1 to 8.

Scenario		**1**	**2**	**3**	**4**	**5**	**6**	**7**	**8**
COP booster [-]	$COP_{booster}$	-	12.7	1	6.6	-	7.7	1	3.2
COP central heat pump [-]	COP_{CH}	2.3	3.6	3.6	4.5	3.6	4.5	4.5	-
Pumping energy [MWh]	E_{pump}	1.2	0.8	0.6	0.9	0.8	0.9	1.0	2.0
Electricity use booster [MWh]	$E_{booster}$	0	42.9	494.4	90.6	0	7.3	22.3	136.4
Electricity use central HP [MWh]	E_{CH}	278.5	163.4	40.4	121.6	130.1	395.4	100.0	0
Total primary energy use [MWh]	E_{tot}	279.7	207.2	535.4	213.1	130.8	96.7	123.3	138.3
DHW demand [MWh]	Q_{DHW}	55.9	55.9	55.9	55.9	55.9	55.9	55.9	55.9
SH demand [MWh]	Q_{SH}	546.0	546.0	546.0	546.0	378.0	378.0	378.0	378.0
Energy efficiency [%]	η_{tot}	215	291	112	282	333	449	352	314

Chapter 6

Sensitivity analysis

In this section, a sensitivity analysis is conducted to assess the impact of varying the COP of the central heat pump and the heat losses in the network on the overall findings. It aims to understand how changes in these parameters affect the conclusions drawn from the analysis in Chapter 5. The network topology, heat demand, and substation layout are assumed to be fixed and specific to this particular case study.

6.1 Coefficient of performance of the central heat pump

The calculation of the COP of the central heat pump is based on the work of Jesper et al. [76] as described in Section 3.3.2. The used empirical formula is based on data obtained from literature or provided by manufacturers. As the network is not currently in operation, the COP of the central heat pump cannot be directly validated. Nonetheless, the COP serves as a crucial parameter that influences the electric energy use of the central heat pump. Hence, in this analysis, the COP is varied to assess its impact on the results and conclusions.

The COP for all scenarios is varied within a range of -20% to +20%, following the approach by Pieper et al. [95]. The variations in total energy use and energy efficiency are depicted in Figure 6.1. It can be observed that the COP of the central heat pump has an influence on the ranking of the scenarios. In non-refurbished buildings, scenario 4 becomes the option with the lowest total energy use and highest efficiency, although the difference with scenario 2 is minimal. The conclusion presented in Chapter 5 does not change. For refurbished buildings, the variation in the COP of the central heat pump influences the ranking of scenarios 5, 7, and 8, as was expected in the analysis of Chapter 5. When the COP of the central heat pump decreases, scenario 8 remains unaffected as it does not involve the use of a central heat pump, and it outperforms scenarios 5 and 7. However, scenario 6 remains the preferred scenario in terms of both total energy use and energy efficiency.

To provide a quantitative overview, Table 6.1 presents the variation in primary energy use and energy efficiency for the extreme cases, where the COP of the central heat pump is increased or decreased by 20%. Observing the table, it is evident that the results of scenarios 1 and 5 are most impacted by variation of the COP of the central heat pump. This can be attributed to the absence of booster units in these scenarios, making the central heat pump's performance relatively more influential. On the other hand, scenario 3 primarily relies on heat from the network for DHW preparation. The electric heaters contribute the largest portion to the total primary energy use in this scenario, thereby reducing the impact of COP variations on the overall results.

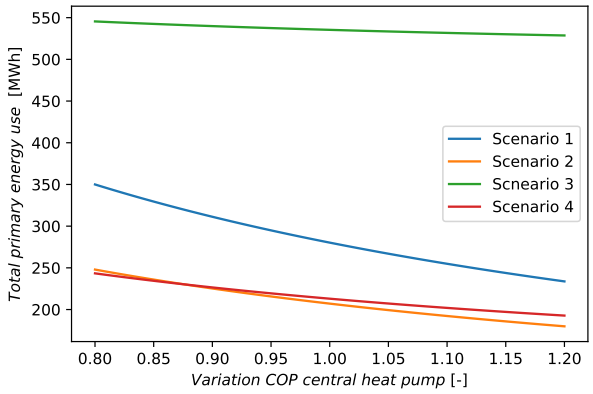

(a) Total energy use non-refurbished buildings

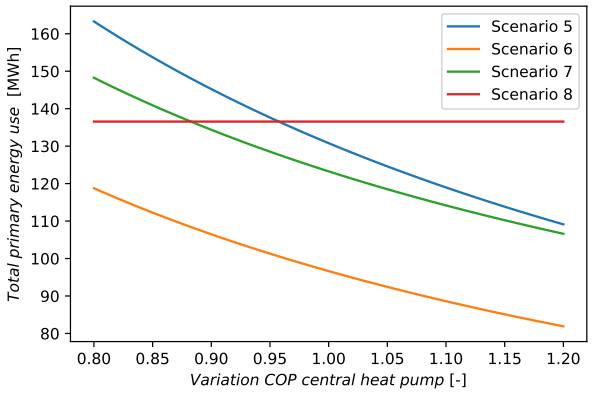

(b) Total energy use refurbished buildings

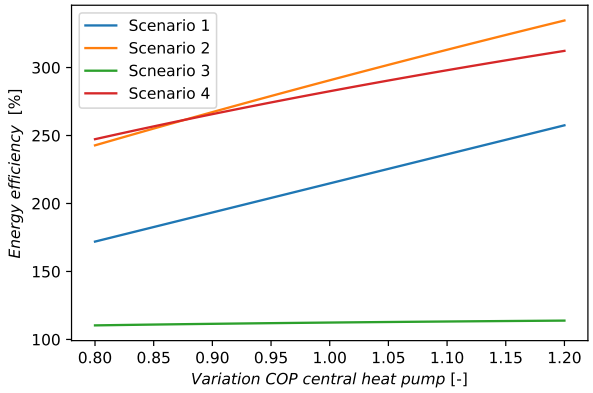

(c) Energy efficiency non-refurbished buildings

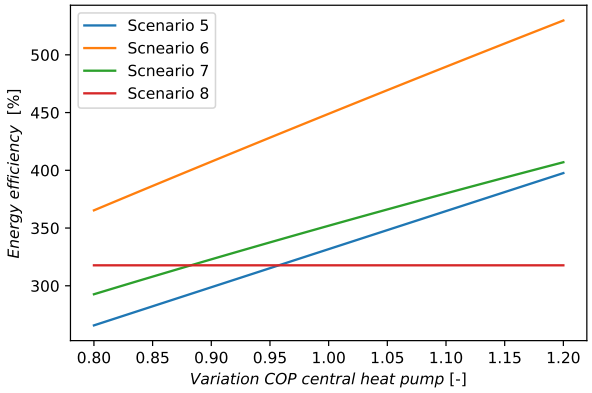

(d) Energy efficiency refurbished buildings

Figure 6.1: Influence on total primary energy use and energy efficiency with a variation of +/-20% of the COP of the central heat pump

Table 6.1: Influence of variations of the COP of the central heat pump on the total primary energy use and energy efficiency of the network.

Scenario	**1**	**2**	**3**	**4**	**5**	**6**	**7**	**8**
Total primary energy use, P_{tot}								
COP +20%	-16.6%	-13.1%	-1.3%	-11.0%	-16.6%	-15.3%	-13.5%	-
COP -20%	+24.9%	+19.7%	+1.9%	16.5%	+24.8%	+22.9%	+20.3 %	-
Energy efficiency, η_{tot}								
COP +20%	+19.9%	+15.1%	+1.3%	+12.4%	+19.9%	+18.0%	+15.6%	-
COP -20%	-19.9%	-16.5%	-1.9%	-14.2%	-19.9%	-18.6%	-16.9%	-

6.2 Heat transfer coefficient

The heat losses in the network are strongly dependent on insulation of the pipes and therefore on the heat transfer coefficient. Higher heat losses increase the temperature drop in the network, which results in higher mass flow rates and increased energy use from the central heat pump. To quantify the influence of the heat transfer coefficient of the pipes on the temperature of the network and the energy use and energy efficiency, the heat transfer coefficient is varied, considering a possible range of values found in literature. In the study of Masatin et al. [96] the heat transfer coefficient is proposed to be a factor for evaluation of the heat loss in a DH network with respect to the pipe inner diameter. The authors present a correlation between the heat transfer coefficient and the pipe inner diameter for low-quality insulation and high-quality insulation, as can be seen in Equation 6.1.

$$K = \frac{Q_{losses}}{2\pi l \Delta T} \tag{6.1}$$

Where K is the heat transfer coefficient [W/m^2/K], Q_{losses} is the heat loss in the DH network [W], l is the pipe length [m] and ΔT is the temperature difference between the water in the pipes and the ambient [K]. The heat transfer coefficient in the study of Masatin et al. is defined differently from the coefficient used in this work, and needs to be multiplied by the pipe's circumference, as can be seen in Equation 6.2.

$$U = 2\pi D_i K \tag{6.2}$$

Where U is the heat transfer coefficient as defined in this study [W/m/K], D_i is the pipe inner diameter [m], and K is the heat transfer coefficient as defined by Masarin et al. [W/m^2/K] [96]. Figure 6.2 presents the values as described in the study of Masatin et al. [96], and the values used in this work. As the heat transfer coefficient already is in the region of high-quality insulated pipes, the sensitivity analysis will consider increased values of the heat transfer coefficient. There is no need to evaluate the performance of the DH network with low quality insulation, as this refers to old DH networks with 50 mm mineral wool insulation, which will not be the case in the new DH network in Ghent. In this sensitivity analysis, the heat transfer coefficient of the pipes is increased by 50% in scenarios 1 and 5, to observe the influence on the results and conclusions drawn in Chapter 5 on two different DH network temperatures.

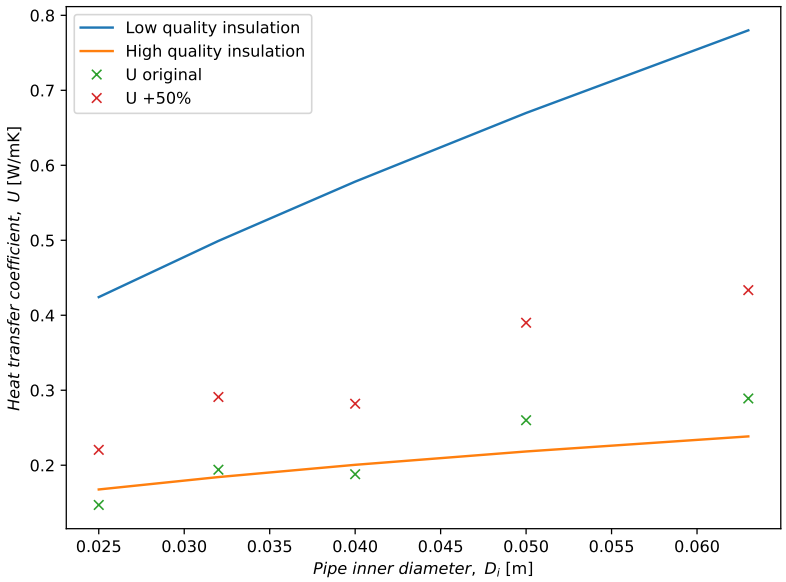

Figure 6.2: Heat transfer coefficients for low quality insulation (blue line) and high quality insulation (orange line) according to Masarin et al. [96], and the heat transfer coefficients used in this study (green crosses) and in the sensitivity analysis (red crosses).

The influence of the increased heat transfer coefficient is shown in Table 6.2. The total primary energy use and energy efficiency are affected more at the high network supply temperature in scenario 1. From this, it can be concluded that the insulation thickness will have the strongest impact in DH networks with high supply temperatures.

Table 6.2: Influence of an increased heat transfer coefficient U of 50% on the total primary energy use and energy efficiency.

	Scenario 1 (75°C)	**Scenario 5 (55°C)**
Total primary energy use, P_{tot}	+ 3.4 %	+ 2.9 %
Energy efficiency, η_{tot}	- 3.3 %	- 3.0 %

Chapter 7

Conclusion

District heating networks are proposed as a solution for decarbonizing the building sector as GHG emissions for space heating and domestic hot water accounts for 35% of the total GHG emissions in Europe. District heating networks offer the advantage of utilizing low-grade heat sources such as waste heat or geothermal heat. Recent studies have focused on lowering the network supply temperature to minimize heat losses in the piping network and enable the integration of low-grade heat or central heat pumps. However, reducing the supply temperature necessitates the use of booster units to meet the temperature requirements for space heating and domestic hot water.

This research analyses the total energy use and energy efficiency of a district heating network with a central heat pump under different network supply temperatures. The study is based on a planned pilot project in Ghent, involving 35 residential buildings. Eight scenarios are investigated, considering both non-refurbished and refurbished buildings, along with booster heat pumps and booster electric heaters. These scenarios are modelled and simulated using Dymola (Modelica).

The findings for non-refurbished buildings demonstrate that lowering the supply temperature to 55°C and 45°C, along with the addition of a booster heat pump, reduces heat losses and improves the performance of the central heat pump, resulting in the lowest total energy use and highest energy efficiency. However, when booster units are not used and the network supply temperature is set at 75°C, the total energy use is only 35% higher compared to the optimal scenario. The latter scenario is worth considering when the investment cost of booster heat pumps is high. The use of electric heaters to increase the temperature for space heating is found to be unfavourable, as it leads to 2.6 times higher total energy use compared to using a booster heat pump and almost twice as high as the scenario without booster units.

For refurbished buildings, a supply temperature of 45°C with decentralized booster heat pumps demonstrates the lowest energy use and highest energy efficiency. The use of booster electric heaters results in only a 28% increase in total energy use and may be an economically viable alternative. The scenario with a supply temperature of 55°C (without booster units) and the scenario with a supply temperature of 10°C (with decentralized heat pumps) show similar results, as the heat losses at 55°C are counterbalanced by the slightly higher performance of the central heat pump compared to the decentralized heat pumps.

The most efficient scenario among the refurbished buildings achieves an efficiency of 449%, whereas the most efficient scenario among the non-refurbished buildings achieves an efficiency of 291%. This indicates that measures to reduces the temperature requirements for SH are beneficial to increase the overall energy efficiency of the network.

A sensitivity analysis shows that the coefficient of performance is a crucial parameter in the analysis of the scenarios with refurbished buildings as it changes the ranking of the scenarios. However, the optimal scenario remains unchanged. On the other hand, variations in heat losses have a limited impact on the results, with more noticeable effects observed at higher supply temperatures.

Future work could focus on optimizing network design and control strategies, which were not covered in this research. A techno-economic analysis can be performed to formulate a conclusion on the optimal scenario from cost perspective.

Bibliography

[1] European Environment Agency. Greenhouse gas emissions from energy use in buildings in Europe, October 2022. https://www.eea.europa.eu/ims/greenhouse-gas-emissions-from-energy.

[2] Aalborg University. Press-Release_roadmap-towards-a-decarbonised-EU-HC-sector.pdf, December 2019. https://heatroadmap.eu/wp-content/uploads/2019/12/Press-Release_Roadmap-towards-a-decarbonised-EU-HC-sector.pdf.

[3] Abdur Rehman Mazhar, Shuli Liu, and Ashish Shukla. A state of art review on the district heating systems. *Renewable and Sustainable Energy Reviews*, 96:420–439, November 2018.

[4] Henrik Lund, Sven Werner, Robin Wiltshire, Svend Svendsen, Jan Eric Thorsen, Frede Hvelplund, and Brian Vad Mathiesen. 4th Generation District Heating (4GDH): Integrating smart thermal grids into future sustainable energy systems. *Energy*, 68:1–11, April 2014.

[5] Katinka Johansen and Sven Werner. Something is sustainable in the state of Denmark: A review of the Danish district heating sector. *Renewable and Sustainable Energy Reviews*, 158:112117, April 2022.

[6] Finnish Energy. Energy Year 2022 - District Heating, January 2023. https://energia.fi/en/newsroom/publications/energy_year_2022_-_district_heating.html#material-view.

[7] Sven Werner. District heating and cooling in Sweden. *Energy*, 126:419–429, May 2017.

[8] Danish energy agency. Energy Statistics 2021. https://ens.dk/sites/ens.dk/files/Statistik/energy_statistics_2021.pdf.

[9] Vlaams energie-en klimaatagentschap. Heating in Flanders. https://energy.ec.europa.eu/system/files/2021-10/be-vlg_ca_2020_en.pdf.

[10] Rasmus Lund and Urban Persson. Mapping of potential heat sources for heat pumps for district heating in Denmark. *Energy*, 110:129–138, September 2016.

[11] Lund H., Mathiesen B.V., Connolly D., and Ostergaard P.A. Renewable energy systems - a smart energy systems approach to the choice and modelling of 100 % renewable solutions. *Chemical Engineering Transactions*, 39:1–6, August 2014.

[12] City of Ghent. Ghent's climate actions | Stad Gent. https://stad.gent/en/city-governance-organisation/city-policy/ghents-climate-actions.

[13] M. A. Sayegh, P. Jadwiszczak, B. P. Axcell, E. Niemierka, K. Brys, and H. Jouhara. Heat pump placement, connection and operational modes in European district heating. *Energy and Buildings*, 166:122–144, May 2018. Place: Lausanne Publisher: Elsevier Science Sa WOS:000429757600010.

[14] Marco Pellegrini and Augusto Bianchini. The Innovative Concept of Cold District Heating Networks: A Literature Review. *Energies*, 11(1):236, January 2018. Number: 1 Publisher: Multidisciplinary Digital Publishing Institute.

[15] Agentschap zorg en gezondheid. Handboek Best Beschikbare Technieken voor Legionellabeheersing | Zorg en Gezondheid, December 2017. https://www.zorg-en-gezondheid.be/handboek-best-beschikbare-technieken-voor-legionellabeheersing.

[16] Henrik Lund, Poul Alberg Ostergaard, Tore Bach Nielsen, Sven Werner, Jan Eric Thorsen, Oddgeir Gudmundsson, Ahmad Arabkoohsar, and Brian Vad Mathiesen. Perspectives on fourth and fifth generation district heating. *Energy*, 227:120520, July 2021. Place: Oxford Publisher: Pergamon-Elsevier Science Ltd WOS:000653079800009.

[17] D. Romanov and B. Leiss. Geothermal energy at different depths for district heating and cooling of existing and future building stock. *Renewable and Sustainable Energy Reviews*, 167:112727, October 2022.

[18] Zhenjun Ma, Paul Cooper, Daniel Daly, and Laia Ledo. Existing building retrofits: Methodology and state-of-the-art. *Energy and Buildings*, 55:889–902, December 2012.

[19] European commision. Energy performance of buildings directive. https://energy.ec.europa.eu/topics/energy-efficiency/energy-efficient-buildings/energy-performance-buildings-directive_en.

[20] European commision. Nearly zero-energy buildings. https://energy.ec.europa.eu/topics/energy-efficiency/energy-efficient-buildings/nearly-zero-energy-buildings_en.

[21] Agoria. Underfloor heating. https://www.agoria.be/en/climate-neutral-building/building-technologies/technical-cards/underfloor-heating.

[22] Wojciech Rzeźnik, Ilona Rzeźnik, and Paweł Hara. Comparison of Real and Forecasted Domestic Hot Water Consumption and Demand for Heat Power in Multifamily Buildings, in Poland. *Energies*, 15(19):6871, January 2022. Number: 19 Publisher: Multidisciplinary Digital Publishing Institute.

[23] M. Z. Pomianowski, H. Johra, A. Marszal-Pomianowska, and C. Zhang. Sustainable and energy-efficient domestic hot water systems: A review. *Renewable and Sustainable Energy Reviews*, 128:109900, August 2020.

[24] Agentschap zorg en gezondheid. Legionella | Zorg en Gezondheid. https://www.zorg-en-gezondheid.be/per-domein/preventie/legionella.

[25] M. Köfinger, D. Basciotti, R. R. Schmidt, E. Meissner, C. Doczekal, and A. Giovannini. Low temperature district heating in Austria: Energetic, ecologic and economic comparison of four case studies. *Energy*, 110:95–104, September 2016.

[26] Torben Ommen, Wiebke Brix Markussen, and Brian Elmegaard. Lowering district heating temperatures – Impact to system performance in current and future Danish energy scenarios. *Energy*, 94:273–291, January 2016.

[27] Brian Elmegaard, Torben Schmidt Ommen, Michael Markussen, and Johnny Iversen. Integration of space heating and hot water supply in low temperature district heating. *Energy and Buildings*, 124:255–264, July 2016.

[28] Xiaochen Yang and Svend Svendsen. Ultra-low temperature district heating system with central heat pump and local boosters for low-heat-density area: Analyses on a real case in Denmark. *Energy*, 159:243–251, September 2018. Place: Oxford Publisher: Pergamon-Elsevier Science Ltd WOS:000442973300022.

[29] E Zvingilaite, T Ommen, B Elmegaard, and M L Franck. LOW TEMPERATURE DISTRICT HEATING CONSUMER UNIT WITH MICRO HEAT PUMP FOR DOMESTIC HOT WATER PREPARATION. page 9, 2012.

[30] Poul Alberg Østergaard and Anders N. Andersen. Booster heat pumps and central heat pumps in district heating. *Applied Energy*, 184:1374–1388, December 2016.

[31] Xiaochen Yang, Hongwei Li, and Svend Svendsen. Evaluations of different domestic hot water preparing methods with ultra-low-temperature district heating. *Energy*, 109:248–259, August 2016. Place: Oxford Publisher: Pergamon-Elsevier Science Ltd WOS:000382591000021.

[32] IRENA. Renewables Take Lions Share of Global Power Additions in 2021, April 2022. `https://www.irena.org/news/pressreleases/2022/Apr/Renewables-Take-Lions-Share-of-Global-Power-Additions-in-2021`.

[33] Abdelazim Abbas Ahmed, Mohsen Assadi, Adib Kalantar, Tomasz Sliwa, and Aneta Sapińska-Śliwa. A Critical Review on the Use of Shallow Geothermal Energy Systems for Heating and Cooling Purposes. *Energies*, 15(12):4281, January 2022. Number: 12 Publisher: Multidisciplinary Digital Publishing Institute.

[34] Carolin Tissen, Kathrin Menberg, Peter Bayer, and Philipp Blum. Meeting the demand: geothermal heat supply rates for an urban quarter in Germany. *Geothermal Energy*, 7(1):9, March 2019.

[35] Stuart J. Self, Bale V. Reddy, and Marc A. Rosen. Geothermal heat pump systems: Status review and comparison with other heating options. *Applied Energy*, 101:341–348, January 2013.

[36] Abdeen Mustafa Omer. Ground-source heat pumps systems and applications. *Renewable and Sustainable Energy Reviews*, 12(2):344–371, February 2008.

[37] J. Hanova and H. Dowlatabadi. Strategic GHG reduction through the use of ground source heat pump technology. *Environmental Research Letters*, 2(4):044001, November 2007.

[38] Jin Luo, Joachim Rohn, Manfred Bayer, Anna Priess, Lucas Wilkmann, and Wei Xiang. Heating and cooling performance analysis of a ground source heat pump system in Southern Germany. *Geothermics*, 53:57–66, January 2015.

[39] Vlaanderen. Warmtepomp. `https://www.vlaanderen.be/zoek?q=temperatuur%20grondwater`.

[40] Xinguo Li, Zhihao Chen, and Jun Zhao. Simulation and experiment on the thermal performance of U-vertical ground coupled heat exchanger. *Applied Thermal Engineering*, 26(14):1564–1571, October 2006.

[41] Kristian Duus and Gerhard Schmitz. Experimental investigation of sustainable and energy efficient management of a geothermal field as a heat source and heat sink for a large office building. *Energy and Buildings*, 235:110726, March 2021.

[42] IEA. Heat Pumps – Analysis. `https://www.iea.org/reports/heat-pumps`.

[43] M. A. Sayegh, J. Danielewicz, T. Nannou, M. Miniewicz, P. Jadwiszczak, K. Piekarska, and H. Jouhara. Trends of European research and development in district heating technologies. *Renewable and Sustainable Energy Reviews*, 68:1183–1192, February 2017.

[44] European heat pump association. Types of heat pumps. `https://www.ehpa.org/about-heat-pumps/types-of-heat-pumps/`.

[45] Andrei David, Brian Vad Mathiesen, Helge Averfalk, Sven Werner, and Henrik Lund. Heat Roadmap Europe: Large-Scale Electric Heat Pumps in District Heating Systems. *Energies*, 10(4):578, April 2017. Number: 4 Publisher: Multidisciplinary Digital Publishing Institute.

[46] K. Kontu, S. Rinne, and S. Junnila. Introducing modern heat pumps to existing district heating systems - Global lessons from viable decarbonizing of district heating in Finland. *Energy*, 166:862–870, January 2019. Place: Oxford Publisher: Pergamon-Elsevier Science Ltd WOS:000455694300071.

[47] A. Volkova, H. Koduvere, and H. Pieper. Large-scale heat pumps for district heating systems in the Baltics: Potential and impact. *Renewable and Sustainable Energy Reviews*, 167:112749, October 2022.

[48] Rasmus Lund, Danica Djuric Ilic, and Louise Trygg. Socioeconomic potential for introducing large-scale heat pumps in district heating in Denmark. *Journal of Cleaner Production*, 139:219–229, December 2016. Place: Oxford Publisher: Elsevier Sci Ltd WOS:000386991600019.

[49] Helge Averfalk, Paul Ingvarsson, Urban Persson, Mei Gong, and Sven Werner. Large heat pumps in Swedish district heating systems. *Renewable & Sustainable Energy Reviews*, 79:1275–1284, November 2017. Place: Oxford Publisher: Pergamon-Elsevier Science Ltd WOS:000410011500091.

[50] Torben Ommen and Brian Elmegaard. Exergetic evaluation of heat pump booster configurations in a low temperature district heating network. page 15, 2012.

[51] R. Lund, D.S. Østergaard, X. Yang, and B.V. Mathiesen. Comparison of low-temperature district heating concepts in a long-term energy system perspective. *International Journal of Sustainable Energy Planning and Management*, 12:5–18, 2017.

[52] Xiaochen Yang and Svend Svendsen. Achieving low return temperature for domestic hot water preparation by ultra-low-temperature district heating. *Energy Procedia*, 116:426–437, June 2017.

[53] Halil Ibrahim Topal, Hakan Ibrahim Tol, Mehmet Kopal, and Ahmad Arabkoohsar. Energy, exergy and economic investigation of operating temperature impacts on district heating systems: Transition from high to low-temperature networks. *Energy*, 251:123845, July 2022. Place: Oxford Publisher: Pergamon-Elsevier Science Ltd WOS:000798568100002.

[54] Marzena Nowak-Oclon and Pawel Oclon. Thermal and economic analysis of preinsulated and twin-pipe heat network operation. *Energy*, 193:1310–1318, February 2020. Place: Oxford Publisher: Pergamon-Elsevier Science Ltd WOS:000518699000103.

[55] Ali Sulaiman Alsagri, Ahmad Arabkoohsar, Milad Khosravi, and Abdulrahman A. Alrobaian. Efficient and cost-effective district heating system with decentralized heat storage units, and triple-pipes. *Energy*, 188:116035, December 2019. Place: Oxford Publisher: Pergamon-Elsevier Science Ltd WOS:000505271100022.

[56] Milad Khosravi and Ahmad Arabkoohsar. Thermal-Hydraulic Performance Analysis of Twin-Pipes for Various Future District Heating Schemes. *Energies*, 12(7):1299, April 2019. Place: Basel Publisher: Mdpi WOS:000465561400116.

[57] Ahmad Arabkoohsar, Ali Sulaiman Alsagri, and Milad Khosravi. Thermal performance analysis of triple pipes for district heating systems: A comparison with twin pipes and the literature results. *Journal of Thermal Analysis and Calorimetry*, 139(3):1993–2003, February 2020. Place: Dordrecht Publisher: Springer WOS:000534480300036.

[58] Mei Gong and Sven Werner. Exergy analysis of network temperature levels in Swedish and Danish district heating systems. *Renewable Energy*, 84:106–113, December 2015.

[59] Poul Alberg Ostergaard and Anders N. Andersen. Economic feasibility of booster heat pumps in heat pump-based district heating systems. *Energy*, 155:921–929, July 2018. Place: Oxford Publisher: Pergamon-Elsevier Science Ltd WOS:000445303100076.

[60] Hanmin Cai, Charalampos Ziras, Shi You, Rongling Li, Kristian Honoré, and Henrik W. Bindner. Demand side management in urban district heating networks. *Applied Energy*, 230:506–518, November 2018.

[61] Jacopo Vivian, Giuseppe Emmi, Angelo Zarrella, Xavier Jobard, Dirk Pietruschka, and Michele De Carli. Evaluating the cost of heat for end users in ultra low temperature district heating networks with booster heat pumps. *Energy*, 153:788–800, June 2018. Place: Oxford Publisher: Pergamon-Elsevier Science Ltd WOS:000436651100071.

[62] Rossano Scoccia, Tommaso Toppi, Marcello Aprile, and Mario Motta. Absorption and compression heat pump systems for space heating and DHW in European buildings: Energy, environmental and economic analysis. *Journal of Building Engineering*, 16:94–105, March 2018.

[63] Yumei Zhang, Pengfei Jie, Chunhua Liu, and Jing Li. Optimizing environmental insulation thickness of buildings with CHP-based district heating system based on amount of energy and energy grade. *Frontiers in Energy*, 16(4):613–628, August 2022.

[64] Sebastian Seebauer. The psychology of rebound effects: Explaining energy efficiency rebound behaviours with electric vehicles and building insulation in Austria. *Energy Research & Social Science*, 46:311–320, December 2018.

[65] BRUGG Pipes. FLEXSTAR pipe system – The flexible and reliable star | BRUGG Pipes. `https://www.bruggpipes.com/en/flexstar/`.

[66] Marouf Pirouti, Audrius Bagdanavicius, Janaka Ekanayake, Jianzhong Wu, and Nick Jenkins. Energy consumption and economic analyses of a district heating network. *Energy*, 57:149–159, August 2013.

[67] H. İ. Tol and S. Svendsen. Improving the dimensioning of piping networks and network layouts in low-energy district heating systems connected to low-energy buildings: A case study in Roskilde, Denmark. *Energy*, 38(1):276–290, February 2012.

[68] Isabelle Best, Janybek Orozaliev, and Klaus Vajen. Impact of Different Design Guidelines on the Total Distribution Costs of 4th Generation District Heating Networks. *Energy Procedia*, 149:151–160, September 2018.

[69] Fabian Ochs, Mara Magni, and Georgios Dermentzis. Integration of Heat Pumps in Buildings and District Heating Systems—Evaluation on a Building and Energy System Level. *Energies*, 15(11):3889, January 2022. Number: 11 Publisher: Multidisciplinary Digital Publishing Institute.

[70] Yu Luo, Yixiang Shi, and Ningsheng Cai. Chapter 2 - Distributed hybrid system and prospect of the future Energy Internet. In Yu Luo, Yixiang Shi, and Ningsheng Cai, editors, *Hybrid Systems and Multi-energy Networks for the Future Energy Internet*, pages 9–39. Academic Press, January 2021.

[71] Google. Google Maps. https://www.google.ca/maps/@51.0785719,3.7317979,18.25z.

[72] Tatu Laajalehto, Maunu Kuosa, Tapio Mäkilä, Markku Lampinen, and Risto Lahdelma. Energy efficiency improvements utilising mass flow control and a ring topology in a district heating network. *Applied Thermal Engineering*, 69(1):86–95, August 2014.

[73] S. E. Haaland. Simple and Explicit Formulas for the Friction Factor in Turbulent Pipe Flow. *Journal of Fluids Engineering*, 105(1):89–90, March 1983.

[74] C. F. Colebrook, C. M. White, and Geoffrey Ingram Taylor. Experiments with fluid friction in roughened pipes. *Proceedings of the Royal Society of London. Series A - Mathematical and Physical Sciences*, 161(906):367–381, January 1997. Publisher: Royal Society.

[75] Wilo. Wilo-Stratos MAXO | Wilo. https://wilo.com/be/nl/Producten-en-competenties/nl/producten-expertise/wilo-stratos-maxo?t=1#c8ae2889e58f131940158f310b6a70d4eTL4_range_description.

[76] Mateo Jesper, Florian Schlosser, Felix Pag, Timothy Gordon Walmsley, Bastian Schmitt, and Klaus Vajen. Large-scale heat pumps: Uptake and performance modelling of market-available devices. *Renewable and Sustainable Energy Reviews*, 137:110646, March 2021.

[77] BDEW Bundesverband der Energie-und Wasserwirtschaft e. V. Energiemarkt_deutschland_2020_englisch.pdf. https://www.bdew.de/media/documents/Energiemarkt_Deutschland_2020_englisch.pdf.

[78] Meteoblue. Weather Archive Ghent. https://www.meteoblue.com/en/weather/archive/era5/ghent_belgium_2797656.

[79] VREG. Wie zijn we? Wat doen we?, December 2018. https://www.vreg.be/nl/wie-zijn-we-wat-doen-we.

[80] VREG. Energieverbruik, December 2018. https://www.vreg.be/nl/energieverbruik.

[81] U. Jordan and K. Vajen. DHWcalc: PROGRAM TO GENERATE DOMESTIC HOT WATER PROFILES WITH STATISTICAL MEANS FOR USER DEFINED CONDITIONS. 2005.

[82] Eddy Janssen. Conceptfiche-0-algemeen_nov2017_v1temp.pdf. https://www.instal2020.be/wp-content/uploads/2016/09/Conceptfiche-0-algemeen_nov2017_V1Temp.pdf.

[83] Silke Verbruggen, Marc Delghust, Jelle Laverge, and Arnold Janssens. Stochastic Occupant Behavior Model Based on Activity And Occupancy Patterns. pages 2310–2317, Rome, Italy.

[84] Ruben Baetens and Dirk Saelens. Modelling uncertainty in district energy simulations by residential occupant behaviour. *Journal of Building Performance Simulation*, 9:431–447, June 2016.

[85] Modelica Association. Modelica Language — Modelica Association. https://modelica.org/modelicalanguage.html.

[86] Dassault Systèmes®. Dymola - Dassault Systèmes®. https://www.3ds.com/products-services/catia/products/dymola/.

[87] Modelica Association. Modelica Libraries — Modelica Association. https://modelica.org/libraries.html.

[88] F. Jorissen, G. Reynders, R. Baetens, D. Picard, D. Saelens, and L. Helsen. Implementation and verification of the IDEAS building energy simulation library. *Journal of Building Performance Simulation*, 11(6):669–688, November 2018.

[89] Michael Wetter, Wangda Zuo, Thierry S. Nouidui, and Xiufeng Pang. Modelica Buildings library. *Journal of Building Performance Simulation*, 7(4):253–270, July 2014. http://www.tandfonline.com/doi/abs/10.1080/19401493.2013.765506.

[90] P. I. D. Tuner. PID Tuner. https://pidtuner.com/.

[91] Rickard Hägg. Dynamic Simulation of District Heating Networks in Dymola. https://lup.lub.lu.se/luur/download?func=downloadFile&recordOId=8883842&fileOId=8883845.

[92] Modelica.org. Modelica.Media.Water.ConstantPropertyLiquidWater. https://doc.modelica.org/Modelica%203.2.3/Resources/helpDymola/Modelica_Media_Water_ConstantPropertyLiquidWater.html.

[93] J. Danielewicz, B. Sniechowska, M. A. Sayegh, N. Fidorow, and H. Jouhara. Three-dimensional numerical model of heat losses from district heating network pre-insulated pipes buried in the ground. *Energy*, 108:172–184, August 2016. Place: Oxford Publisher: Pergamon-Elsevier Science Ltd WOS:000382414200019.

[94] Stanislav Chicherin. A method for assessing heat losses in developing countries with a focus on operational data of a district heating (DH) system. *Sustainable Energy, Grids and Networks*, 30:100616, June 2022.

[95] Henrik Pieper, Torben Ommen, Jonas Kjær Jensen, Brian Elmegaard, and Wiebke Brix Markussen. Comparison of COP estimation methods for large-scale heat pumps used in energy planning. *Energy*, 205:117994, August 2020.

[96] Vladislav Masatin, Eduard Latõšev, and Anna Volkova. Evaluation Factor for District Heating Network Heat Loss with Respect to Network Geometry. *Energy Procedia*, 95:279–285, September 2016.

Appendix A

Data sheets

A.1 FLEXSTAR UNO

Sortiment FLEXSTAR

FLEXSTAR UNO (Heizung 6 bar)

FLEXSTAR
in Ringen:
Dimensionen:
FXS Ø 70 - 105 mm

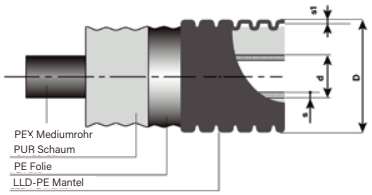

FLEXSTAR Heizung 6 bar, UNO

Typ	Innenrohr PEX d x s mm	Nennweite DN	Zoll "	Aussenmantel D x s1 mm	Minimaler Wickelradius m	Volumen Innenrohr l/m	Gewicht kg/m	maximale Lieferlänge m
25/ 70	25 x 2.3	20	¾	71 x 1.5	0.30	0.32	0.73	200
32/ 70	32 x 2.9	25	1	71 x 1.5	0.30	0.53	0.84	200
40/ 90	40 x 3.7	32	1¼	90 x 1.6	0.30	0.83	1.25	200
50/ 90	50 x 4.6	40	1½	90 x 1.6	0.30	1.30	1.44	200
63/105	63 x 5.8	50	2	106 x 1.7	0.30	2.07	2.07	200

Grössere oder kürzere Lieferlängen können auf Anfrage auf Trommeln geliefert werden.

Bei Bestellung auf die Baustelle bitte Gesamtgewicht des Ringes beachten (Abwickelvorrichtungen)

Druckverlustdiagramm

FLEXSTAR (Heizung 6 bar)

Wassertemperatur 80 °C
Oberflächenrauhigkeit ε = 0.007 mm (PEX)
(1 mmWS = 9.81 Pa)

$$\dot{m} \approx \frac{Q \cdot 860}{\Delta T}$$

$\dot{m}$	=	Durchfluss in kg/h
Q	=	Leistungsbedarf in kW
ΔT	=	Temperaturdifferenz VL/RL in °C

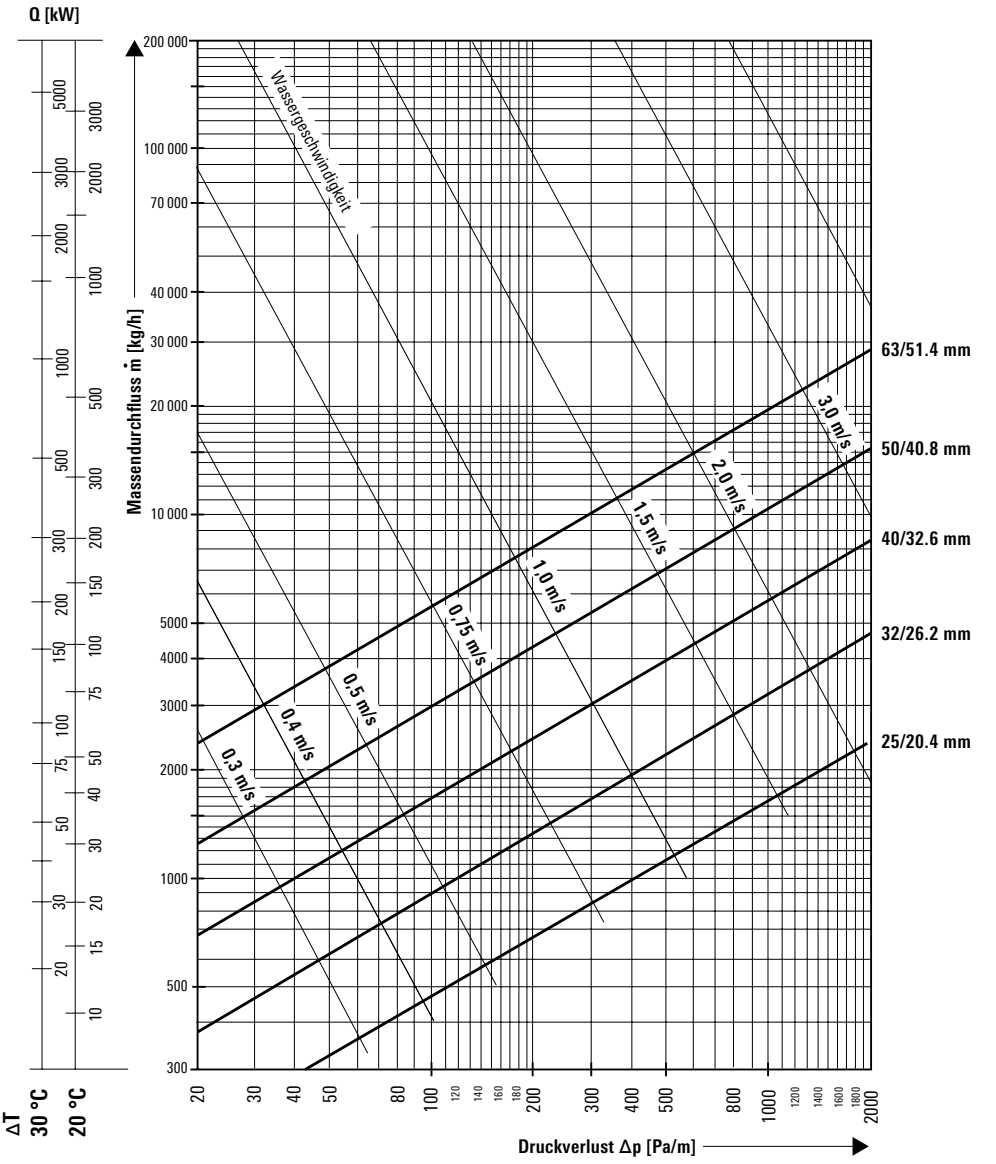

28.03.2023
Technische Änderungen vorbehalten.

BRUGG Pipes

Wärmeverlust

FLEXSTAR (Heizung 6 bar)

FLEXSTAR UNO

Wärmeverluste q [W/m] für ein UNO Rohr							
Typ	**U-Wert**	**mittlere Betriebstemperatur T_B [°C]**					
	[W/mK]	**40°**	**50°**	**60°**	**70°**	**80°**	**90°**
25/ 70	0.1470	4.41	5.88	7.35	8.82	10.29	11.76
32/ 70	0.1940	5.82	7.76	9.70	11.64	13.58	15.52
40/ 90	0.1880	5.64	7.52	9.40	11.28	13.16	15.04
50/ 90	0.2600	7.80	10.40	13.00	15.60	18.20	20.80
63/105	0.2890	8.67	11.56	14.45	17.34	20.23	23.12

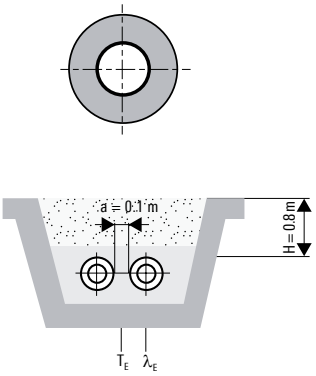

FLEXSTAR DUO (Vorlauf und Rücklauf in einem Rohr)

Wärmeverluste q [W/m] für ein DUO Rohr							
Typ	**U-Wert**	**mittlere Betriebstemperatur T_B [°C]**					
	[W/mK]	**40°**	**50°**	**60°**	**70°**	**80°**	**90°**
25 + 25/ 90	0.2280	6.84	9.12	11.40	13.68	15.96	18.24
32 + 32/105	0.2510	7.53	10.04	12.55	15.06	17.57	20.08
40 + 40/125	0.2620	7.86	10.48	13.10	15.72	18.34	20.96
50 + 50/150	0.2820	8.46	11.28	14.10	16.92	19.74	22.56

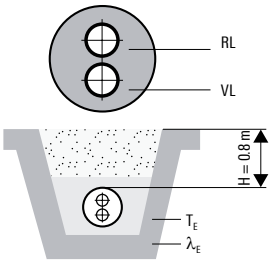

Verlegeart FXS UNO:	2-Rohr erdverlegt
Verlegeart FXS DUO:	1-Rohr erdverlegt
Rohrabstand:	a = 0.10 m
Überdeckungshöhe:	H = 0.80 m
Erdreichtemperatur:	T_E = 10 °C
Leitfähigkeit des Bodens:	λ_E = 1.0 W/mK
Leitfähigkeit des PUR-Schaumes:	λPU = 0.024 W/mK
* Leitfähigkeit des PEX-Rohres:	λPEX = 0.38 W/mK
Leitfähigkeit des PE-Mantels:	λPE = 0.33 W/mK
Messtemperatur für λ:	T_λ = 50 °C

Wärmeverlust im Betrieb:

$q = U (T_B - T_E)$ [W/m]

U = Wärmedurchgangskoeffizient [W/mK]

T_B = Mittlere Betriebstemperatur [°C]

T_E = Mittlere Erdreichtemperatur [°C]

VL = Vorlauf

RL = Rücklauf

28.03.2023

Technische Änderungen vorbehalten.

BRUGG Pipes

A.2 Wilo Stratos MAXO 25/0,5-8 PN10-R7

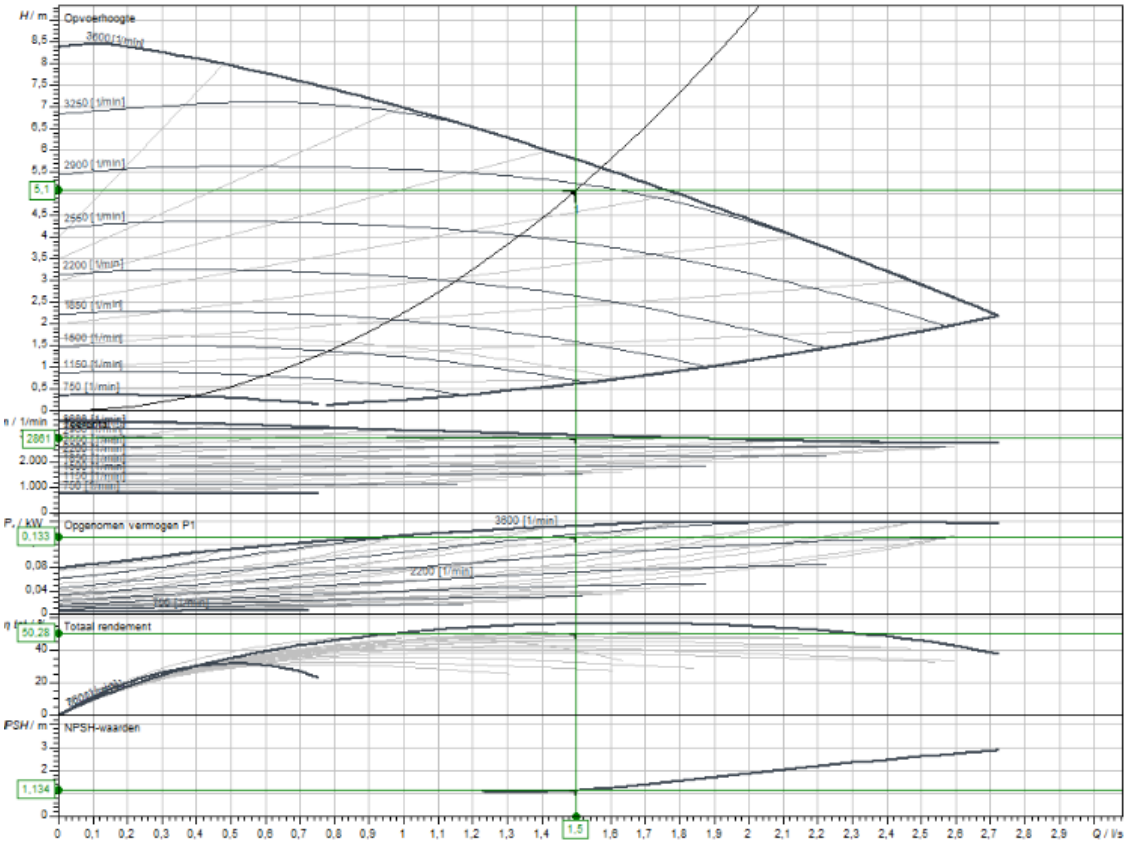

Vloeistof	Water 100 %
Mediumtemperatuur *T*	20,00 °C
Debiet *Q*	1,50 l/s
Opvoerhoogte (drukeenheid)	5,10 m (49,94 kPa)
Geleverd debiet	1,50 l/s
Opvoerhoogte (drukeenheid) in het bedrijfspunt	5,10 m (49,94 kPa)
Toerental op het bedrijfspunt	2.861 1/min
Totaal opgenomen elektrisch vermogen op bedrijfspunt	0,13 kW
Totaal asvermogen op bedrijfspunt	0,09 kW
NPSH pump @ BP	1,13 m
Hydraulisch rendement in het bedrijfspunt	80,11 %
Totaal rendement in het bedrijfspunt	50,28 %

A.3 Wilo Stratos MAXO 30/0,5-12 PN 16

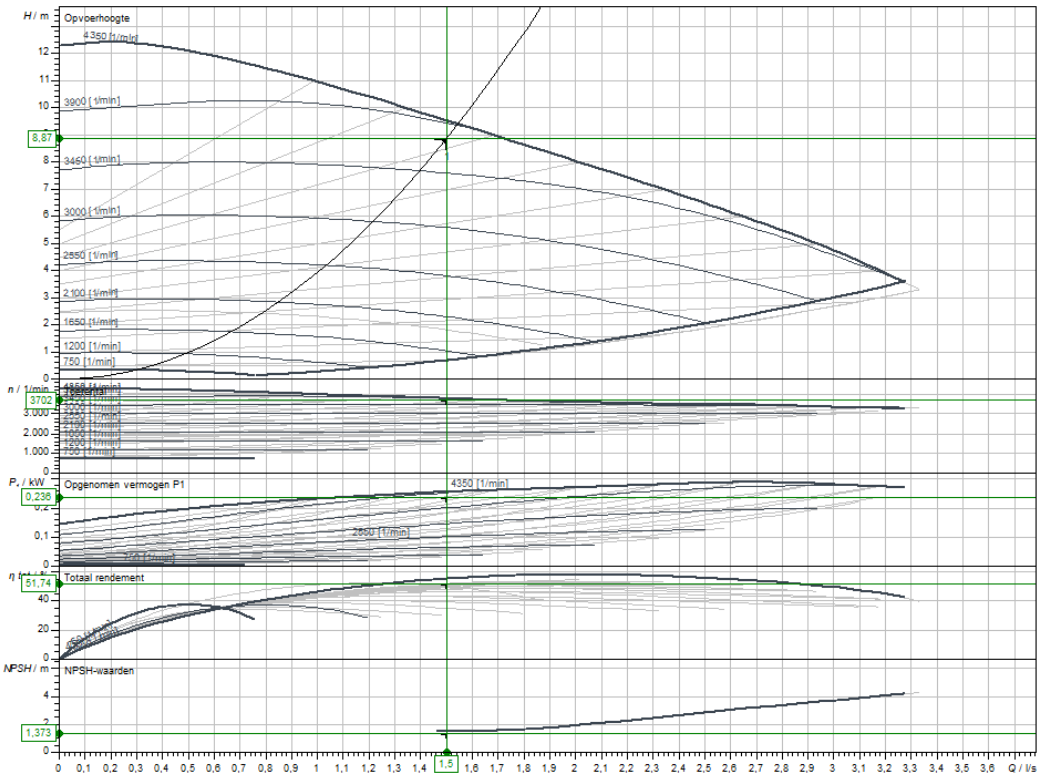

Vloeistof	Water 100 %
Mediumtemperatuur *T*	20,00 °C
Debiet *Q*	1,50 l/s
Opvoerhoogte (drukeenheid)	8,87 m (86,86 kPa)
Geleverd debiet	1,50 l/s
Opvoerhoogte (drukeenheid) in het bedrijfspunt	8,87 m (86,86 kPa)
Toerental op het bedrijfspunt	3.702 1/min
Totaal opgenomen elektrisch vermogen op bedrijfspunt	0,24 kW
Totaal asvermogen op bedrijfspunt	0,18 kW
NPSH pump @ BP	1,37 m
Hydraulisch rendement in het bedrijfspunt	73,04 %
Totaal rendement in het bedrijfspunt	51,74 %

A.4 Wilo Stratos MAXO 32/0,5-12 PN6/10-R7

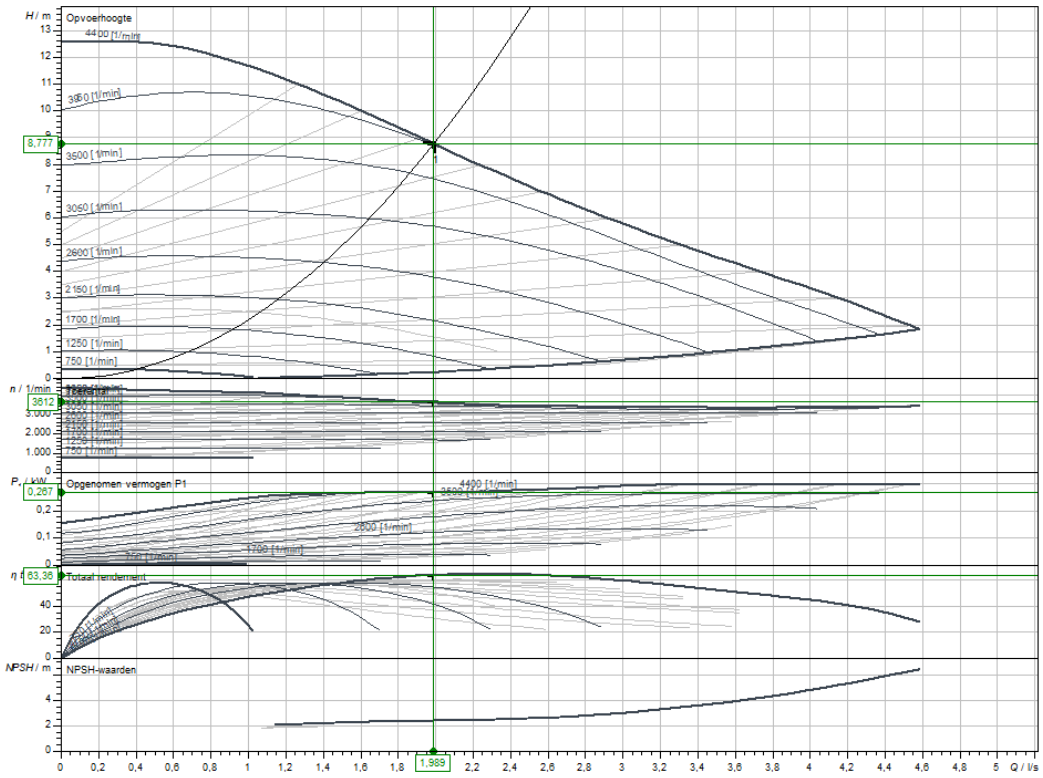

Vloeistof	Water 100 %
Mediumtemperatuur *T*	20,00 °C
Debiet *Q*	2,00 l/s
Opvoerhoogte (drukeenheid)	8,87 m (86,86 kPa)
Geleverd debiet	1,99 l/s
Opvoerhoogte (drukeenheid) in het bedrijfspunt	8,78 m (85,94 kPa)
Toerental op het bedrijfspunt	3.612 1/min
Totaal opgenomen elektrisch vermogen op bedrijfspunt	0,27 kW
Totaal asvermogen op bedrijfspunt	0,20 kW
NPSH pump @ BP	2,40 m
Hydraulisch rendement in het bedrijfspunt	83,81 %
Totaal rendement in het bedrijfspunt	63,36 %

A.5 Wilo Stratos MAXO 40/0,5-12 PN 16

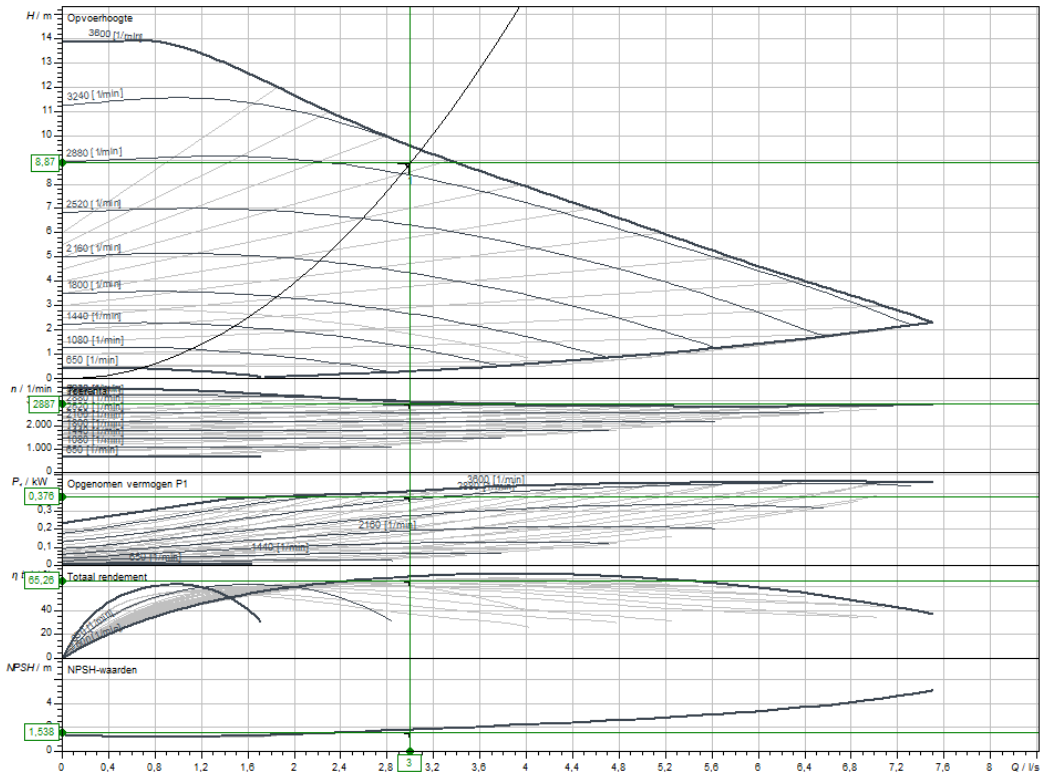

Vloeistof	Water 100 %
Mediumtemperatuur *T*	20,00 °C
Debiet *Q*	3,00 l/s
Opvoerhoogte (drukeenheid)	8,87 m (86,86 kPa)
Geleverd debiet	3,00 l/s
Opvoerhoogte (drukeenheid) in het bedrijfspunt	8,87 m (86,86 kPa)
Toerental op het bedrijfspunt	2.887 1/min
Totaal opgenomen elektrisch vermogen op bedrijfspunt	0,38 kW
Totaal asvermogen op bedrijfspunt	0,30 kW
NPSH pump @ BP	1,54 m
Hydraulisch rendement in het bedrijfspunt	84,86 %
Totaal rendement in het bedrijfspunt	65,26 %

A.6 Wilo Stratos MAXO 50/0,5-12 PN16

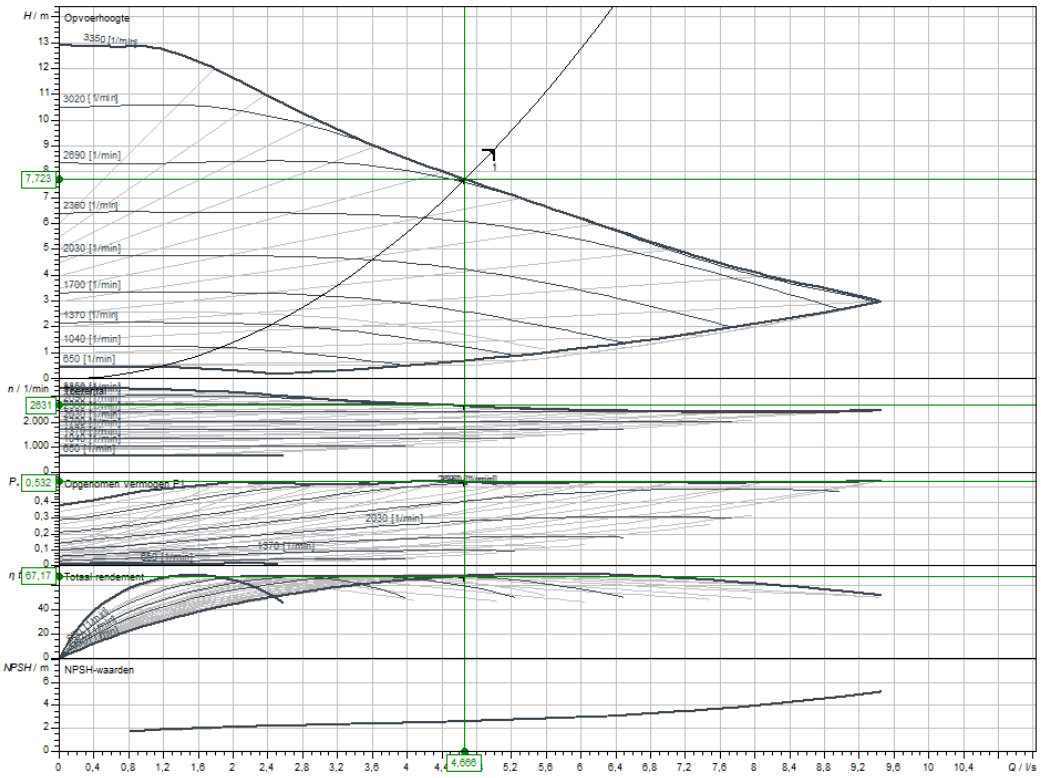

Vloeistof	Water 100 %
Mediumtemperatuur *T*	20,00 °C
Debiet *Q*	5,00 l/s
Opvoerhoogte (drukeenheid)	8,87 m (86,86 kPa)
Geleverd debiet	4,67 l/s
Opvoerhoogte (drukeenheid) in het bedrijfspunt	7,72 m (75,63 kPa)
Toerental op het bedrijfspunt	2.631 1/min
Totaal opgenomen elektrisch vermogen op bedrijfspunt	0,53 kW
Totaal asvermogen op bedrijfspunt	0,42 kW
NPSH pump @ BP	2,62 m
Hydraulisch rendement in het bedrijfspunt	84,60 %
Totaal rendement in het bedrijfspunt	67,17 %

Appendix B

Pipe dimensions

Table B.1: Dimensions segments supply pipe.

Scenario		**1**	**2**	**3**	**4**	**5**	**6**	**7**	**8**
Pipe segment	*Length [m]*				*Diameter [m]*				
1	20	0.05	0.05	0.04	0.063	0.05	0.05	0.063	0.09
2	5	0.05	0.05	0.04	0.063	0.05	0.05	0.063	0.09
3	5	0.05	0.05	0.04	0.063	0.05	0.05	0.063	0.09
4	5	0.05	0.05	0.04	0.063	0.05	0.05	0.063	0.09
5	5	0.05	0.05	0.04	0.063	0.05	0.05	0.063	0.09
6	5	0.05	0.05	0.04	0.063	0.05	0.05	0.063	0.09
7	5	0.05	0.05	0.04	0.063	0.05	0.05	0.05	0.09
8	5	0.05	0.05	0.04	0.063	0.05	0.04	0.05	0.09
9	5	0.05	0.05	0.04	0.063	0.05	0.04	0.05	0.09
10	5	0.05	0.05	0.04	0.063	0.05	0.04	0.05	0.09
11	5	0.05	0.04	0.04	0.063	0.05	0.04	0.05	0.09
12	5	0.05	0.04	0.04	0.063	0.05	0.04	0.05	0.09
13	5	0.05	0.04	0.04	0.063	0.05	0.04	0.05	0.09
14	5	0.05	0.04	0.04	0.063	0.05	0.04	0.05	0.09
15	5	0.05	0.04	0.04	0.063	0.05	0.04	0.05	0.09
16	5	0.05	0.04	0.04	0.063	0.04	0.04	0.05	0.09
17	5	0.05	0.04	0.04	0.05	0.04	0.04	0.05	0.063
18	5	0.04	0.04	0.04	0.05	0.04	0.04	0.05	0.063
19	5	0.04	0.04	0.032	0.05	0.04	0.04	0.05	0.063
20	5	0.04	0.04	0.032	0.05	0.04	0.04	0.04	0.063
21	5	0.04	0.04	0.032	0.05	0.04	0.032	0.04	0.063
22	5	0.04	0.04	0.032	0.05	0.04	0.032	0.04	0.063
23	5	0.04	0.032	0.032	0.05	0.04	0.032	0.04	0.063
24	5	0.04	0.032	0.032	0.05	0.04	0.032	0.04	0.063
25	5	0.04	0.032	0.032	0.05	0.032	0.032	0.04	0.063
26	5	0.032	0.032	0.032	0.04	0.032	0.032	0.04	0.05
27	5	0.032	0.032	0.025	0.04	0.032	0.032	0.032	0.05
28	5	0.032	0.032	0.025	0.04	0.032	0.032	0.032	0.05
29	5	0.032	0.025	0.025	0.04	0.032	0.025	0.032	0.05
30	5	0.032	0.025	0.025	0.04	0.032	0.025	0.032	0.05
31	5	0.025	0.025	0.025	0.032	0.025	0.025	0.032	0.04
32	5	0.025	0.025	0.025	0.032	0.025	0.025	0.025	0.04
33	5	0.025	0.025	0.025	0.032	0.025	0.025	0.025	0.032
34	5	0.025	0.025	0.025	0.025	0.025	0.025	0.025	0.032
35	5	0.025	0.025	0.025	0.025	0.025	0.025	0.025	0.025

Table B.2: Dimensions segments return pipe.

Scenario		**1**	**2**	**3**	**4**	**5**	**6**	**7**	**8**
Pipe segment	*Length [m]*				*Diameter [m]*				
1	5	0.025	0.025	0.025	0.025	0.025	0.025	0.025	0.025
2	5	0.025	0.025	0.025	0.025	0.025	0.025	0.025	0.032
3	5	0.025	0.025	0.025	0.032	0.025	0.025	0.025	0.032
4	5	0.025	0.025	0.025	0.032	0.025	0.025	0.032	0.04
5	5	0.025	0.025	0.025	0.032	0.025	0.025	0.032	0.04
6	5	0.032	0.025	0.025	0.04	0.032	0.025	0.032	0.05
7	5	0.032	0.025	0.025	0.04	0.032	0.025	0.032	0.05
8	5	0.032	0.032	0.025	0.04	0.032	0.025	0.032	0.05
9	5	0.032	0.032	0.025	0.04	0.032	0.032	0.032	0.05
10	5	0.032	0.032	0.032	0.04	0.032	0.032	0.04	0.05
11	5	0.04	0.032	0.032	0.05	0.032	0.032	0.04	0.063
12	5	0.04	0.032	0.032	0.05	0.04	0.032	0.04	0.063
13	5	0.04	0.032	0.032	0.05	0.04	0.032	0.04	0.063
14	5	0.04	0.04	0.032	0.05	0.04	0.032	0.04	0.063
15	5	0.04	0.04	0.032	0.05	0.04	0.032	0.04	0.063
16	5	0.04	0.04	0.032	0.05	0.04	0.04	0.04	0.063
17	5	0.04	0.04	0.032	0.05	0.04	0.04	0.05	0.063
18	5	0.04	0.04	0.032	0.05	0.04	0.04	0.05	0.063
19	5	0.05	0.04	0.04	0.05	0.04	0.04	0.05	0.063
20	5	0.05	0.04	0.04	0.063	0.04	0.04	0.05	0.09
21	5	0.05	0.04	0.04	0.063	0.05	0.04	0.05	0.09
22	5	0.05	0.04	0.04	0.063	0.05	0.04	0.05	0.09
23	5	0.05	0.04	0.04	0.063	0.05	0.04	0.05	0.09
24	5	0.05	0.04	0.04	0.063	0.05	0.04	0.05	0.09
25	5	0.05	0.04	0.04	0.063	0.05	0.04	0.05	0.09
26	5	0.05	0.05	0.04	0.063	0.05	0.04	0.05	0.09
27	5	0.05	0.05	0.04	0.063	0.05	0.04	0.05	0.09
28	5	0.05	0.05	0.04	0.063	0.05	0.04	0.05	0.09
29	5	0.05	0.05	0.04	0.063	0.05	0.05	0.05	0.09
30	5	0.05	0.05	0.04	0.063	0.05	0.05	0.063	0.09
31	5	0.05	0.05	0.04	0.063	0.05	0.05	0.063	0.09
32	5	0.05	0.05	0.04	0.063	0.05	0.05	0.063	0.09
33	5	0.05	0.05	0.04	0.063	0.05	0.05	0.063	0.09
34	5	0.05	0.05	0.04	0.063	0.05	0.05	0.063	0.09
35	100	0.05	0.05	0.04	0.063	0.05	0.05	0.063	0.09

Appendix C

Dymola components

In this Appendix, a brief explanation of the used components is provided. For the modelling and simulation in this work, the Modelica Standard Library (version 4.0.0) [87], IDEAS library (version 3.0.0) [88] and Buildings Library (version 9.0.0) [89] are used. Figure C.1 shows the icon of all used components in Dymola. The models are described in the same order.

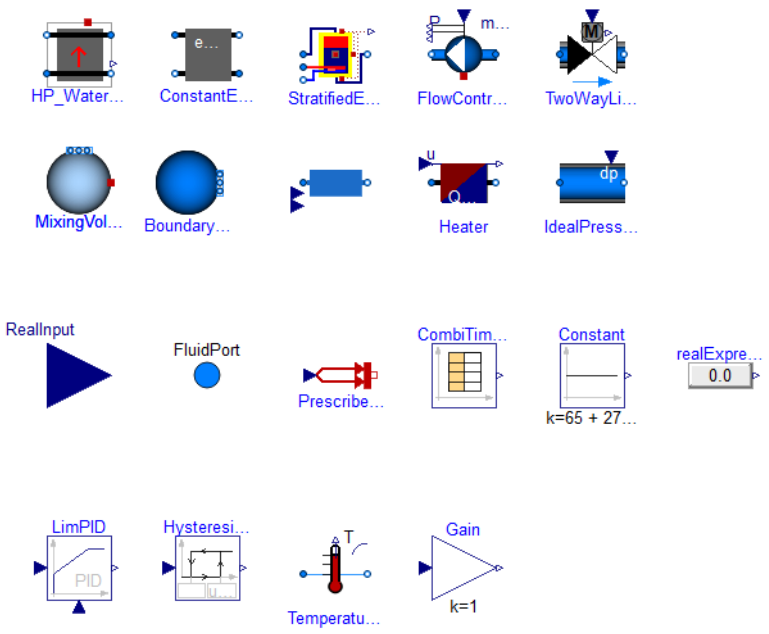

Figure C.1: Components used in Dymola.

Water-to-water heat pump The IDEAS.Fluid.HeatPumps.HP_WaterWater_OnOff model is used to represent a booster heat pump. The model implements a water-to-water heat pump with given performance map. Performance maps of existing Vitocal heat pumps are available, but the user can provide performce data as well. The heat pump is switched on or off based on a temperature setpoint or an external signal. The model provides the possibility to modulate the heat pump power output. The COP remains constant but the electric power is scaled according to a given input.

Heat exchanger The IDEAS.Fluid.HeatExchangers.ConstantEffectiveness model transfers heat in the amount of $\dot{Q} = \epsilon \dot{Q}_{\max}$ where ϵ is a constant effectiveness and $\dot{Q}_{\max}$ is the maximum heat that can be transferred. The equations that are implemented in the model are given in

Equation 3.4-3.7

Storage tank with internal heat exchanger The IDEAS.Fluid.Storage.StratifiedEnhanced InternalHex model represents a storage tank for thermal energy storage with a built-in heat exchanger. The tank's volume, the tank's dimensions and heat exchanger properties are to be specified by the user.

Pump The IDEAS.Fluid.Movers.FlowControlled_m_flow model describes a fan or pump with prescribed mass flow rate. Also the IDEAS.Fluid.Movers.FlowControlled_dp model and IDEAS.Fluid.Movers.SpeedControlled_y model are used and are pressure and speed controlled, but have the same icon. Based on a given performance map and pressure curve, defined in record 'per', the efficiency is computed. Existing data from a Wilo Stratos are available in the IDEAS library.

Valve The IDEAS.Fluid.Actuators.Valves.TwoWayLinear valve has a linear opening characteristic. The model requires a nominal mass flow and nominal pressure drop to size the valve. The actuator position can be given as input.

Storage tank The IDEAS.Fluid.MixingVolumes.MixingVolume model represents a instantaneously mixed volume. Potential and kinetic energy at the port are neglected and there is no pressure drop over the ports. Heat transfer can be applied by the user. When 'precribedHeatFlowRate' is set equal to 'true', a heat flow rate can be specified. When 'precribedHeatFlowRate' is set equal to 'false' the heat flow is computed as a function of the temperature difference between the mixing volume and the ambient.

Boundary IDEAS.Fluid.Sources.Boundary_pT models can be added to prescribe the temperature and/or pressure at a certain position in the circuit. In closed circuits, it is necessary to include a boundary model to provide a reference value.

Pipe The pipe model used the district heating network model is part of this work and described in Section 4.2.1. The purpose of creating a new pipe model is to reduce simulation time.

Ideal heater The IDEAS.Fluid.HeatExchangers.HeaterCooler_u model adds or removes a prescribed amount of heat from the medium, $Q_{flow} = uQ_{flow,nominal}$, where u is an input signal.

Ideal pressure source With the IDEAS.Fluid.Movers.BaseClasses.IdealSource model either the mass flow rate or pressure difference between the two fluid ports is set to the value of the input connector.

Real input connector The Modelica.Blocks.Interfaces.RealInput connector is used to transfer values of the type 'Real' from outside to inside the model. It can be used to exchange data from one layer to another.

Fluid port The Modelica.Blocks.Interfaces.FluidPort connector is used to connect the hydraulic circuit of different models.

Predescribed heat flow The Modelica.Thermal.HeatTransfer.Sources.PredescribedHeatFlow model is used to allow a specified amount of heat to be injected into a thermal system. The real input specifies the heat flow to be transferred. The output is a heat port to which a thermal connector can be connected.

Time table The Modelica.Blocks.Sources.CombiTimeTable is used to include the space heating and domestic hot water profiles in the model. The model has multiple outputs, such that data files with multiple profiles can be imported. The output signals is determined by executing a constant, linear or cubic hermite spline interpolation in the table.

Constant The Modelica.Blocks.Sources.Constant model is used to provide a constant real input value for other models. The value is provided by the user and remains fixed during the simulation.

Real expression The Modelica.Blocks.Sources.RealExpression model generates a real output depending on the expression given by the user. This can be a fixed value or a time varying output containing variables of other components.

PID Controller In the Modelica.Blocks.Continuous.LimPID model either P, PI, PD or PID can be selected. A gain 'k', integrator time constant 'Ti' and/or derivative time constant 'Td' should be given. Both minimum and maximum limits can be set according to the user's specification.

Hysteresis The IDEAS.Control.Discrete.HysteresisRelease model transforms a real input signal into a real output signal. When the output is false and the input becomes greater than the specified parameter uHigh, the output switches to true. The opposite happens when the input becomes less than the specified parameter uLow.

Temperature sensor IDEAS.Fluid.Sensors.TemperatureTwoPort sensors are added in the circuit to measure the temperature of the passing fluid. The output of the temperature sensor can be used for visualisation or post-processing, or as an input for another model in the circuit.

Gain The Modelica.Blocks.Math.Gain model multiplies a given input 'u' by a gain 'k' specified by the user, and returns the result as an output.

Appendix D

Simulation scenario 6

Due to an unexpected increase in simulation time, scenario 6 was simulated differently compared to the other scenarios. As can be seen in Figure D.1, the mass flow rate in summer is small, but includes sudden changes. Where the mass flow rate increases abruptly after being at the lowest point, the calculation time could extend to several hours. This is probably caused by difficulties with finding a suitable solution for the next time step. To address this problem, the simulation was executed for the remaining part of the year, as depicted in Figure D.2a. For the missing days, the available data from day 152 to 175 (orange) and from day 175 to 202 (green) is repeated, hereby following the trend as observed in the simulations of the other scenarios. The result is presented in Figure D.2b.

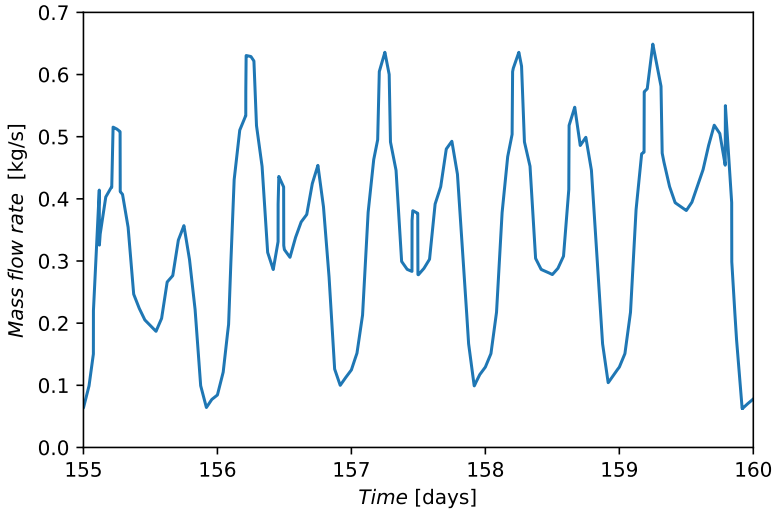

Figure D.1: Illustration of the problem in simulating scenario 6.

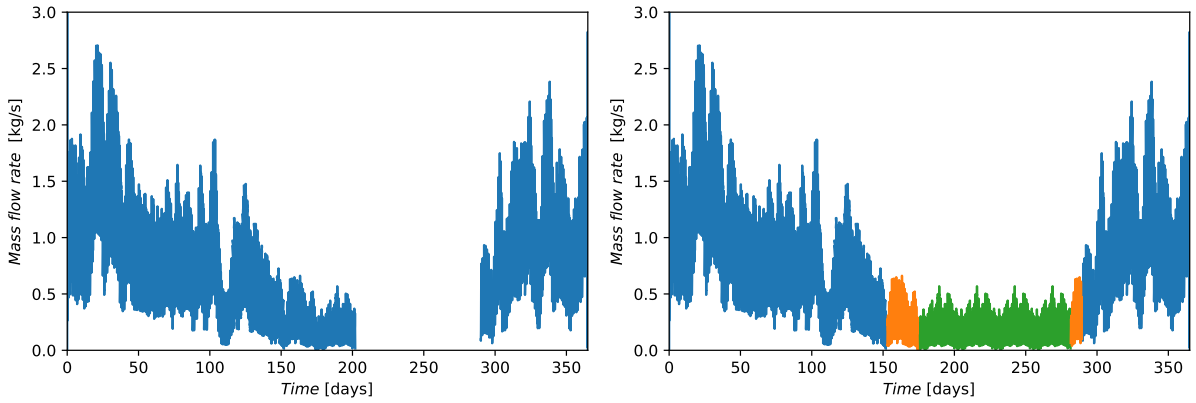

(a) Simulated part of scenario 6.

(b) Extended simulation.

Figure D.2: Total mass flow rate in the network before and after extension of the available data.

In order to evaluate the influence of this approach, the energy use during the specific period is compared to the energy use throughout the entire year. The duration from day 202 to 290 accounts for 9.4% of the total energy use, thereby having a limited impact on the drawn conclusions. To further examine the influence on total energy use and energy efficiency, the energy use for the days within the range of 202 to 290 is varied by +/- 25%. The results of these analyses are presented in Table D.1.

Table D.1: Influence of the variation of the energy use of day 202 to 290 on the overall total primary energy use and energy efficiency.

	Total primary energy use	**Energy efficiency**
Energy use of day 202 to 290: +25%	+2.36%	-2.30%
Energy use of day 202 to 290: -25%	-2.36%	+2.41%